In presenting the dissertation as a partial fulfillment of the requirements for an advanced degree from the Georgia Institute of Technology, I agree that the Library of the Institute shall make it available for inspection and circulation in accordance with its regulations governing materials of this type. I agree that permission to copy from, or to publish from, this dissertation may be granted by the professor under whose direction it was written, or, in his absence, by the Dean of the Graduate Division when such copying or publication is solely for scholarly purposes and does not involve potential financial gain. It is understood that any copying from, or publication of, this dissertation which involves potential financial gain will not be allowed without written permission.

3/17/65
b

QUADRUPOLE HYPERFINE STRUCTURE IN THE MICROWAVE SPECTRA OF PHOSPHOROUS TRICHLORIDE AND PHOSPHORYL CHLORIDE

A THESIS

Presented to

The Faculty of the Graduate Division

by

Carl Rodney Nave

In Partial Fulfillment

of the Requirements for the Degree

Doctor of Philosophy in the School of Physics

Georgia Institute of Technology

June 1966

QUADRUPOLE HYPERFINE STRUCTURE IN THE

MICROWAVE SPECTRA OF PHOSPHOROUS TRICHLORIDE

AND PHOSPHORYL CHLORIDE

Approved:

Chairman

Date approved by Chairman 26 May 1966

ACKNOWLEDGMENTS

The author is grateful to Drs. J. Q. Williams and T. L. Weatherly for their patient supervision. The research was made much more enjoyable by their unfailing good humor and helpfulness in the time of difficulty. A special note of appreciation is due my wife, Brenda, for her encouragement and understanding during the time of being the wife of a student.

This research was supported in part by the National Science Foundation.

TABLE OF CONTENTS

TABLE OF CONTENTS (Continued)

LIST OF TABLES

LIST OF ILLUSTRATIONS

LIST OF ILLUSTRATIONS (Continued)

SUMMARY

The low rotational transitions in the microwave spectra of the molecules phosphorous trichloride, PCl_3^{35}, and phosphoryl chloride, POC_3^{35}, have been investigated. The theory of the electric quadrupole interaction in symmetric-top molecules with three identical quadrupolar muclei has been reviewed and then extended to calculate the Stark effect in the presence of the hyperfine structure. The J=1 to J=2 transition spectrum, including the effects of the Stark interaction, has been calculated with the aid of a computer program. The lines were pressure broadened according to the Van Vleck-Weisskopf relation and added to obtain a spectrum for direct comparison with the experimental spectrum recordings. The separations of the two strongest hyperfine components in the J=1 to J=2 transitions of PCl_3 and $POCl_3$ were measured. The measured separations were compared to the calculated spectra to obtain values for the P-Cl bond axis quadrupole coupling constants, eqQ. The coupling constants obtained for PCl_3 and $POCl_3$ were -53.3 Mc/sec and -55.4 Mc/sec respectively. The effects of pressure broadening and the Stark interaction upon the above measurements were evaluated. The Stark effect in the J=1 to J=2 and J=2 to J=3 transitions was analysed to obtain the values 0.56 ± 0.02 debye and 2.54 ± 0.04 debye for the dipole moments of PCl_3 and $POCl_3$ respectively. A phase-lock klystron stabilization technique was utilized in recording the spectra to improve the resolution of the spectrograph.

CHAPTER I

INTRODUCTION

The microwave spectra of symmetric-top molecules are often very easy to measure and analyse. For this reason, a large number of such molecules have been studied. However, if the molecule contains a nucleus with spin 1 or greater, the molecular rotation states are split by the interaction of the quadrupole moment of this nucleus with the average electric field gradient at the nucleus. This splitting gives rise to hyperfine structure in the microwave absorption spectrum of the molecule. The resulting lines are weaker and often very close together, but if they can be resolved they supply information about the electric quadrupole interaction.

The effect of the quadrupole interaction upon atomic spectra has been treated in detail by Casimir (1). The quadrupole hyperfine structure in molecular rotational spectra can be treated in a similar manner. The application to microwave spectroscopy has been outlined by Townes and Schawlow (2). The complexity of the quadrupole hyperfine structure increases rapidly with the number of quadrupolar nuclei in the molecule. The case of three identical quadrupolar nuclei in a symmetric-top molecule is a particularly interesting and difficult one. The splitting of each rotational transition into a large number of hyperfine components results in very low intensities for the individual components, and consequently measurement of the spectrum is difficult. The theory for the quadrupole interaction in such cases has also presented some problems.

Bersohn (3) (4) discussed the calculation of the quadrupole hyperfine structure for this case and calculated the matrix elements of the hamiltonian which are necessary for a calculation of the hyperfine splitting. P. N. Wolfe (5) (6) then compared the J=2 to J=3 rotational spectrum of $CHCl_3$ with the spectrum calculated from Bersohn's theory and obtained the value -80.39 Mc/sec for the quadrupole coupling constant of the chlorine nuclei. Long (7) (8) measured the J=1 to J=2 transitions in $CFCl_3$ and $CHCl_3$ and obtained the quadrupole coupling constants -103.5 Mc/sec and -110.8 Mc/sec respectively. The pure quadrupole resonance experiments of Livingston (9) had yielded the values 76.90 Mc/sec and 79.63 Mc/sec for the quadrupole coupling constants of $CHCl_3$ and $CFCl_3$ respectively in the solid state. The solid state and microwave measurements of the quadrupole coupling constants in other molecules have been in much better agreement than this.

In order to produce agreement with Bersohn's theory, Long found that it was necessary to assign values to the centrifugal distortion coefficients of both $CHCl_3$ and $CFCl_3$ which were much larger than the theoretical values. In addition, the centrifugal distortion coefficient D_J was negative and changed with J, while previous investigations had yielded only positive, constant values for D_J in molecules of this type. Johnson (10) studied centrifugal distortion in several symmetric-top molecules. Upon comparison of the theoretical and experimental results, he found agreement in every case except for the reported distortion coefficients for $CFCl_3$ and $CHCl_3$. Subsequently, Favero and Mirri (11) investigated the spectra of $CFCl_3$ and $CHCl_3$ in the range J=15 to J=29 where the splitting due to the quadrupole interaction is negligible. They obtained

values for the centrifugal distortion coefficients which were in good agreement with the theoretical values, in contradiction to the results of Long.

Long suggested that the discrepancies mentioned above might be caused by errors in the quadrupole interaction theory. Weatherly (12) calculated the hyperfine structure of $CFCl_3$ using a different approach, taking care to choose wavefunctions which behaved properly under exchange of any two of the identical nuclei. Using Long's experimental results, Weatherly obtained the quadrupole coupling constant -81.5 Mc/sec and his calculation indicated that the centrifugal distortion coefficients would be near the theoretical values. Weatherly's calculation differed from Bersohn's in that it included some non-zero matrix elements linking states characterized by K=1 and K=-1. It was concluded that Bersohn's theory gave incorrect results because it failed to take into account properly the effects of the Pauli exclusion principle.

Weatherly's approach had the disadvantage that the wave functions chosen did not take full advantage of the permutation symmetry of the three identical quadrupolar nuclei. The resulting calculation for the frequencies and intensities of the quadrupole hyperfine lines proved to be inconveniently large, even with the use of a high-speed digital computer. Svidzinskii (13), in a rather general treatment of multipole interactions in molecular rotational spectra, showed how to use the symmetry properties of the molecule to maximum advantage in the calculation of hyperfine structure. Svidzinskii included a discussion of the appropriate state functions to use when identical nuclei are involved.

Using the method suggested by Svidzinskii, A. A. Wolf (14) has

given a theoretical treatment of the quadrupole hyperfine structure of symmetric-top molecules with three identical quadrupolar nuclei. He calculated the complete hyperfine structure pattern for the J=1 to J=2 and J=2 to J=3 transitions of $CHCl_3$ and $CFCl_3$ with the aid of the computer program included in Appendix B of this thesis. Wolf calculated exact expressions for the strongest hyperfine lines and intensities up through the J=4 to J=5 transition. He obtained the values -77.9 Mc/sec and -79.9 Mc/sec for the quadrupole coupling constants of $CHCl_3$ and $CFCl_3$ respectively. These values are in agreement with the solid state measurements.

In order to provide additional confirmation of the theory, the molecules phosphorous trichloride, PCl_3^{35} and phosphoryl chloride, $POCl_3^{35}$, were chosen for this investigation. The hyperfine structures for both of these molecules have been analysed to obtain values for their quadrupole coupling constants. The theory has been extended to calculate the Stark effect in the presence of the hyperfine structure, and dipole moment measurements have been made by analysis of the Stark effect.

The molecules PCl_3 and $POCl_3$ have been studied rather extensively. A brief outline of the previous work is presented here. The structure of PCl_3 has been determined by Kisliuk and Townes (15) using microwave methods and by Swingle (16) and Hedberg and Iwasaki (17) using electron diffraction. A microwave determination of the structure of $POCl_3$ has been carried out by Williams et al. (18), and electron diffraction studies have been made by Badgley and Livingston (19). The experimentally determined structural parameters are given in Table 1 and the method of investigation is indicated in each case. The values 100.27 ± .09 and 103.5 ± 1.0 degrees for the Cl-P-Cl angles in PCl_3 and $POCl_3$ respectively

were used in the calculations for this investigation.

A recent review of the Raman investigations of $POCl_3$ has been written by Ziomek and Piotrowski (20). They compared seven different measurements of the Raman displacements and seven sets of measured depolarization factors. They chose as the most probable data the Raman displacements and relative intensities of Langseth (21) and the depolarization factors of Cabannes and Rousset (22). The Raman displacements of Langseth are listed in Table 2. Infrared measurements in $POCl_3$ have been reported by Daasch and Smith (23) and by Baudler et al. (24). Ziomek and Piotrowski (20) did a normal coordinate analysis of $POCl_3$ and calculated some of its thermodynamic properties. More recently, Nakai and Mori (25) have made force constant calculations for both PCl_3 and $POCl_3$.

The Raman and infrared spectra for PCl_3 have recently been measured by Frankiss and Miller (26). Earlier Raman measurements were made by Cabannes and Rousset (22) and by Nielsen and Ward (27). The infrared spectrum was measured by Davis (28) in the liquid and by Lorenzelli (29) in the gaseous state. A number of bond force constant calculations have been carried out. The most recent are those of Venkateswarlu (30), Nakai and Mori (25), and Mirri et al. (31). The latter measured the millimeter wave spectrum for PCl_3 and obtained the values 1.17 ± .01 kc/sec and -1.879 ± .008 kc/sec for the centrifugal distortion coefficients D_J and D_{JK} respectively. These coefficients appear in the equation

$$\nu = 2(J+1)(B-D_{JK}K^2) - 4D_J(J+1)^3 \qquad (I-1)$$

Table 1. Experimentally Determined Structural Parameters for PCl_3 and $POCl_3$

Molecule	P-Cl Distance in Å	Cl-P-Cl in Degrees	P-O Distance in Å	B_0 in Mc/sec	Method*	Reference
PCl_3^{35}	2.043 ± 0.003	100.1 ± 0.3		2,617.1 ± 0.1	M	(15)
	2.03 ± 0.02	100.5 ± 1.5			E.D.	(16)
	2.039 ± 0.0014	100.27 ± 0.09			E.D.	(17)
$POCl_3^{35}$	1.99 ± 0.02**	103.6 ± 2.0	1.45 ± 0.03	2,015.20 ± 0.05	M	(18)
	1.99_5 ± 0.02	103.5 ± 1.0	1.45 ± 0.05		E.D.	(19)

*M = Microwave, E.D. = Electron Diffraction.

**Assumed.

for the frequency of a rotational transition J to J+1 in a symmetric-top molecule (32).

Both PCl_3 and $POCl_3$ belong to the symmetry point group C_{3v}. The normal vibrational modes are shown in Figures 1 and 2 for PCl_3 and $POCl_3$ respectively. The perpendicular modes v_2 and v_4 for PCl_3 and v_2, v_4, and v_6 for $POCl_3$ are doubly degenerate. The infrared and Raman spectra which were discussed above yield the frequencies for excitation of these modes, although the identification of the mode corresponding to a given frequency is sometimes difficult. The frequency for the excitation of a molecule into the first excited vibrational state in a single mode will be referred to as the fundamental frequency of that mode. The experimental fundamental frequencies for PCl_3 and $POCl_3$ are listed in Table 2. The Boltzmann factors which give the populations of the first excited states relative to that of the ground state are included in Table 2. The corresponding data for $CHCl_3$ and $CFCl_3$ are also listed for comparison.

If an appreciable fraction of the molecules are in an excited vibrational state, then rotational transitions corresponding to that state may be observed. These rotational transitions are characterized by a rotational constant of the form (33)

$$B_v = B_e - \sum_s (v_s + \frac{g_s}{2}) \alpha_s \ , \qquad \text{(I-2)}$$

where B_e is the equilibrium rotational constant, v_s is the vibrational quantum number, and g_s is the degeneracy of the s^{th} vibrational mode. The frequency of a rotational transition is given by

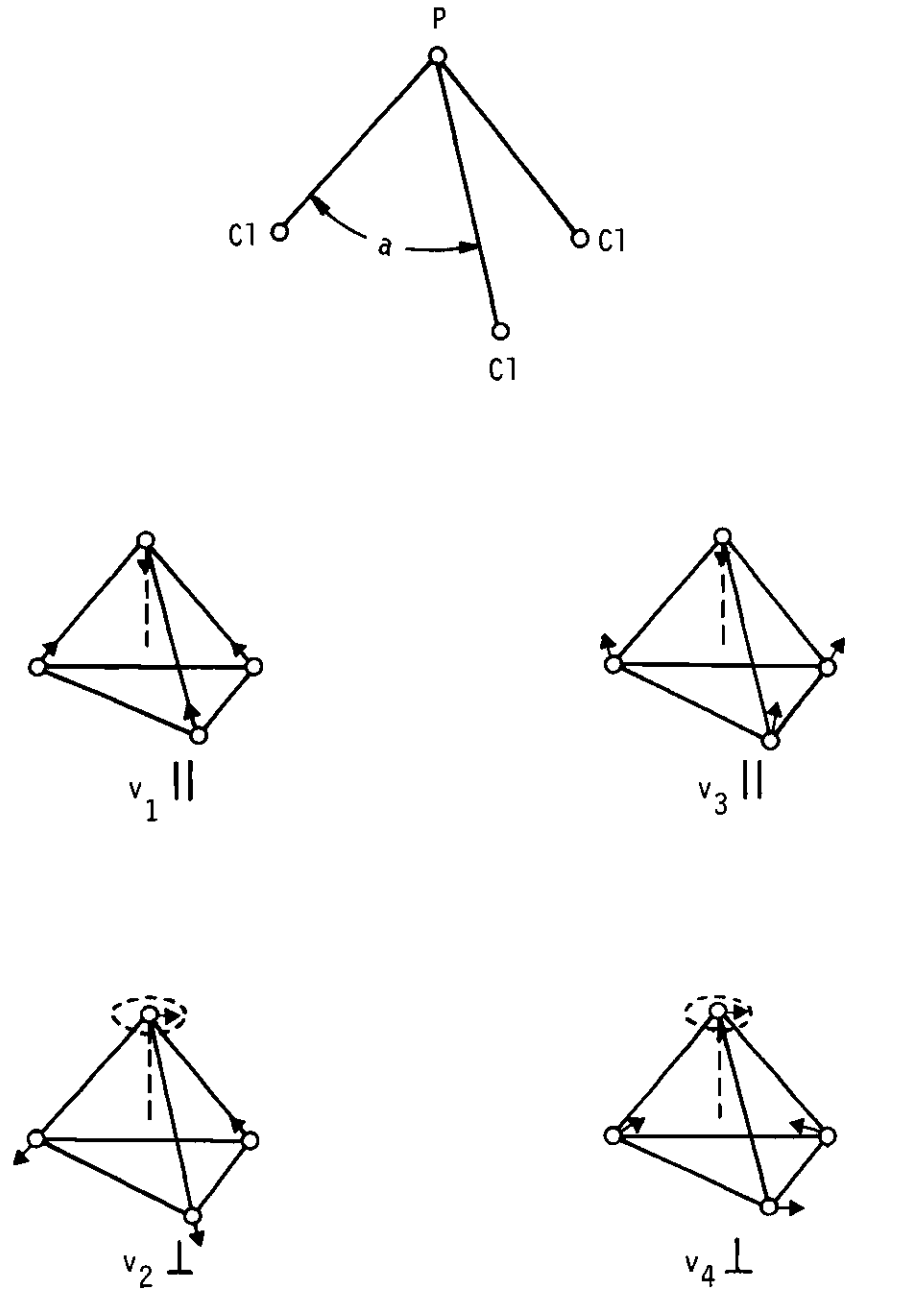

Figure 1. Vibrational Modes of Phosphorous Trichloride.

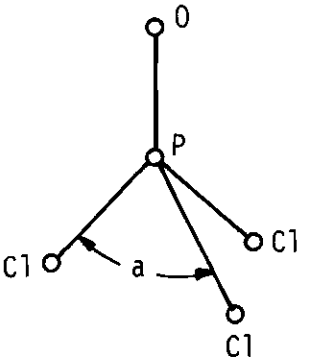

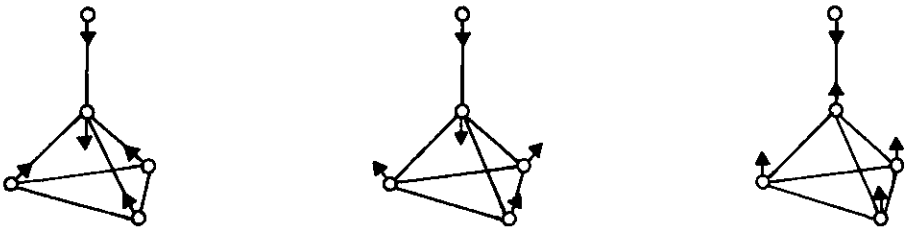

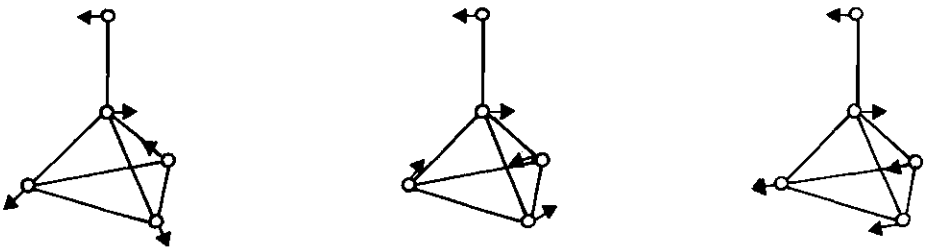

Figure 2. Vibrational Modes of Phosphoryl Chloride.

$$\nu = 2B_o(J+1) - 2(J+1)\sum_s \alpha_s v_s \ , \qquad \text{(I-3)}$$

where $B_o = B_e - \sum_s \frac{g_s}{2} \alpha_s$.

Kisliuk and Townes (15) have observed excited state lines in the spectrum of PCl_3 and have assigned these lines to modes v_2 and v_4. From the observed spectrum they have calculated the interaction constants $\alpha_2 = 1.9 \pm 0.3$ Mc/sec and $\alpha_4 = -1.9 \pm 0.3$ Mc/sec. With these constants, the excited vibration state lines for the J=1 to J=2 transition would be expected to fall 7.6 Mc/sec on each side of the ground state line center.

Excited state lines have not been reported for $POCl_3$, but the Boltzmann population factors in Table 2 indicate that they should be of approximately the same relative strength as those in PCl_3. From examination of the Boltzmann factors it appears that excited state lines should not be so easily observable in $CFCl_3$ and $CHCl_3$ as in PCl_3 and $POCl_3$.

The dipole moments of PCl_3 and $POCl_3$ have been measured by various methods and with rather widely varying results. These results are summarized in Table 5. No microwave measurements of the dipole moments have been made prior to this investigation and no measurement of the dipole moment of $POCl_3$ in the gaseous state has been reported to date.

In this investigation, the quadrupole splitting of the low rotational transitions in PCl_3 and $POCl_3$ was examined. A review of the theoretical treatment of A. Wolf (14) is given. The theory is then extended to treat the Stark effect in the presence of the quadrupole

Table 2. Fundamental Excitation Frequencies for Vibrational Modes and the Populations of Excited States Relative to the Ground State

Mode	PCl_3			$POCl_3$			$CHCl_3$			$CFCl_3$		
	ω	Population		ω	Population		ω	Population		ω	Population	
	(cm^{-1})	200°K	300°K	(cm^{-1})	200°K	300°K	(cm^{-1})	200°K	300°K	(cm^{-1})	200°K	300°K
ω_1	510	.03	.09	486	.03	.10	672	.01	.04	534	.02	.08
ω_2	491	.06	.18	581	.03	.12	760	.01	.05	846	.00	.03
ω_3	260	.15	.29	267	.15	.28	363	.07	.18	351	.08	.19
ω_4	190	.51	.80	193	.50	.79	261	.30	.57	245	.24	.62
ω_5				1290	.00	.00	3030	.00	.00	1085	.00	.01
ω_6				337	.18	.40	1217	.00	.01	400	.11	.29

References for frequencies: PCl_3, Reference 26; $POCl_3$, Reference 21; $CHCl_3$, Reference 2; $CFCl_3$, R. B. Bernstein, J. P. Zeitlow, and F. F. Cleveland, J. Chem. Phys. 21, 1778 (1953).

hyperfine structure for symmetric-top molecules with three identical quadrupolar nuclei. A computer program has been written to calculate the hyperfine structure of the J=1 to J=2 rotational transition, both in the presence and absence of an applied electric field. The lines were pressure broadened according to the Van Vleck-Weisskopf relation and added to get a resultant spectrum for direct comparison with the experiment.

The J=1 to J=2 transition is the most advantageous for analysis of the hyperfine structure since its quadrupole splitting is the largest. The quadrupole splittings in PCl_3 and $POCl_3$ are smaller than in the molecules previously investigated, i.e., $CHCl_3$ and $CFCl_3$. For this reason, a phase-lock technique for stabilizing the klystron was utilized to enhance the resolution. The technique is similar to that described by Narath and Gwinn (34). It is discussed in detail in Chapter II.

The J=1 to J=2 transitions in PCl_3 and $POCl_3$ were analysed to obtain values for the quadrupole coupling constant eqQ. These values were compared to the solid state values obtained by Livingston (35). The Stark effect in the J=1 to J=2 and J=2 to J=3 transitions was examined and dipole moment measurements were made for these molecules.

In the text of this thesis, the chemical formulae PCl_3 and $POCl_3$ will indicate the abundant symmetric-top species PCl_3^{35} and $POCl_3^{35}$ unless otherwise specified.

CHAPTER II

INSTRUMENTATION AND TECHNIQUE

The microwave spectrograph used in this investigation is the conventional Stark modulation type, utilizing an 85 kc/sec square wave for the modulation. It has been described in detail by Clayton (36) and Long (7), but a brief description will be repeated here in order to explain recent modifications.

The microwave radiation from a klystron is introduced into a waveguide which contains the sample. An 85 kc/sec square wave is applied to an electrode centered in the waveguide to produce electric fields up to 1200 volts/cm in the sample. The absorption of the gas is modulated by this square wave, and the resulting 85 kc/sec signal is detected by a crystal and amplified by means of a phase-sensitive lock-in amplifier. The signal from the amplifier is displayed on an oscilloscope or plotted on a recorder.

Because the detection system is phase-sensitive, the absorption line in the presence of the electric field and that in the absence of the field give D.C. signals of opposite polarity. If the signals overlap in frequency due to pressure broadening, etc., then the resultant signal obtained is the difference between the field-on and field-off signals. If the signals do not overlap appreciably, this feature is convenient, because it provides a means for distinguishing between the unperturbed absorption lines and the lines as perturbed by the Stark effect. If the klystron is swept slowly and uniformly over the frequency range of interest

while recording the signal from the detector, a plot of absorption as a function of frequency is obtained.

The frequency resolution of the spectrograph is dependent upon the bandwidth of the detector and the stability of the klystron oscillator. The bandwidth of the phase-sensitive detector can be made as small as desired by increasing the time constant of the RC output network. If the stability of the klystron can be increased, then presumeably not only the frequency resolution but also the sensitivity can be increased because of the possibility of using longer time constants.

In this investigation the klystron was stabilized by means of a double phase-lock stabilization technique similar to that described by Narath and Gwinn (34). A block diagram of the stabilization circuit is shown in Figure 3. Two Dymec Model DY-2650A Oscillator-Synchronizers were used to provide the phase-lock stabilization. These units utilize a 30 Mc/sec crystal oscillator as a reference frequency. For normal operation of the Oscillator-Synchronizer, harmonics of a 100 Mc/sec crystal-controlled oscillator are generated and mixed with a sample of the klystron output to obtain a 30 Mc/sec beat frequency. This beat frequency is phase-locked to the 30 Mc/sec reference oscillator. A D.C. correction voltage is generated and applied to the klystron reflector when the klystron starts to drift.

In the arrangement shown in Figure 3, klystron #1 is stabilized at a single frequency as described above. The stabilized output of klystron #1 is then mixed with the output of klystron #2 and further mixed with a third signal from a transfer oscillator, the frequency of which can be varied from 100 to 220 Mc/sec. The resultant 30 Mc/sec beat

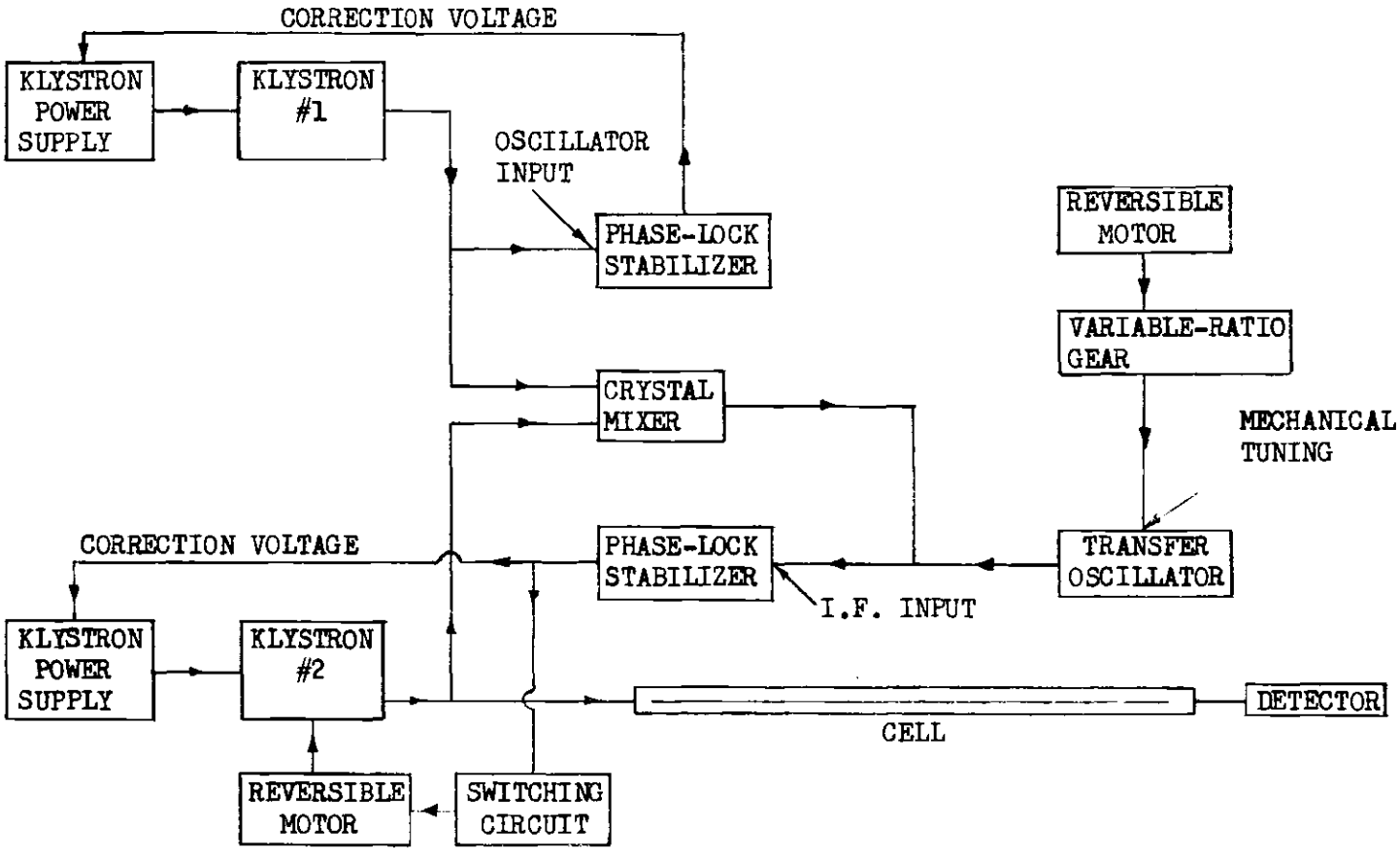

Figure 3. Block Diagram of Klystron Stabilization and Tuning Circuit

frequency is introduced into another Dymec stabilizer at the I.F. input to be directly compared with the 30 Mc/sec reference oscillator. Once the lock-in condition is obtained, the second phase-lock stabilizer will keep the beat frequency of the three signals at 30 Mc/sec by applying a correction voltage to the reflector of klystron #2. If the transfer oscillator is now tuned slowly, the phase-lock circuit will retune klystron #2 to keep the beat frequency at 30 Mc/sec. Since the phase-lock circuit can produce only a limited correction voltage, it is necessary to mechanically retune the cavity of klystron #2 to keep the error voltage within the allowed limits, which are about ±20 volts. To accomplish this, the correction voltage is also applied to a switching circuit such as that shown schematically in Figure 5, which drives a small reversible motor. The motor acts through a reduction gear to retune the klystron cavity to give zero error voltage.

By this method, klystron #2 can be electrically tuned, continuously and slowly, over a large frequency range while maintaining the phase-lock stabilization. The uniformity of the tuning is practically that of the transfer oscillator, which represents a significant improvement over other methods presently used for klystron tuning. The Dymec stabilizer can presumeably compensate for noise up to 100 kc/sec in the klystron reflector circuit.

As an example of the lock-in procedure, consider the case of the J=1 to J=2 rotational transition of PCl_3, the line center of which is at 10,468 Mc/sec. The lock-in arrangement is illustrated in Figure 4. The reference klystron, in this case a Varian X-13B, was stabilized at 10,230 Mc/sec by locking it 30 Mc/sec above the 102nd multiple of the 100 Mc/sec

oscillator in the Dymec stabilizer.

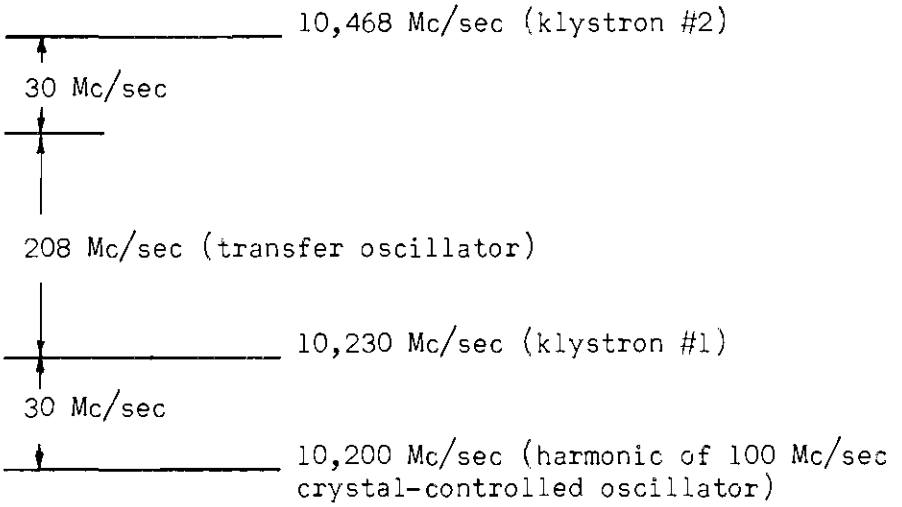

Figure 4. Relation of the Frequencies Used in Measuring the J=1 to J=2 Transition of PCl_3.

The signals from the two klystrons and the transfer oscillator are mixed as described earlier. The signal klystron, a Varian X-13, is then locked 30 Mc/sec above the sum of the reference klystron (#1) and transfer oscillator frequencies. For a transfer oscillator frequency of 208 Mc/sec, this puts the signal klystron (#2) at 10,468 Mc/sec, the line center frequency for the J=1 to J=2 transition. If the transfer oscillator is tuned from 198 to 218 Mc/sec, the signal klystron is 'pushed' from 10,458 to 10,478 Mc/sec. This covers all of the significant hyperfine structure while maintaining the phase-lock condition. The klystron has been tuned over ranges in excess of 100 Mc/sec by this method; the continuous tuning range is limited only by the width of the klystron mode. By use of a two-speed, reversible motor and a variable-ratio gear, tuning speeds from 0.1 to 15.0 Mc/min were obtained.

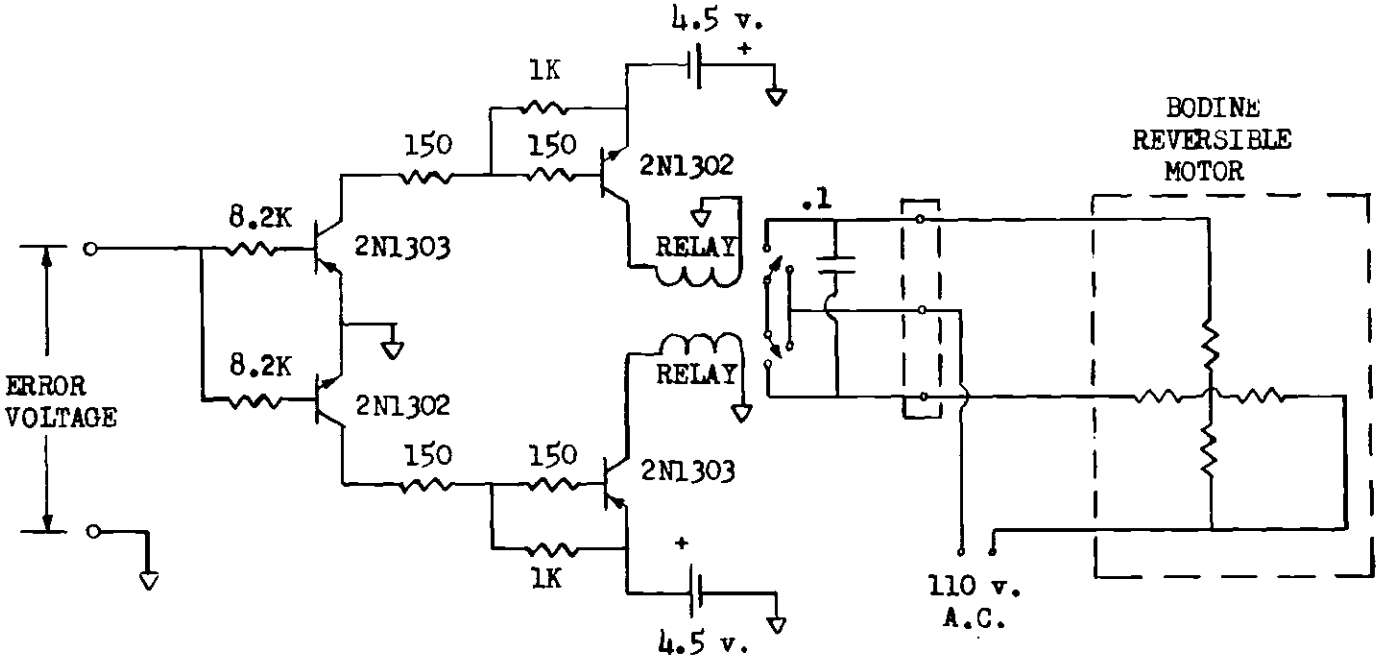

Figure 5. Switching Circuit for Klystron Cavity Retuning Motor

Frequency measurements were made by means of a Hewlett-Packard Model 5245L electronic frequency counter. The counter was calibrated by adjusting a crystal oscillator to give a 5 Mc/sec reading on the counter. Upon comparison of this oscillator with the signal from the National Bureau of Standards, WWV, a beat frequency of 1 cycle/sec or less was obtained. The counter was then used to count the transfer oscillator frequency. The signal was counted for 0.1 seconds and then the frequency was displayed. At convenient intervals a marker was placed on the recorder chart, and the transfer oscillator frequency was recorded. The recordings were made at tuning rates less than 5 Mc/min so the 0.1 second average leads to frequency errors less than 0.01 Mc/sec at the display time. The time lag in placing the marker on the chart probably leads to an additional error of about the same size. Examination of Figure 4 makes it clear that the uncertainty in the reference klystron (#1) frequency must be added to the above mentioned error. The source of this uncertainty is the 100 Mc/sec crystal-controlled oscillator in the phase-lock stabilizer. This oscillator was monitored and found to drift not more than 0.01 kc/sec in a 24 hour period. This leads to a maximum uncertainty of 0.001 Mc/sec in the case of the J=1 to J=2 transition for PCl_3, since the 102nd multiple of the 100 Mc/sec oscillator was used. The largest source of uncertainty lies in the assignment of peak positions on the spectrum. This will be discussed in connection with the experimental results. This frequency measurement technique is advantageous in that it provides an almost continuous readout of the frequency while sweeping over the spectrum. This makes the measurement of the separation of hyperfine lines and the measurement of linewidths more convenient than with previous techniques.

The lock-in procedure described above has been used for frequencies as high as 20,150 Mc/sec in examining the J=4 to J=5 transition in $POCl_3$. In this case the reference klystron frequency was doubled and then mixed with the transfer oscillator and the signal klystron. With proper mixing, the lock-in technique should be applicable up to 30 Kmc/sec and perhaps higher. Besides the increased stability, this procedure offers a much more convenient method for frequency measurement than those commonly used in this frequency range.

The spectrograph used for this investigation had previously utilized an 85 kc/sec preamplifier and a lock-in amplifier which have been described by Clayton (36). The lock-in amplifier was replaced by an improved model, the Model HR-8 manufactured by Princeton Applied Research Corporation. Since the preamplifier in this model is untuned, it was found to be advantageous to use the 85 kc/sec preamplifier mentioned above before the HR-8 cut down the off-frequency noise. Otherwise, this noise saturated the first stages of the HR-8 in the cases where very weak signals required large amplifications. This lock-in amplifier has calibrated time constants up to 100 seconds. By slowing the tuning rate of the klystron, time constants up to 30 seconds were used to advantage in data collection.

Data Collection Procedures

The vapor pressure of phosphorous trichloride, PCl_3, at dry ice temperature (-78.5 degrees Centigrade) appeared to be about 0.06 mm Hg. This agrees with a calculated value of 0.06 mm Hg using the formula:

$$\log_{10}(P) = \frac{-0.05223a}{T} + b$$

obtained from the Handbook of Chemistry and Physics published by the Chemical Rubber Company. The empirical parameters a and b were determined for pressures 1, 5 and 10 mm Hg from data given in the Handbook and used for an approximation at -80 degrees Centigrade. The vapor pressure P is in mm Hg and T is the temperature in degrees Centigrade. All data on PCl_3 was taken at a temperature of about -80 degrees Centigrade, obtained by placing dry ice directly on the waveguide.

The reliability of the pressure measurements made in the course of this experiment is not known. The pressure measurements were made with a Pirani gauge which must be calibrated for each individual gas; measurements for different gases can vary several percent. Calibrations have not been obtained for PCl_3 and $POCl_3$. The ordinary procedure is to calibrate the Pirani gauge for a given gas using a McLeod gauge. This is impractical in the case of PCl_3 and $POCl_3$ since they would react strongly with the mercury in the McLeod gauge. The Pirani gauge was calibrated for air using the McLeod gauge. The agreement of the calculated vapor pressure with the Pirani gauge reading indicates that the calibration for Pcl_3 is not drastically different from that for air.

The spectrum of PCl_3 proved to be very sensitive to the microwave power level. The microwave power was attenuated until an optimum spectrum was obtained. Increasing the power above the optimum led to general lowering of the peak intensities and some apparent alteration of the relative intensities of the hyperfine lines.

It was found that the power saturation problem could be minimized by working at low pressures. Low pressures also enhance the resolution and minimize the effect of the pressure broadening on the hyperfine line

separations. The best results for PCl_3 were obtained by pumping continuously on the cell after it had reached an equilibrium near -80 degrees Centigrade. The pumping process could be carried on for several hours while the condensed PCl_3 in the waveguide evaporated to maintain a fairly uniform pressure. The main disadvantage of this method was that no accurate indication of the pressure in the waveguide was obtainable while pumping.

The sample, at room temperature, was introduced into the cooled waveguide at the end opposite the pump. The source was then shut off and the sample in the waveguide allowed to condense down to its vapor pressure. The waveguide was then pumped until all the sample was removed. Data was taken during this time which, as mentioned above, was sometimes several hours.

Phosphoryl chloride, $POCl_3$, is a solid at -80 degrees Centigrade and does not have enough vapor pressure to produce a detectable microwave spectrum. However, it must be cooled below zero degrees Centigrade in order to obtain the rotational energy level population necessary for a satisfactory signal-to-noise ratio. With thin plastic foam strips placed on the waveguide and with dry ice placed on the strips, the temperature was found to drift downward slowly enough that data could be taken at temperatures ranging from zero degrees Centigrade downward. This process usually reached an equilibrium with the vapor pressure of $POCl_3$ somewhere between 5 and 20 microns Hg, as indicated by the Pirani gauge. Pressures lower than this could be obtained by pumping. The most useful data was taken between 5 and 30 microns Hg. The pressure broadening of the lines in $POCl_3$ is quite large because of the molecule's large dipole

moment, so pressures below 30 microns Hg were necessary to obtain satisfactory resolution of the hyperfine structure. The spectrum of $POCl_3$ was not so sensitive to the microwave power level as that of PCl_3.

CHAPTER III

QUADRUPOLE INTERACTION THEORY

The theory of the electric quadrupole interaction for the case of three identical quadrupolar nuclei in a symmetric-top molecule has been treated in detail by Svidzinskii (13) and by A. Wolf (14). Wolf utilized the work of Svidzinskii and also the earlier treatments of Bersohn (3) and P. N. Wolfe (5). A summary of A. Wolf's work is given here in order to provide the results necessary for the calculation of the hyperfine structure and to establish a foundation for the treatment of the Stark effect. In Chapter IV the theory is extended to treat the Stark effect in the presence of hyperfine structure.

Svidzinskii and A. Wolf took full advantage of the symmetry of the molecular system. The amount of labor involved in the hyperfine structure calculation was greatly reduced by choosing nuclear spin eigenvectors which are basis vectors for irreducible representations of the group of permutations of the three identical nuclei. There are no matrix elements of the Hamiltonian between basis vectors of different irreducible representations, so this reduces the number of matrix elements which must be calculated.

The basic assumptions involved in the theory are listed below:

1. The electronic charge does not penetrate the nucleus.
2. The quadrupole interaction Hamiltonian is diagonal in the rotational angular momentum J. (This is a reasonable assumption since the separation between rotational levels is much

larger than the quadrupole interaction energy.)

3. The electrostatic potential is symmetric about the Cl-X axis in the XCl_3 structure.

The State Function

For the hyperfine structure calculation, the rotational part of the wavefunction and the spin part will be discussed separately. The total wave function must satisfy the Pauli exclusion principle under the exchange of two identical nuclei by changing sign if the spins are half-integral and maintaining the same sign if the spins are integral. This imposes some restrictions on the eigenvectors used for construction of the state function.

The Hamiltonian remains unchanged under any permutation of the three identical nuclei. This is equivalent to saying that the Hamiltonian commutes with the permutation operators. If linear combinations of the resultant spin eigenvectors can be found which will serve as the basis vectors for one irreducible representation of the group of permutations of three objects, then there will be no matrix elements of the quadrupole Hamiltonian between these basis vectors and the basis vectors for other irreducible representations. This is a result of group theory (37), and it will allow a considerable simplification of the quadrupole hyperfine structure calculation.

As is well known, the group of permutations of three objects has three irreducible representations: totally symmetric, $A^{(1)}$; antisymmetric, $A^{(2)}$; and the two-dimensional representation, E. The matrices representing the elements of this group are given in Appendix A. If O_R represents

any operator in the group and U_i a complete set of linearly independent functions, then a representation R of the operator can be generated by

$$O_R U_i = \sum_{j=1}^{n} R_{ji} U_j \qquad \text{(III-1)}$$

where R_{ji} is an element of the representation matrix R.

The set of functions U_i is a basis for the representation R and a set U_i exists such that R is an <u>irreducible</u> representation. If there is more than one irreducible representation, then there will be corresponding sets of vectors $U_i^{(v)}$ such that

$$O_R U_i^{(v)} = \sum_{j=1}^{n} R_{ji}^{(v)} U_j^{(v)} \qquad \text{(III-2)}$$

where $R_{ji}^{(v)}$ is an element of the v^{th} irreducible representation of the operator O_R.

In order to obtain a linear combination of resultant spin eigenvectors which will serve as a basis for an irreducible representation of the group, a projection operator P is defined which will operate on the spin eigenvectors to give a function which will transform like one row of an irreducible representation (if there is more than one row). That is,

$$P_k^{(w)} U = U_k^{(w)} \qquad \text{(III-3)}$$

where U is any function which can be expressed in terms of the basis set of the w^{th} irreducible representation, and $U_k^{(w)}$ is a function which belongs

to the k^{th} row of the w^{th} representation. Such an operator has the form (38)

$$P_k^{(w)} = \frac{n_w}{g} \sum_R R_{kk}^{(w)*} O_R \qquad \text{(III-4)}$$

where n_w is the dimension of the w^{th} irreducible representation and g is the order of the group.

Referring to Figure 6, the resultant nuclear spin is obtained by coupling the spin of nucleus 2 to that of nuceus 3 to obtain an intermediate angular momentum L, and then coupling the spin of nucleus 1 to L to obtain the resultant angular momentum I. The resultant vector is denoted by u(LI).

A normalized eigenvector $u(w_k I)$ which transforms like the k^{th} row of the w^{th} representation can be obtained by use of the projection operator as follows (34):

$$u(w_k I) = \frac{\sum_{L'} (u(L'I), P_k^{(w)} u(LI)) u(L'I)}{\left[(u(LI), P_k^{(w)} u(LI)) \right]^{1/2}} \qquad \text{(III-5)}$$

where $(u(LI), P_k^{(w)} u(LI))$ is a matrix element of the projection operator. From the definition of the projection operator, equation III-4, these matrix elements have the form

$$(U(L'I), P_k^{(w)} u(LI)) = \frac{n_w}{g} \sum_R R_{kk}^{(w)*} (u(L'I), S_R u(LI)) \qquad \text{(III-6)}$$

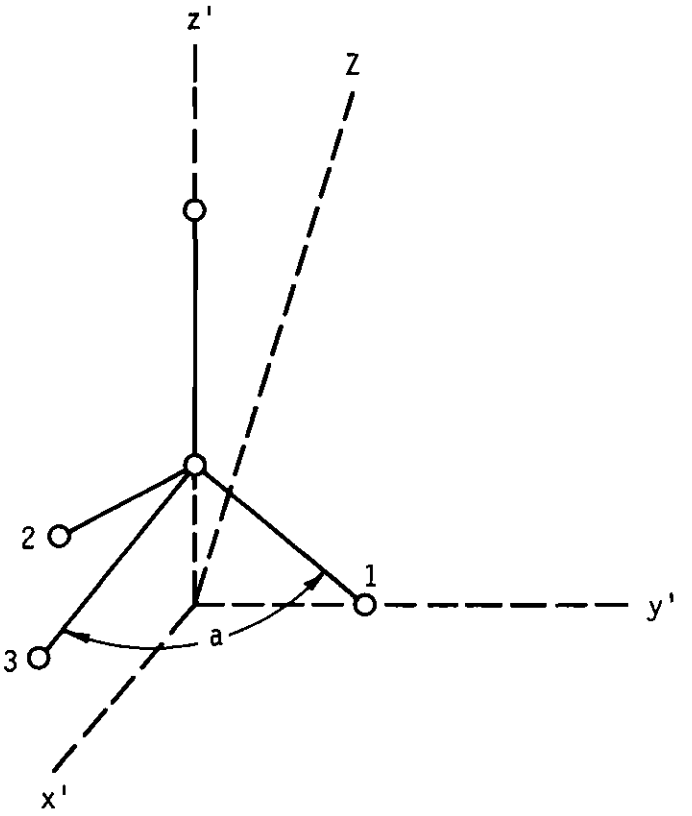

Figure 6. Geometry of Molecular System.

where S_R are the operators which permute the spin coordinates among the identical nuclei. The matrix elements of these permutation operators have been evaluated by Wolf and are reproduced in Appendix A.

The expansion coefficients in equation III-5 above are called genealogical coefficients or coefficients of fractional parentage. They are also tabulated in Appendix A. If these coefficients are denoted by $G(w_k LI)$ then equation III-5 becomes

$$u(w_k I) = \sum_{L'} G(w_k L'I)u(L'I) \ . \qquad \text{(III-7)}$$

Note that the genealogical coefficients are dependent upon the intermediate angular momentum L. However, this dependence is apparent only in the phase of the coefficients. For the one dimensional representations $A^{(1)}$ and $A^{(2)}$ the choice of phase is immaterial. For the two dimensional representation E, either both upper or both lower signs for the E_1 and E_2 coefficients under a given I must be chosen. This does not affect the choice of signs under any other value of I.

The spin functions in equation III-5 have the desired form and their behavior under permutation of the spin coordinates is known. The vibration and rotation parts of the wavefunction will have the required symmetry under interchange of the spatial coordinates of the identical nuclei.

The rotational part of the wavefunction is characterized by the quantum numbers J and K, representing the rotational angular momentum and its projection along the molecular symmetry axis respectively. The

two lowest vibrational states for molecules of the form YX_3 or ZYX_3 are characterized by the quantum numbers v=0 and v=1 and have the symmetry $(-1)^v$ under inversion of the molecule. This is most familiar in the case of NH_3. In molecules like PCl_3 and $POCl_3$ these states are essentially degenerate and together constitute the gound vibrational state. Since the process for permuting identical nuclei includes an inversion operation (40), the quantum number v is necessary for characterizing the state function. When the vibration and rotation parts of the wavefunction are included, the resultant function is denoted by $u(vJKw_kIF)$ where F is the total angular momentum obtained by coupling I and J. Linear combinations of the functions $u(vJKw_\kappa IF)$ can be found which have the proper symmetry under exchange of any two of the identical nuclei.

If K is zero or a multiple of three, only linear combinations of functions having spin parts of symmetry $A^{(1)}$ or $A^{(2)}$ can give the proper symmetry of the total wavefunction. The appropriate state functions for this case are (41)

$$u(E_{vJK}A^{(1)}IF) = \frac{1}{\sqrt{2}}\left[u(vJKA^{(1)}IF) + (-1)^{J+v+2j}\, u(vJ-KA^{(1)}IF)\right] \qquad \text{(III-8)}$$

and

$$u(E_{vJK}A^{(2)}IF) = \frac{1}{\sqrt{2}}\left[u(vJKA^{(2)}IF) - (-1)^{J+v+2j}\, U(vJ-KA^{(2)}IF)\right]$$

where E_{vJK} indicates the rotation and vibration part of the wavefunction and j is the spin of each of the identical nuclei.

For K is not a multiple of three, combinations of functions with symmetry E are required to give the proper symmetry for the total wavefunction. The proper wavefunction is (42)

$$u(E_{vJK}EIF) = \frac{1}{2}\left[u(vJKE_2IF) + (-1)^{J+v+2j}\, u(vJ-KE_2IF)\right] \qquad \text{(III-9)}$$

$$+ \frac{1}{2}\left[u(vJKE_1IF) - (-1)^{J+v+2j}\, u(vJ-KE_1IF)\right]$$

where the subscripts 1 and 2 on E indicate the rows of the two dimensional representation.

Matrix Elements of the Quadrupole Interaction Hamiltonian

The electrostatic potential energy of a nucleus due to the surrounding electrons in a molecule is of the form

$$W = -\int \bar{U}_m \bar{U}_n e^2 \sum_{i,j} \frac{1}{|\vec{r}_{ei} - \vec{r}_{pj}|} U_m U_n \, dv_m \, dv_n \qquad \text{(III-10)}$$

where U_m and U_n are the state functions of the molecular electrons and the nucleus respectively, $\vec{r}_{ei}$ is the position vector of the i^{th} electron in a space-fixed frame, $\vec{r}_{pj}$ is the position vector of the j^{th} proton in a space-fixed frame, and the integral is evaluated over the coordinates of all electrons and protons.

A multipole expansion of the above yields the familiar result

$$H_Q = \vec{\nabla}\vec{E} : \vec{\vec{Q}} \qquad \text{(III-11)}$$

for the quadrupole part of the Hamiltonian, where $\vec{\vec{E}}$ is the electric field at the nucleus, and $\vec{\vec{Q}}$ is the electric quadrupole moment operator for the nucleus. This Hamiltonian is the scalar product of second rank irreducible tensor operators. Wolf writes this Hamiltonian as

$$H = A \cdot B \qquad \text{(III-12)}$$

so this notation will be used hereafter in this treatment.

The total interaction energy of the three quadrupolar nuclei is just three times the interaction energy of one of them taken separately (43). The energy will be expressed in terms of nucleus 1 (Figure 6). The coupling scheme is:

$$j_2 + j_3 = L \; ; \; j_1 + L = I \; ; \; J + I = F. \qquad \text{(III-13)}$$

Using the representation u(vJKIF) without regard to symmetry gives

$$(u(vJK'I'F), A \cdot B\, u(vJKIF)) = \qquad \text{(III-14)}$$

$$(-1)^{J+I'+F} \begin{Bmatrix} F & I' & J \\ 2 & J & I \end{Bmatrix} (vJK' \| A \| vJK)(I' \| B \| I)$$

for the matrix elements of the Hamiltonian (44). In this expression the curly brackets $\{\ \}$ represent the Wigner 6-J symbol (47). The reduced matrix element of A is non-zero only for $K'-K = 0$ or ± 2. The non-zero elements are (45)

$$(vJK \| A \| vJK) = (-1)^{J+K}(2J+1) \begin{pmatrix} J & 2 & J \\ -K & 0 & K \end{pmatrix} \frac{q \cos(a)}{2} \qquad \text{(III-15)}$$

$$(vJ-1\|A\|vJ1) = (vJ1\|A\|vJ-1) = (-1)^{J-1}(2J+1)\begin{pmatrix} J & 2 & J \\ 1 & -2 & 1 \end{pmatrix}\frac{q\sqrt{6}\,(\cos(a)-1)}{12}\,.$$

The large brackets $\begin{pmatrix} \end{pmatrix}$ represent the Wigner 3-J symbol (47). The symbol q represents $\frac{\partial^2 V}{\partial a^2}$, where V is the potential at the nucleus due to the electrons, and a represents a coordinate along the bond axis. In obtaining the above expressions in terms of the second derivative of the potential with respect to the bond axis coordinate, the charge distribution was assumed to be symmetric about the bond axis. The angle a is the bond angle Cl-X-Cl. If the symmetry axis of the charge distribution is not along the bond axis due to an interaction with some other nucleus in the molecule, e.g. the oxygen nucleus in $POCl_3$, then the effective value of 'a' in equation III-15 would be altered.

The reduced matrix element of B is given by

$$(I'\|B\|I) = (-1)^{j_1+L+I+2}\,[(2I+1)(2I'+1)]^{1/2}\begin{Bmatrix} j_1 & I' & L \\ I & j_1 & 2 \end{Bmatrix}(j_1\|B\|j_1) \qquad \text{(III-16)}$$

where j_1 is the spin of nucleus 1 and L is the intermediate angular momentum obtained by coupling j_2 and j_3. The reduced matrix element $(j_1\|B\|j_1)$ is

$$(j_1\|B\|j_1) = \frac{eQ}{2\begin{pmatrix} j_1 & 2 & j_1 \\ -j_1 & 0 & j_1 \end{pmatrix}} = \sqrt{5}\;\; eQ$$

in this case, where $j_1 = 3/2$ for the chlorine nucleus. The term eQ is the quadrupole moment defined by

$$eQ = \int \bar{U}_n e(3z^2 - r^2) U_n dv_n \qquad \text{(III-18)}$$

where the integral is to be evaluated for the state in which the angular momentum has its maximum projection along the space-fixed z axis.

When the wavefunctions are transformed according to equation III-7 and a factor of three introduced to account for the sum over the three quadrupolar nuclei, the matrix elements take the form

$$(u(vJK'w_kI'F), A\cdot B\ u(vJKw_kIF)) = \qquad \text{(III-19)}$$

$$3(-1)^{J+I'+F}\begin{Bmatrix} F & I' & J \\ 2 & J & I \end{Bmatrix} (vJK' \| A \| vJK)(w_kI' \| B \| w_kI)$$

where

$$(w_kI' \| B \| w_kI) = \sum_{L'} G(w_kL'I)(L'I \| B \| L'I)G(w_kL'I).$$

Equation III-19 reduces to

$$(u(vJK'w_kI'F),\ A\cdot B\ u(vJKw_kIF)) = \qquad \text{(III-20)}$$

$$(-1)^{j+J+F}\begin{Bmatrix} F & I' & J \\ 2 & J & I \end{Bmatrix} (vJK' \| A \| vJK)(j \| B \| j)C(w_iI'I)$$

with the use of equation III-16, where $C(w_kI'I)$ is a nuclear reduction coefficient defined by

$$C(w_k I'I) = 3(-1)^{I'+I}\,[(2I+1)(2I'+1)]^{1/2} \qquad \text{(III-21)}$$

$$\sum_{L'} (-1)^{L'}\, G(w_k L'I')\, \begin{Bmatrix} j & I' & L' \\ I & j & 2 \end{Bmatrix} G(w_k L'I).$$

These reduction coefficients are reproduced in Appendix A. The coefficients listed there are obtained by using either all the upper signs or all the lower signs in the genealogical coefficient table. The reduction coefficients are symmetric in I' and I .

As a final step, linear combinations of these elements must be taken to get the matrix elements with the correct state functions given by III-8 and III-9. The result for K=0 or K equal to a multiple of three is

$$(u(E_{JK}A^{(1,2)}{}_{I'F}), A\cdot B\; u(E_{JK}A^{(1,2)}{}_{IF})) = \qquad \text{(III-22)}$$

$$(-1)^{J+F+j} \begin{Bmatrix} F & I' & J \\ 2 & J & I \end{Bmatrix} (vJK\|\, A\|\, vJK)(j\|\, B\|\, j)C(A^{(1,2)}{}_{I'I})$$

For K not equal to a multiple of three the matrix elements are given by

$$(u(E_{JK}EI'F), A\cdot B\; u(E_{JK}EIF)) = \qquad \text{(III-23)}$$

$$(-1)^{J+F+j} \begin{Bmatrix} F & I' & J \\ 2 & J & I \end{Bmatrix} (j\|\, B\|\, j)[C(+,I',I)(vJK\|\, A\|\, vJK)$$

$$+ (-1)^{J+v+2j}\, C(-,I',I)(vJK\|\, A\|\, vJ{-}K)]$$

where

$$C(+,I',I) = \frac{1}{2}\left[C(E_2 I'I) + C(E_1 I'I)\right]$$

$$C(-,I',I) = \frac{1}{2}\left[C(E_2 I'I) - C(E_1 I'I)\right] .$$

Note that the term $(vJK\|\ A\|\ vJK-K)$ in equation III-23 is non-zero only when K=1 and thus the v=0 and v=1 states are degenerate except when K=1.

Relative Intensities of Hyperfine Components

The relative intensities of the quadrupole hyperfine components are proportional to the square of the dipole moment matrix elements between the initial and final states. When the matrices of the quadrupole interaction Hamiltonian are diagonalized, the state function for a given hyperfine level, T, is

$$u(E_{JK}T) = \sum_I B_{TI}\, u(E_{JK} w_k I F M_F)$$

where B_{TI} are the matrix elements of the diagronalizing transformation, and M_F is the projection of the total angular momentum F onto the space fixed z axis. The relative intensity for a transition from an initial state T to a final state T' as worked out by Wolf (46) is

$$N = \left(\frac{(J+1)^2 - K^2}{3(J+1)}\right) d^2(2F^i + 1)(2F^f + 1)$$

$$\left[\sum_I B^i_{TI} B^f_{T'I} (-1)^{J+I+F^f+1} \begin{Bmatrix} J & F^i & I \\ F^f & (J+1) & 1 \end{Bmatrix} \right]^2$$

wher 'd' is the dipole moment of the molecule. For microwave absorption transitions, the rotational angular momentum goes from J to J+1. The development of the above relationship will be discussed in more detail in Chapter IV where the Stark effect in the presence of hyperfine structure is presented.

CHAPTER IV

STARK EFFECT WITH QUADRUPOLE INTERACTION

The theory of the Stark effect on symmetric-top molecules with nuclear quadrupole interaction has been treated by Low and Townes (48). However, the choice of wavefunctions in that treatment is not convenient for the case of interest here, namely the case of molecules with three identical quadrupolar nuclei. The eigenvectors worked out by Svidzinskii (49) are more convenient since they take advantage of the symmetry inherent in this type of molecule. These eigenvectors are listed in equations III-8 and III-9.

The intermediate field case discussed by Low and Townes is the case which is appropriate for this calculation since the Stark and quadrupole interactions are of comparable magnitude for the electric field strengths of interest. The interaction Hamiltonian which must be used for the first order energy calculation is of the form

$$H_{Interaction} = H_s + H_{q1} + H_{q2} + H_{q3} \qquad (IV\text{-}1)$$

where H_{qi} is the quadrupole interaction Hamiltonian for nucleus i and H_s is the Stark interaction Hamiltonian.

As discussed in the previous chapter, the representations given by equations III-8 and III-9 are appropriate for the calculation of the quadrupole matrix elements. These representations will also be used for the calculation of the matrix elements of the above interaction

Hamiltonian. The matrix elements of the quadrupole part $H_{q_1} + H_{q_2} + H_{q_3}$ are those listed in equations III-22 and III-23. The matrix elements of the Stark part H_s contain several terms, typical of which is the following:

$$(vJKw_kIFM_F|H_s|v'J'K'w_kF'M_F').$$

In this expression w_k represents the k^{th} row of the w^{th} irreducible representation of the group of permutations of three objects. The quantum number M_F was not included in the discussion of Chapter III since the quadrupole Hamiltonian is independent of the spatial orientation of F. With the use of equation III-7 this term can be expressed as

$$\sum_L G^*(w_kLI)G(w_kLI)(vJKLIFM_F|H_s|v'J'K'LIF'M_F').$$

Use will be made of the fact that H_s is diagonal with respect to all spin quantum numbers since it does not interact with the spin. The matrix elements above are independent of the intermediate spin angular momentum L, and therefore it can be eliminated from the notation. Due to the normalization of the eignvectors in equation III-7, carrying out the summation above yields

$$(vJKIFM_F|H_s|v'J'K'IF'M_F'),$$

as may be verified by substituting the genealogical coefficients $G(w_kLI)$ from Appendix A for any w_k.

With the use of equations III-8 and III-9, the matrix elements of H_s for any value of K are seen to be

$$\frac{1}{2}\left[(vJKIFM_F|H_s|v'J'K'IF'M_F') + (-1)^{J+J'+v+v'}(vJ-KIFM_F|H_s|v'J'-K'IF'M_F')\right] . \quad \text{(IV-2)}$$

For the first order Stark calculation, elements off-diagonal in J will be neglected.

The spherical tensor notation defined by Edmonds (50) is convenient for writing the matrix elements of the Stark effect Hamiltonian. In this notation the Hamiltonian can be written

$$H_s = \sum_{\mu} d_{\mu}^{(1)} E_{\mu} \quad \text{(IV-3)}$$

where (1) denotes a tensor of rank one, and μ can take the values 1, 0, and -1 with the following connotations:

$$d_1^{(1)} = \frac{-1}{2}\left(d_x^{(1)} + id_y^{(1)}\right)$$

$$d_0^{(1)} = d_z^{(1)}$$

$$d_{-1}^{(1)} = \frac{-1}{2}\left(d_x^{(1)} - id_y^{(1)}\right)$$

The matrix elements required are of the form

$$(vJKIFM_F|d_{\mu}^{(1)} E_{\mu}|v'J'K'IF'M_F') . \quad \text{(IV-4)}$$

By use of the Wigner-Eckert Theorem (51), equation IV-4 can be put in the form

$$(-1)^{F-M_F}\begin{pmatrix} F & 1 & F' \\ -M_F & \mu & M_F' \end{pmatrix}(vJKIF \| d^{(1)} \| v'J'K'IF')\mu E \qquad \text{(IV-5)}$$

where $(vJKIF \| d^{(1)} \| v'J'K'IF')$ is the reduced matrix element of the dipole moment operator, and the large parentheses represent a Wigner 3-J symbol. If the space-fixed z-axis is chosen as the direction of the uniform electric field, only the $\mu = 0$ component of d will contribute to the Stark interaction. The subscript μ will subsequently be dropped from E_μ with the assumption that E is along the z-axis. The matrix elements of the dipole moment operator are then diagonal in M_F since the sum of the indices in the bottom row of the 3-J symbol must be zero for the 3-J symbol to be non-zero.

The use of equation 7.1.7 of Edmonds (52) gives

$$(vJKIF \| d^{(1)} \| v'J'K'IF') = \qquad \text{(IV-6)}$$

$$(-1)^{J'+I+F'+1}[(2F+1)(2F'+1)]^{1/2}\begin{Bmatrix} J & F & I \\ F' & J' & 1 \end{Bmatrix}(vJK \| d^{(1)} \| v'J'K')$$

for the reduced matrix element of equation IV-5. Parity considerations lead one to the conclusion that the dipole moment matrix elements are non-zero only for $v = v' \pm 1$. Since the dipole moment is an odd operator, it can connect only states of different inversion symmetry. This is the effect which leads to the zero first order Stark effect in the inversion spectrum of the NH_3 molecule.

The matrix element $(vJK\| d^{(1)} \| v'J'K')$ can be further reduced as follows (53):

$$(vJK\| d^{(1)} \| v'J'K') = \tag{IV-7}$$

$$= [(2J+1)(2J+1)]^{1/2}(-1)^{J-K} \begin{pmatrix} J' & J & 1 \\ K' & -K & 0 \end{pmatrix} d \quad \text{if } v' - v = \pm 1$$

$$= 0 \text{ if } v' - v = 0$$

The symbol d now represents the dipole moment of the molecule of interest. The symmetry properties of the 3-J symbol lead to the selection rule $\Delta K = 0$. The 3-J symbol property (54)

$$\begin{pmatrix} j_1 & j_2 & j_3 \\ m_1 & m_2 & m_3 \end{pmatrix} = (-1)^{j_1+j_2+j_3} \begin{pmatrix} j_1 & j_2 & j_3 \\ -m_1 & -m_2 & -m_3 \end{pmatrix}$$

gives the result

$$(vJK\| d^{(1)} \| v'J'K) = -(vJ-K\| d^{(1)} \| v'J'-K) \text{ if } J = J'$$

$$= (vJ-K\| d^{(1)} \| v'J'-K) \quad \text{if } J = J' \pm 1 .$$

The matrix elements of the Stark effect part of the interaction Hamiltonian IV-1 can now be evaluated. The matrix elements for any value of K may be obtained by substituting into equation IV-2. These matrix elements are given by

$$(vJKwIFM_F|H_s|v'J'K'wIF'M_F') = (-1)^{F+F'+J+J'-K+I+1} \qquad \text{(IV-8)}$$

$$\cdot [(2J+1)(2J'+1)(2F+1)(2F'+1)]^{1/2} \begin{pmatrix} F & 1 & F' \\ -M_F & 0 & M_F' \end{pmatrix} \begin{pmatrix} J' & 1 & J \\ K' & 0 & K \end{pmatrix} \begin{Bmatrix} J & F & I \\ F' & J' & 1 \end{Bmatrix} Ed$$

if $v'=v\pm1$. If $v'=v$ the matrix elements are zero. In the above expression 'w' represents any one of the irreducible representations $A^{(1)}$, $A^{(2)}$, and E of the group of permutations of three objects. As previously mentioned, the condition that the bottom three elements in the 3-J symbol sum to zero allows non-zero matrix elements only if

$$K' = K; \; M_F' = M_F \; .$$

The top three angular momenta a, b, and c in a 3-J symbol must satisfy the triangular conditions

$$a+b-c \geq 0; \; a-b+c \geq 0; \; -a+b+c \geq 0$$

and the sum a+b+c must be an integer. These conditions give the additional requirements

$$F' - F = 0, \pm1$$

$$J' - J = 0, \pm1$$

for non-zero matrix elements. Only the terms for which $J'=J$ are included in the first order Stark calculation. Therefore, equation IV-8 reduces to

$$(vJKwIFM_F|H_S|v'JKwIF'M_F) = (2J+1)(-1)^{F+F'-M_F+I-K+1} \qquad \text{(IV-9)}$$

$$\cdot [(2F+1)(2F'+1)]^{1/2} \begin{pmatrix} F & 1 & F' \\ -M_F & 0 & M_F \end{pmatrix} \begin{pmatrix} J & 1 & J \\ K & 0 & -K \end{pmatrix} \begin{Bmatrix} J & F & I \\ F' & J & 1 \end{Bmatrix} Ed.$$

As a preliminary check on this expression for the Stark effect matrix element, it can be assumed for no coupling that I=0 and F=J. The matrix element above reduces to

$$(-1)^{J-M_J+1} \begin{pmatrix} J & 1 & J \\ -M_J & 0 & M_J \end{pmatrix} (2J+1) \begin{Bmatrix} J & J & 0 \\ J & J & 1 \end{Bmatrix} \frac{\sqrt{2J+1}}{\sqrt{J(J+1)}} \; KEd.$$

With the use of explicit expressions for the 3-J and 6-J symbols given by Edmonds (55), the above expression becomes

$$\frac{M_J KEd}{J(J+1)}$$

which is the result for the Stark splitting of a rotational level in the absence of the quadrupole interaction (56).

The matrices for the interaction Hamiltonian IV-1 can be calculated with the use of equation IV-9 and the appropriate choice of either III-22 or III-23, depending upon the value of K. Note that the quadrupole part of the Hamiltonian is diagonal with respect to the inversion symmetry v. This feature made possible the separation of the v=0 and v=1 levels in the quadrupole calculation in the absence of an applied electric field. The Stark effect part of the Hamiltonian is off-diagonal in v, a fact which increases the order of the secular equations which must be solved

for the energy levels of the Hamiltonian IV-1. In the quadrupole calculation for the J=1 to J=2, K=1 transition the largest secular equation was of order four. However, when the Stark effect is added, the largest secular equation is of order 28.

By use of the Burroughs B-5500 computer, the matrices for J=1 and J=2, K=1 were calculated and diagonalized, and the transition frequencies and intensities for all lines in the J=1 to J=2, K=1 rotational transition were obtained. The intensity calculation is discussed below, and the computer solution is discussed in Appendix B. A typical matrix is shown in Figure 8, with the allowed ranges of the various quantum numbers. This particular matrix is for the case J=1 and $M_F = 7/2$ (The Hamiltonian is diagonal in M_F.). The letter S represents a Stark effect element and Q a quadrupole interaction element.

		F =	9/2	9/2	7/2	7/2	7/2	7/2
		I =	7/2	7/2	7/2	7/2	5/2	5/2
F	I	v =	0	1	0	1	0	1
9/2	7/2	0	Q	S	0	S	0	0
9/2	7/2	1	S	Q	S	0	0	0
7/2	7/2	0	0	S	Q	S	Q	0
7/2	7/2	1	S	0	S	Q	0	Q
7/2	5/2	0	0	0	Q	0	Q	S
7/2	5/2	1	0	0	0	Q	S	Q

Figure 7. Illustration of Matrix for J=1, $M_F = 7/2$, K=1

Note that the maximum value that I can take is 7/2 in this case where K is not a multiple of three. A resultant spin of 9/2 would correspond to having all three spins in the same direction. A wavefunction with the correct symmetry under exchange of identical nuclei cannot be constructed when the three spins are parallel unless the spatial part of the wavefunction is antisymmetric under exchange of any two identical nuclei. This occurs only when K=0 or K equal to a multiple of three.

The other matrices can be built up in a similar manner by consideration of the selection rules and the limits on the various quantum numbers. In no case do the non-zero matrix elements extend more than five elements away from the diagonal, but the matrices constructed as in the illustration cannot be broken down into smaller matrices. As previously mentioned, the matrices are as large as 28 x 28 in some cases.

One property of the Stark matrices does produce a simplification in the calculation which is not apparent upon first examination of the matrix elements. The dependence of the Stark matrix elements upon the quantum number M_F from equation IV-9 is

$$(-1)^{F-M_F}\begin{pmatrix} F & 1 & F' \\ -M_F & 0 & M_F \end{pmatrix} \quad .$$

If M_F is replaced by $-M_F$ this becomes

$$(-1)^{F+M_F}\begin{pmatrix} F & 1 & F' \\ M_F & 0 & -M_F \end{pmatrix} = (-1)^{F+1+F'}(-1)^{F-M_F}\begin{pmatrix} F & 1 & F' \\ -M_F & 0 & M_F \end{pmatrix}.$$

Thus the dependence on the sign of M_F is expressed by

$$(-1)^{F+1+F'} .$$

Depending on the values of F and F', the element may change sign or retain the same sign upon replacing M_F by $-M_F$. Thus it appears that the calculation of the eigenvalues must be done separately for the plus and minus M_F values. However, when the secular equations are constructed, the elements which change sign M_F always occur in even order products so that the same secular equations are obtained for plus and minus M_F. As a confirmation of this, the computer program was run with both plus and minus values of M_F and identical results were obtained. This circumstance reduces the amount of calculation that must be done by a factor of two.

Intensity Calculation

If $|f_1)$ and $|f_2)$ represent the eigenvectors associated with the eigenvalues f_1 and f_2, the intensity of a transition from f_1 to f_2 is proportional to

$$|(f_1|d^{(1)}|f_2)|^2$$

where $d^{(1)}$ is the dipole moment operator. The expression for this quantity in terms of a particular representation was discussed in Chapter III. The appropriate representation here is $|vJKIFM_F)$, after the non-essential spin parts are removed.

The expression for the relative intensity of a transition from f_1 to f_2 is then

$$I = \left[\sum_{\substack{I, M_F, F, F' \\ v = v'}} (vJKIFM_F|f_1)(v'J'KIF'M_F|f_2) \right.$$

$$\left. \cdot (vJKIFM_F|d^{(1)}|v'JIKIF'M_F) \right]^2 . \qquad \text{(IV-10)}$$

The matrix element of the dipole moment appearing above is given by equation IV-8 if the electric field E is deleted in that equation. That is, this matrix element is the same as that calculated for the Stark interaction except for a factor of electric field strength. The elements for J'=J+1 are of interest here. The coefficients in equation IV-10 are the eigenvector components obtained from the diagonalizing transformation. These quantities were obtained and the intensities calculated with the aid of the computer program in Appendix B.

Stark Effect in the Absence of Quadrupole Splitting

The first order splitting of a rotational level in a symmetric top molecule due to the presence of an electric field E is given by (57)

$$\frac{-\mu E M_J K}{J(J+1)} \qquad \text{(IV-11)}$$

in the absence of perturbing effects such as the quadrupole interaction. In this case μ is the dipole moment and J, M_J, and K are the symmetric-top quantum numbers. When the applied field E is parallel to the microwave E vector, the selection rule on M_J is $\Delta M_J = 0$. For a transition J to J+1 the above splitting leads to an absorption frequency

$$\nu = 2B(J+1) + \frac{2M_J K\mu E}{J(J+1)(J+2)h} \quad . \tag{IV-12}$$

The term $2B(J+1)$ is the unperturbed frequency of the rotational transition, therefore the Stark displacement is given by

$$\Delta\nu = \frac{2M_J K\mu E}{J(J+1)(J+2)h} \quad . \tag{IV-13}$$

For large fields E, the quadrupole interaction can be treated as a perturbation on the Stark effect, and one would expect the hyperfine structure to be centered around the positions of the symmetric-top Stark effect lines given by equation IV-13.

The Stark displacements are obtained in Mc/sec by the relation

$$\Delta\nu = \frac{2M_J K\mu V}{J(J+1)(J+2)d} \left(\frac{0.50348 \text{ Mc/sec}}{\text{debye volt/cm}} \right) \tag{IV-14}$$

where V is the Stark voltage, and d is the separation between the Stark electrode and the waveguide wall. The separation d was determined by analysing the Stark effect of the J=0 to J=1 transition of carbonyl sulfide, OCS. This separation was found to be 0.481 ± .005 centimeters.

CHAPTER V

BROADENING OF SPECTRAL LINES

In order to closely approximate the experimental spectra, the line spectra calculated from the theory must be appropriately broadened. Broadening of the spectrum is particularly important when there are a large number of components since overlap of the lines may affect the appearance of the spectrum considerably. Overlap of lines can shift the apparent peak positions and give rise to erroneous frequency assignments. In order to at least qualitatively evaluate these effects, the broadening of spectral lines is briefly reviewed here.

A number of perturbations on the molecular energy levels spread the allowed levels over a finite range and thus give rise to broadening of the lines. The relevant sources of broadening, according to Townes and Schawlow (58), are:

1. Natural line width
2. Doppler effect
3. Pressure broadening
4. Saturation broadening
5. Collisions between molecules and the walls of the containing vessel.

The natural line width is negligible in ordinary microwave absorption experiments. When the frequency of operation is significantly removed from the cut-off frequency of the waveguide, the broadening due to the Doppler effect is approximated by (59)

$$\Delta\nu = \frac{\nu}{c}\sqrt{2kN_o \ln(2)}\sqrt{\frac{T}{M}} = 3.58 \times 10^{-7}\sqrt{\frac{T}{M}}\ \nu \qquad \text{(V-1)}$$

where

ν = frequency

N_o = Avagadro's number

k = Boltzmann's constant

T = temperature in degrees Kelvin

M = molecular weight.

For PCl_3 with a molecular weight of 137 and a J=1 to J=2 transition frequency of 10468 Mc/sec, the Doppler effect half-width at room temperature is

$$\Delta\nu \simeq 0.006 \text{ Mc/sec.}$$

For $POCl_3$ this figure is about 0.004 Mc/sec. As will be shown, this is quite small compared to other sources of broadening.

An estimate of the broadening due to collisions with the walls of the waveguide may be obtained from an elementary approach given by Townes and Schawlow (60). The approximate linewidth due to such collisions is given by the expression

$$\Delta\nu = 1.00 \times 10^4 \frac{A}{V}\ M^{-1/2} \qquad \text{(V-2)}$$

where

A = area of walls in $\mathring{A}^2$

V = volume of cell in $\mathring{A}^3$

M = molecular weight.

Again the molecule PCl_3 with M = 137 will be considered. In the Stark absorption cell used in the experiment, the separation between the Stark septum and waveguide wall is 4.81 mm, giving a line width

$$\Delta\nu = 0.003 \text{ Mc/sec}$$

which is approximately the same as that calculated for $POCl_3$.

Townes and Schawlow give a treatment of saturation broadening, but it is difficult to obtain an estimate of the magnitude of the effect because the expressions for the broadening contain parameters such as the mean time between collisions which are not easily obtainable experimentally.

Qualitatively, the effects of saturation broadening are:

1. lowering of the peak intensity by a factor $(1 + aI)^{-1}$
2. broadening the line by a factor proportional to $(1 + aI)^{1/2}$

where I is the intensity of the microwave radiation. It is notable that the magnitude of this effect may differ for different components of the line which are split by quadrupole interaction, Stark effect, etc. The reason for this is that the factor 'a' in the expressions above contains a matrix element of the dipole moment which may vary with the different components of the spectrum.

Since the effects of saturation cannot be easily calculated, the alternative is to try to eliminate them by decreasing the intensity of the microwave radiation. As was mentioned in Chapter II, a saturation problem of some type is apparently present in the case of PCl_3. It was necessary in that case to reduce the microwave power until the relative peak heights of the hyperfine components became independent of the power. It was then assumed that the saturation effects were negligible.

Pressure Broadening

"Pressure broadening" is the term applied to broadening caused by collisions between molecules, although 'collision' in this context does not necessarily mean the same thing as it does in kinetic theory. As will be discussed further below, the cross-section for interactions between molecules which give rise to appreciable spectral broadening is considerably larger than the cross-section for kinetic theory type collisions.

Van Vleck and Weisskopf (61) have obtained an expression for the broadening of a spectral line due to collisions under the following basic assumptions:

1. The collisions are so strong that the Boltzmann energy distribution is restored after each collision.
2. The duration of a collision is short enough that the electric field does not change appreciably during the collision.

Assumption 1 is equivalent to saying that the collisions are violent enough that the phase of the oscillation after the collision depends only slightly upon the phase before the collision, but that there is thermodynamic equilibrium between the molecule and the electric field immediately after the collision.

With the exception of the negative frequency resonance term which is negligible at the pressures of interest, the line shape obtained by Van Vleck and Weisskoph is

$$\gamma = \frac{8\pi^2 Nf}{3ckT} |\mu_{ij}|^2 \nu^2 \left[\frac{1/(2\pi\tau)}{(\nu - \nu_o)^2 + 1/(2\pi\tau)^2} \right] \qquad (V-3)$$

where

γ = absorption coefficient

N = number of molecules per unit volume

f = fraction of molecules in the lower of the transition states

c = speed of light

k = Boltzmann's constant

T = temperature in degrees Kelvin

μ_{ij} = matrix element of the dipole moment

ν_o = natural molecular frequency

τ = mean time between collisions.

For a wide range of low pressures (up to a few mm of Hg), this relation has the following properties:

1. Peak intensity does not vary with pressure.
2. The apparent resonant frequency is independent of the pressure.
3. The line width is directly proportional to the pressure.

These properties have been experimentally verified for NH_3 (62) and a few other molecules.

The dependence of the line width at half-maximum upon the pressure is expressed by

$$\Delta\nu = 1/\pi\tau = 2bp$$

where p is the pressure and 'b' is some constant which will subsequently be referred to as the line width parameter. When $\Delta\nu \ll \nu$, the term ν^2

in equation V-3 can be approximated by a constant. In the case of the J=1 to J=2 transition of $POCl_3$, which lies at about 8060 Mc/sec, the frequency range over which the hyperfine structure spreads is about 40 Mc/sec. The term ν^2 would change by only about one percent over that range. Since the frequency ranges of interest will ordinarily be less than 40 Mc/sec, the term ν^2 will subsequently be approximated by a constant. With this approximation the line shape formula becomes

$$\gamma = \frac{Cbp}{(\nu - \nu_o)^2 + (bp)^2} \qquad (V-4)$$

Since only relative intensities will be considered in this treatment, the magnitude of the constant C is of no interest. The line width parameter 'b' gives an indication of the cross-section for line-broadening interactions. This parameter can be varied to fit the experimental line width, and a rough measurement of the collision cross-section can be obtained. This cross-section will ordinarily be larger than that obtained from kinetic theory since, due primarily to the interaction of the dipole moments of the molecules, the molecules do not have to undergo a kinetic theory type collision in order to perturb the molecular energy levels.

A typical value for the line width parameter is 20 Mc/mm Hg. For a pressure of 0.025 mm Hg, which is typical for this experiment, the pressure broadening line width is about 1 Mc/sec. This is much larger than the other sources of broadening discussed.

A considerable amount of theoretical work has been done on the finer details of pressure broadening (63), but the experimental work is rather sparse. Since the spectra in this investigation are so complex,

they do not provide a satisfactory tool for the investigation of the finer details, therefore they will not be discussed here. Under the experimental conditions of this investigation, the line shapes obtained by more refined methods do not differ significantly from the Van Vleck-Weisskopf relation. Consequently, equation V-4 above will be used to broaden each component line. The broadened lines will then be added to obtain a qualitative fit of the experimental spectra.

CHAPTER VI

CALCULATED SPECTRA

Chapters III, IV and V contain all the material which is necessary for a calculation of the quadrupole structure of symmetric-top molecules with three identical quadrupolar nuclei.

Without consideration of the Stark effect, a calculation of the line positions and intensities of the quadrupole spectrum can be made using the material of Chapter III. In particular, for the J=1 to J=2, K=1, transition, the matrix elements given by equation III-23 are appropriate. These matrices were calculated and diagonalized, and the line positions and intensities were obtained by means of the computer program in Appendix B. The line spectrum for the J=1 to J=2, K=1 transition contains 194 lines, the strongest of which are shown in Figure 8. The quadrupole coupling constant eqQ and bond angle 'a' characteristic of PCl_3 were used in Figure 8. This particular rotational transition is the most important for analysis of the quadrupole interaction since the quadrupole splitting is greater for the lower rotational transitions. The splitting of the strongest quadrupole components varies approximately as J^{-2} (64). The J=0 to J=1, K=0 and J=1 to J=2, K=0 transitions are not observed at low fields with a Stark modulation spectrometer because they have no first order Stark effect.

Note that the spectrum is dominated by two very strong lines of equal intensity, denoted in Figure 8 by A and B. There is another pair, C and D, of equal intensity which have the same separation as A and B.

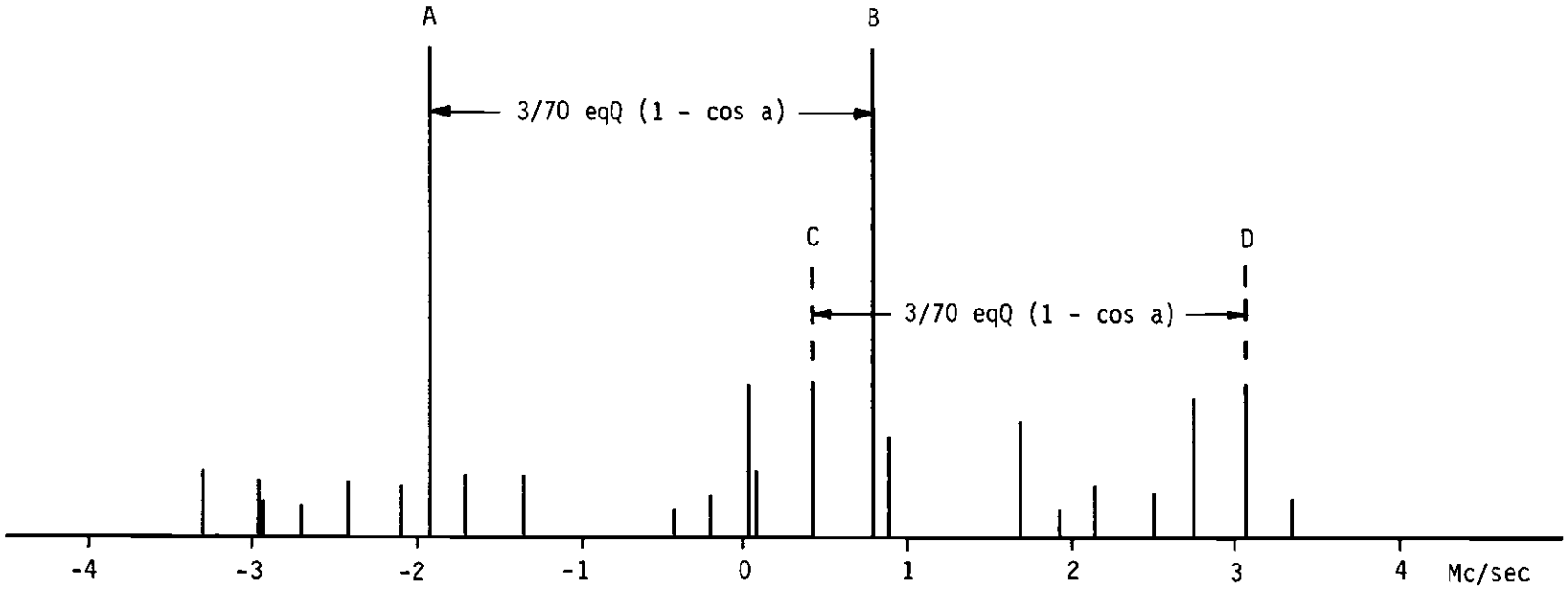

Figure 8. Line Spectrum for PCl_3, J = 1 to J = 2 Transition.

Exact expressions have been worked out for the positions of the strongest lines of the spectrum in terms of the quadrupole coupling constant eqQ and the Cl-X-Cl bond angle 'a' (65). The separations A-B and C-D are given by

$$\Delta\nu = \frac{3}{70} eqQ(1-\cos a). \qquad \text{(VI-1)}$$

Since the bond angle 'a' is known for the molecules of interest, the quadrupole coupling constant eqQ can be determined if the separation of the lines A and B can be reliably measured. The present experiment does not provide a means for separating the quadrupole moment eQ from the second derivative of the potential q.

Depending upon eqQ and the bond angle, the weaker lines of the spectrum, including the secondary pair C and D, are shifted with respect to the primary pair A and B. This fact affects the appearance of the observed spectrum. The line spectrum in Figure 8, calculated with the parameters of PCl_3, shows that line C lies quite close to line B. When broadened by the pressure, these lines overlap, giving a higher absorption at position B than at A. Thus the higher frequency member of the pair A-B appears stronger, as illustrated in Figures 13 and 14. In the case of $CFCl_3$, the pair C-D is shifted out so that little overlap occurs. A group of smaller lines around A cause it to appear higher, as illustrated in Figures 17 and 18. In the calculated spectrum shown in Figure 9a, the components have been broadened according to the Van Vleck-Weisskopf relation, equation V-4, and added by the computer. The value bp = 0.4 in equation V-4 was used for the broadening.

As discussed in Chapter II, the nature of the Stark modulation

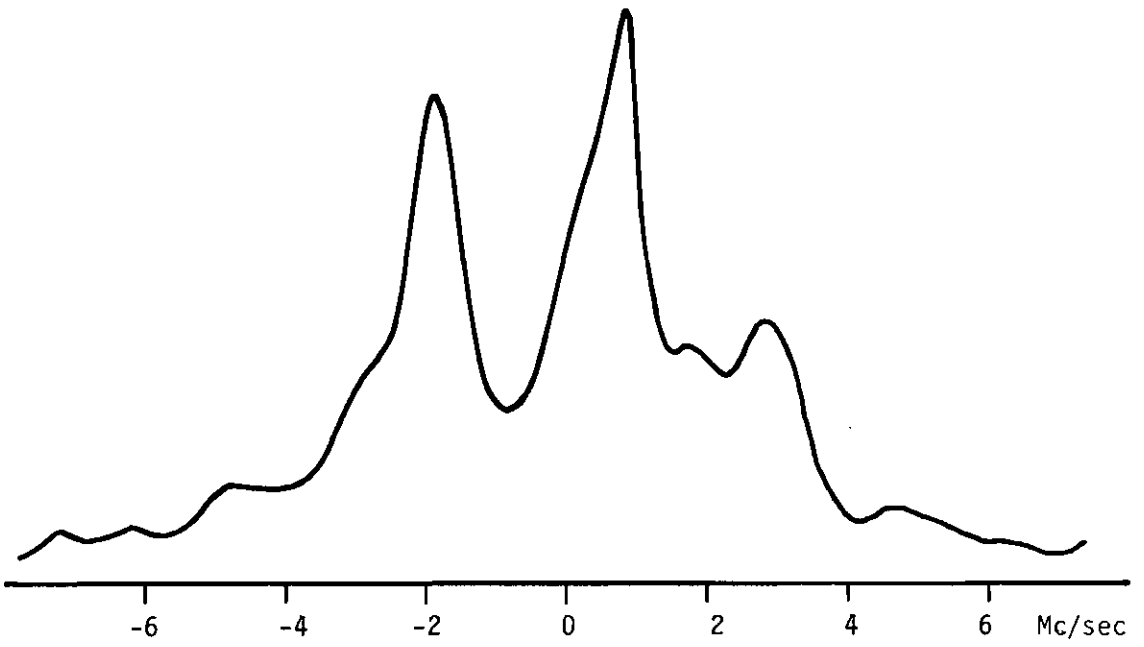

(a) WITHOUT STARK EFFECT

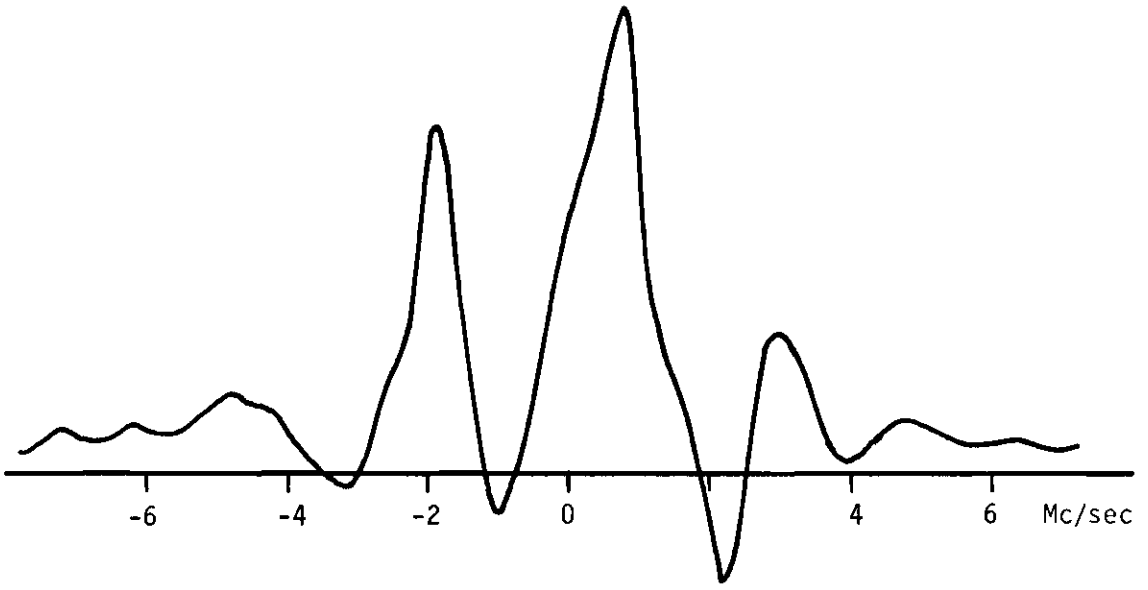

(b) WITH STARK EFFECT

Figure 9. Calculated Quadrupole Spectrum for PCl_3 With and Without Stark Effect.

spectrometer is such that the resultant spectrum is the difference between the unperturbed and the Stark effect perturbed spectra. If these spectra overlap appreciably, the effect of the detection technique on the spectrum must be evaluated. For that reason, the Stark perturbed spectrum for the J=1 to J=2, K=1 transition has been calculated.

A sample calculation using the PCl_3 parameters and several different values for the Stark voltage is shown in Figure 10. The lines were broadened using bp=1 in the Van Vleck-Weisskopf relation, equation V-4.

The general features of the spectrum consist of two groups of lines which move out approximately linearly with the voltage and which are approximately symmetrical about the line center and a third group of lines close to the line center which moves very little with increasing voltage. The group of lines which are concentrated around the line center cannot be removed by increasing the Stark voltage and thus must be analyzed carefully to determine whether or not they will appreciably alter the measured spacing between lines A and B of Figure 8. This point will be discussed in more detail later.

If there were no quadrupole splitting, the Stark effect for the J=1 to J=2, K=1 transition would be expressed by equation IV-13. It would be composed of two symmetrically placed components which move out from the center line (i.e., the unperturbed transition frequency 2(J+1)B) according to the relation $\Delta\nu = \mu E/3$. For large electric fields E, the Stark effect of the symmetric-top molecule with quadrupole splitting would be expected to approach this behaviour. That is, the centers of the two groups of lines would be expected to move out according to

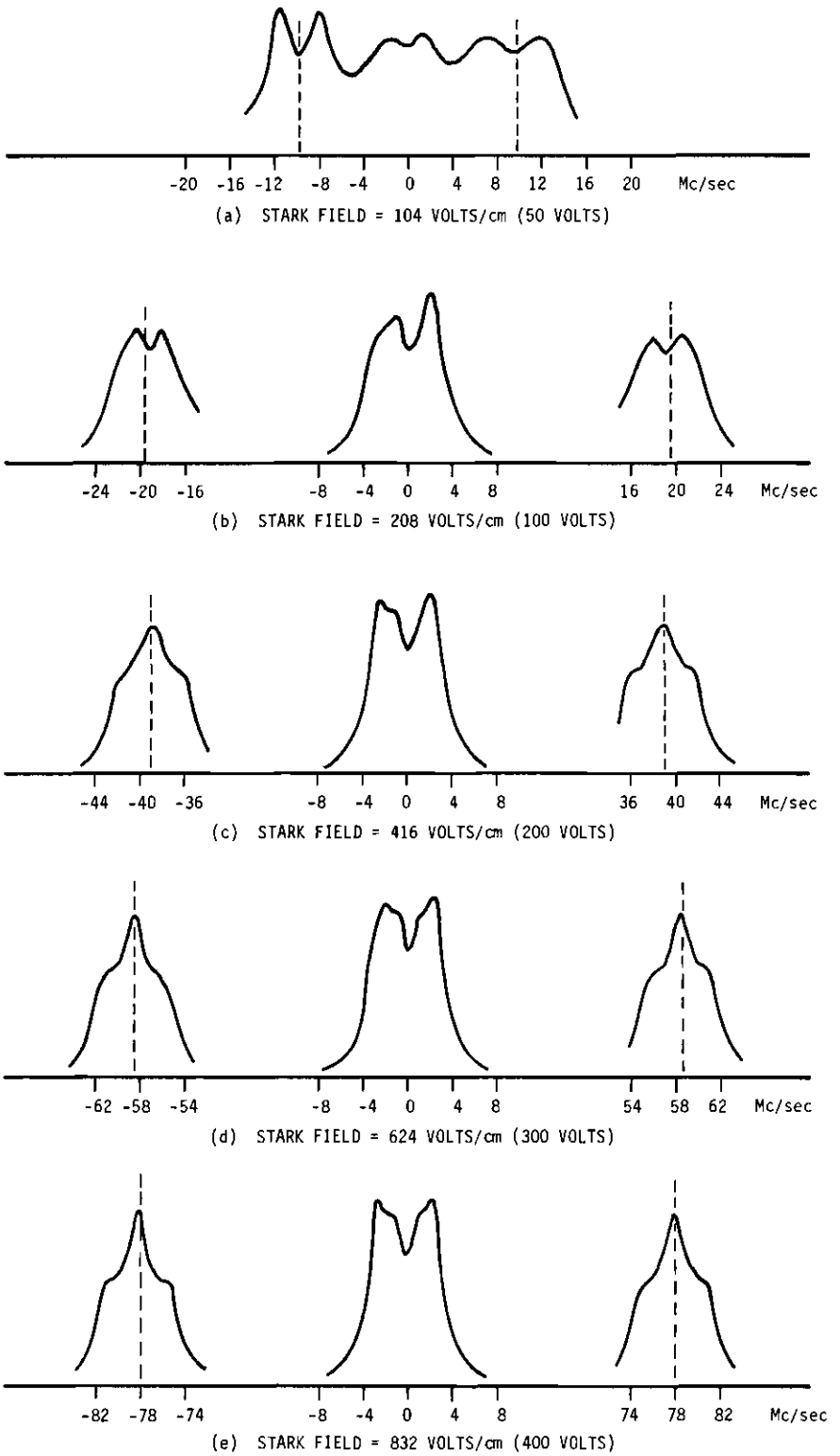

Figure 10. Calculated Stark Spectrum for the J = 1 to J = 2 Transition in PCl_3.

the relation $\Delta\nu = \mu E/3$. When the two groups of lines mentioned above are pressure broadened and added together, they form a 'line' or Stark lobe which moves out in a linear fashion with the Stark voltage, or electric field. The symmetric-top Stark displacement $\mu E/3$ is marked by a dashed line on the spectra in Figure 10. As can be seen, for $\mu E > 100$ Mc/sec (voltage > 200 volts in the figure) the line center or peak of the Stark component is within less than one percent of the position given by $\mu E/3$. Thus for large voltages, the center of the Stark component gives a measurement of the dipole moment of the molecule if the electric field E is known.

If one attempted to decide a priori what field strength would be required to obtain a good measurement of μ, the most likely criterion would be $\mu E/3 \gg W_{Qmax}$, where W_Q is the splitting of one of the quadrupole interaction components. This would be the condition such that the quadrupole interaction could be treated as a perturbation on the Stark effect. For the PCl_3 parameters, W_{Qmax} is approximately 28 Mc/sec. To make $\mu E/3$ an order of magnitude larger than this would require voltages in excess of 1400 volts on the Stark electrode. The main contributions to the quadrupole interaction in PCl_3 occur for W_Q less than 5 Mc/sec. Even in this case it is not clear from a superficial examination of the theory that a dipole moment measurement of PCl_3 could be made with voltages as low as 200 volts. However, the detailed calculation illustrated in Figure 10 indicates that measurements can be made with such low voltages.

To show how some of the individual components of the complex Stark spectrum behave, the displacements of some of the strong components of

the spectrum as a function of the field strength are plotted in Figure 11.

The actual calculation of the Stark perturbed spectrum involves an extremely large number of computations. The 194 lines of the J=1 to J=2, K=1 spectrum are further split by the Stark effect, which removes the degeneracy in M_F. The J=1 to J=2 Stark split spectrum is composed of 1532 lines. Only about 40 to 70 of these lines contribute more than 0.5 percent each of the total absorption. The number depends upon the magnitude of the Stark Hamiltonian μE. As the field strength is increased, this relatively small number of important components contributes an increasing fraction of the total absorption. For μE greater than 150 Mc/sec, this set of strong lines contributes more than 90 percent of the total absorption. For example, in the case of PCl_3 with μ = 0.56 debye, if μE = 176 Mc/sec corresponding to a 300 volt Stark voltage, 62 strong lines contribute more than 0.5 percent each and the sum of the absorptions for these lines is 95 percent of the total absorption. The calculation for 50 volts on the Stark electrode yields 49 strong lines which contribute 43 percent of the total intensity, i.e., the absorption is more diffusely spread among the large number of other components. This leads to a more or less uniform absorption near the center line, as illustrated in Figure 10 for 50 volts.

To get the resultant spectrum for comparison with the experiment, the Stark perturbed spectrum (illustrated in Figure 10) is subtracted from the quadrupole spectrum (Figure 9a) to yield a resultant spectrum like that in Figure 9b. Other examples are Figures 13 and 17 which are compared to the experiment in Figures 14 and 18 respectively. In

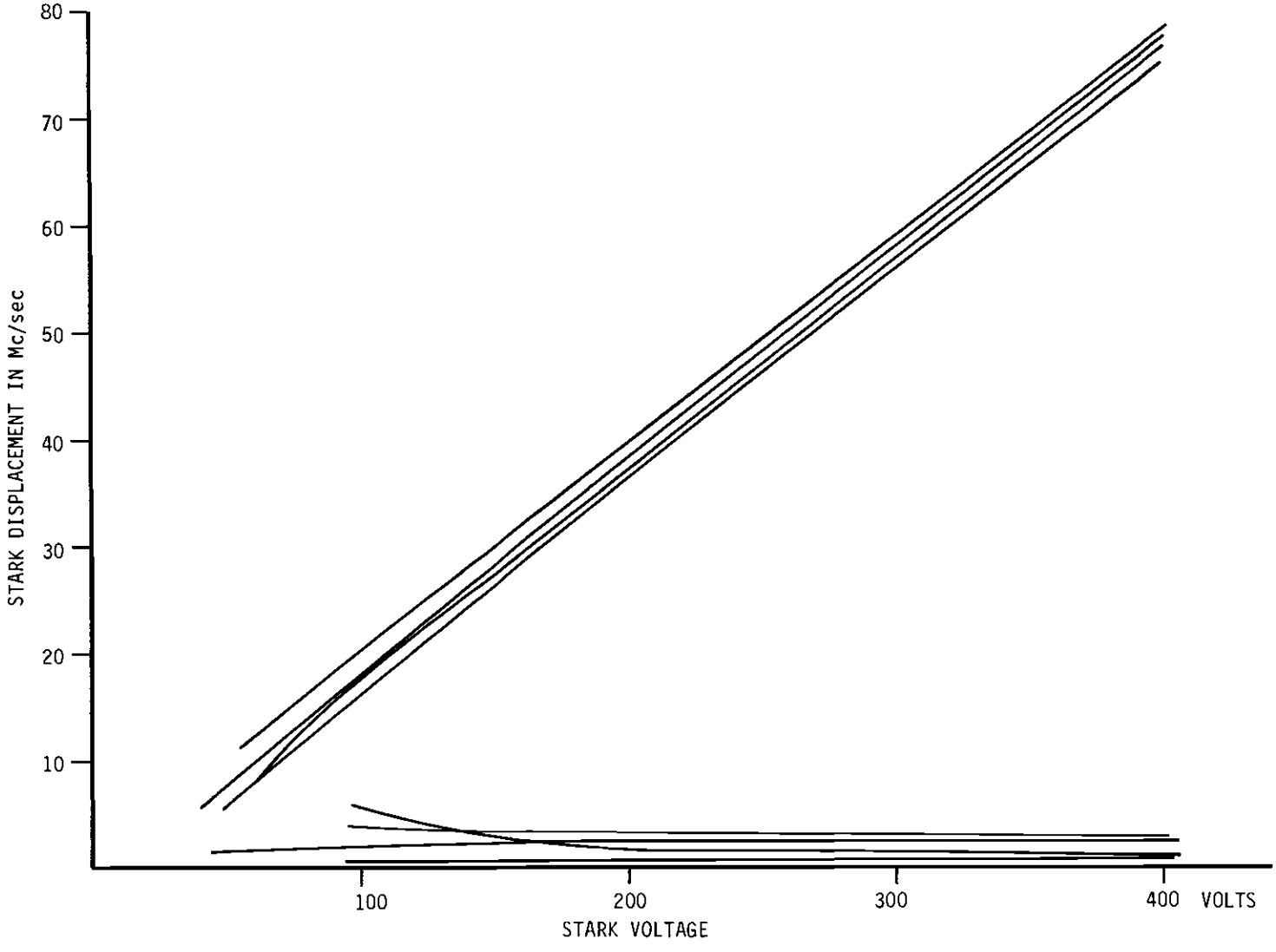

Figure 11. Calculated Stark Displacement for Selected Lines in PCl_3, J = 1 to J = 2 Transition.

subtracting the two spectra, it was assumed in accordance with the spectral stability principle (66) that the total microwave absorption is the same when the quadrupole interaction alone is present as when the system is further perturbed by the Stark field. It was further assumed that the interactions leading to the pressure broadening are independent of the Stark field, i.e., the same value for the product bp is used in equation V-4 for pressure broadening the spectrum with the Stark field on as with it off.

It is clear from Figure 9 that the Stark effect does change the qualitative appearance of the spectrum. The most important question is whether or not the Stark effect changes the measured separation of the two main peaks A and B (Figure 8) which is used to evaluate the quadrupole coupling constant eqQ. Obviously, pressure broadening can also affect the separation. A calculation of the peak separation as a function of pressure for different voltages is plotted in Figure 12. The calculation was made with the parameters of $POCl_3$, but the results are essentially the same for PCl_3. Note that for μE = 63 Mc/sec (corresponding to 25 volts on the Stark electrode for $POCl_3$) the separation of the two main peaks is essentially independent of the pressure up to bp=1. However, for μE = 260 Mc/sec (Stark voltage = 100 volts in $POCl_3$) the Stark effect can decrease the separation up to five percent at pressures where pressure broadening alone would have little effect. Therefore, to obtain reliable measurements of the peak separation it is desirable to utilize not only low pressures but also low Stark voltages. At a given pressure, the separation of the peaks would be expected to decrease with increasing Stark voltage if high enough Stark voltages were used.

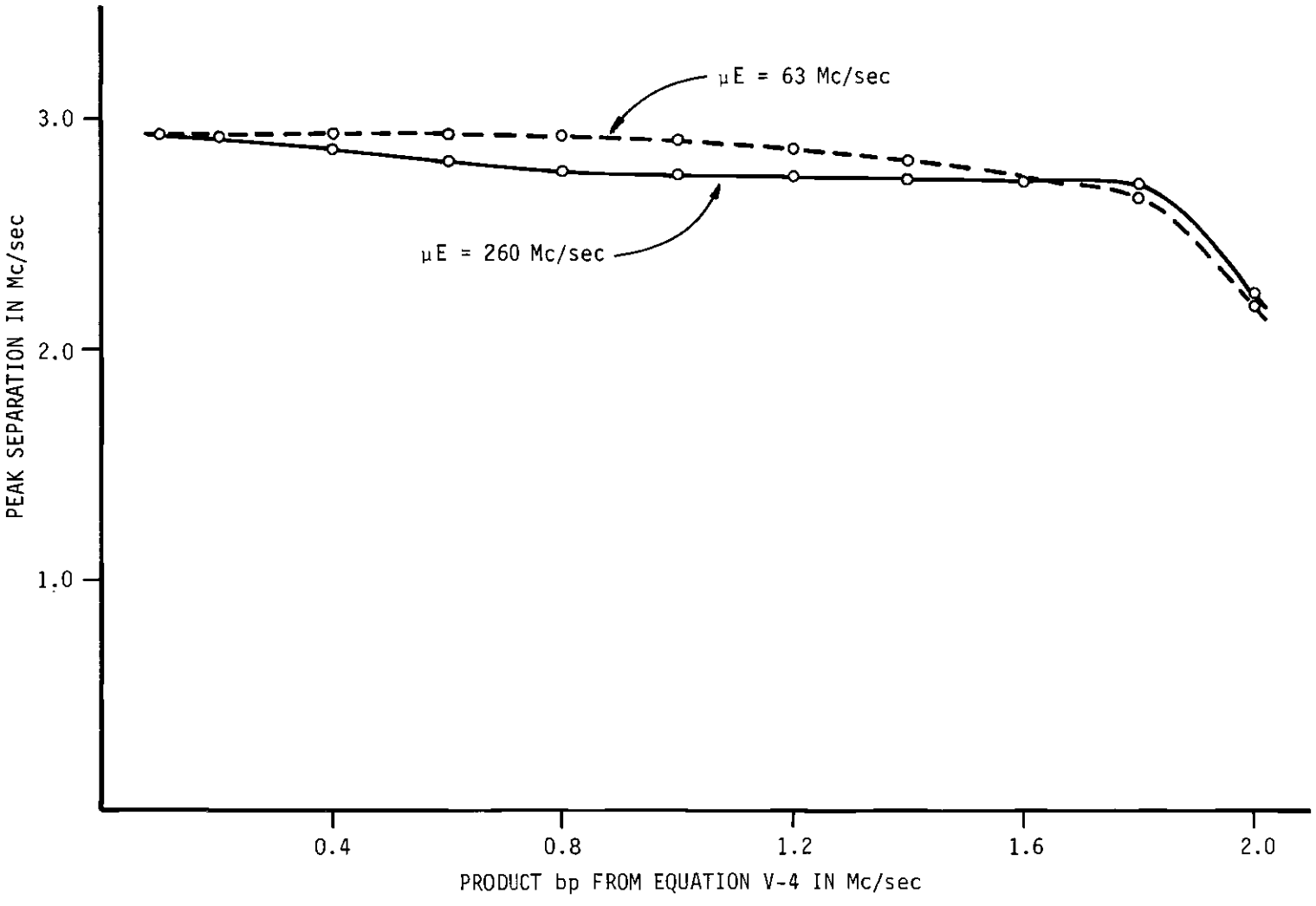

Figure 12. Calculated Peak Separation as a Function of Pressure for Different Stark Fields.

To summarize the results of the calculations, it appears that for $bp \leq 1$ and $\mu E \leq 60$ Mc/sec, a reliable measurement of the separation of lines A and B and thus a reliable measurement of the quadrupole coupling constant eqQ can be made. This value for μE corresponds to Stark voltages of 25 volts and 125 volts for $POCl_3$ and PCl_3 respectively. Errors in the separation should be two percent or less for μE up to 260 Mc/sec if $bp \leq 0.4$ Mc/sec. Furthermore, the value of the dipole moment should be obtainable by measurement of the Stark displacement for $\mu E > 100$ Mc/sec.

CHAPTER VII

EXPERIMENTAL SPECTRA

The strongest lines in the J=1 to J=2 rotational transition are denoted A and B in Figure 8, and their separation is given by

$$\Delta\nu = \frac{3}{70} eqQ \left[1 - \cos(a)\right].$$

The bond angles a for PCl_3 and $POCl_3$ are listed in Table 1. Measurements of the separation of lines A and B will be used to calculate the quadrupole coupling constants eqQ.

Before discussing the actual measurements of the line separations, however, the sources of uncertainty in these measurements will be considered in detail. The most important sources of uncertainty are:

1. Klystron instability
2. Pressure broadening
3. Stark effect
4. Excited vibrational state lines
5. Frequency measurement errors.

The klystron stabilization technique discussed in Chapter II should effectively eliminate klystron instability as an appreciable source of uncertainty.

Pressure broadening is a major factor and is usually the limiting factor in the resolution of hyperfine structure. If the pressure is low enough to resolve the hyperfine components, the signal strength is also

very low and poor signal-to-noise ratios tend to destroy the resolution. The calculation illustrated in Figure 12 indicates that below bp = 0.4, the systematic error due to the Stark effect will be less than two percent, even with μE as high as 260 Mc/sec. With the use of low Stark voltages, the systematic error can be essentially eliminated. However, the pressure at which the error becomes negligible cannot be directly calculated because the product bp must be determined by comparison with the experiment. This comparison is qualitative in nature and cannot give an accurate value for bp. A further difficulty in determining b is the fact that the reliability of the pressure measurements is not known. Nevertheless, the calculation in Figure 12 is useful, because it indicates that for pressures below a given value the separation no longer appreciably depends upon the pressure. Below this value, a reliable measurement of the separation of peaks A and B can be made. The experimental procedure for minimizing the uncertainty due to pressure broadening is to lower the pressure until the separation no longer depends on the pressure, i.e., no longer changes as the pressure is lowered. This procedure was used in data collection. Data was taken for several low values of the field strength to make sure that the separation was not being affected by the Stark effect.

The Boltzmann factors listed in Table 2 indicate that some of the first excited vibrational states of PCl_3 and $POCl_3$ will be appreciably populated, even at -80 degrees Centigrade. The line center of a transition corresponding to an excited vibrational state is given by equation I-3. If the coefficient α for a given vibrational mode is sufficiently small, the lines for the excited state could lie close to those for the

ground state and could cause a shift in one of the lines A and B. This possibility will be discussed along with the discussion of the details of the spectra of PCl_3 and $POCl_3$.

The frequency measurement errors inherent in the instrumentation were discussed in Chapter II. The largest source of error is the uncertainty in locating the peak positions of the lines. This error is reflected in the probable error limits on the data given below and will be discussed in connection with this data.

Quadrupole Spectrum of Phosphorous Trichloride

As mentioned in Chapter II, the vapor pressure of PCl_3 at -80 degrees Centigrade was calculated to be 60 microns Hg. The Pirani gauge read in the range 50-60 microns Hg at equilibrium with dry ice on the waveguide so apparently the calibration of the Pirani gauge for PCl_3 does not differ drastically from that for air in this pressure range. Data was taken for pressures less than 50 microns Hg. Pumping on the cell to lower its pressure did not appreciably alter the measured separation of the two main lines so it was assumed that pressure broadening was not shifting the peak positions significantly.

A recorder trace of the J=1 to J=2, K=1 transition is shown in Figure 14. The pressure is about 50 microns Hg according to the Pirani gauge. A calculated spectrum where the line width parameter b has been adjusted for the best fit is shown in Figure 13. The best fit was obtained for a line width parameter b = 12 Mc/mm Hg. It is difficult to assign a probable error to this parameter since the fit is qualitative and the pressure value is questionable. For the line separation measurements, the spectrum shown in Figure 14 was spread out by using a slower

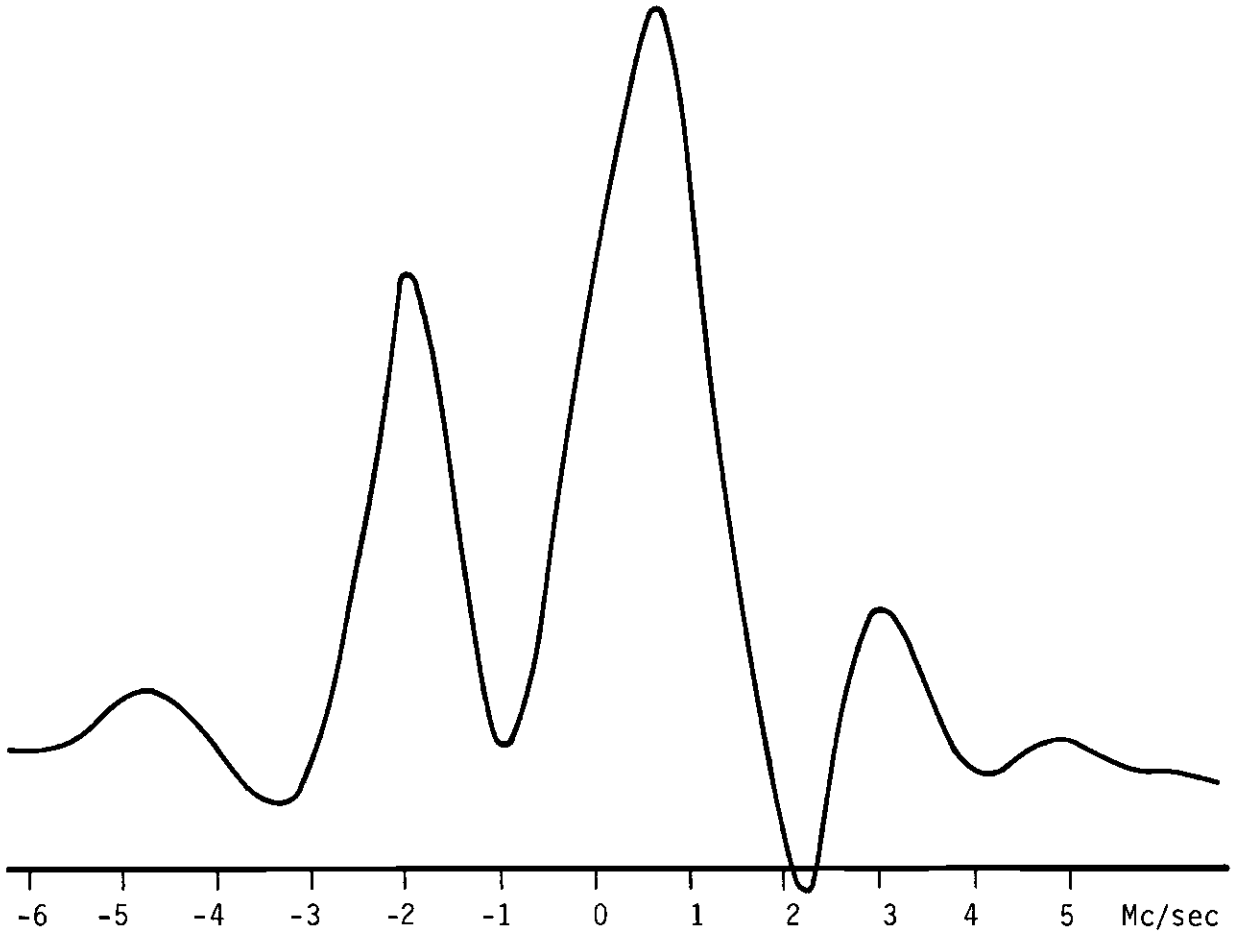

Figure 13. Calculated J = 1 to J = 2 Transition for PCl_3.

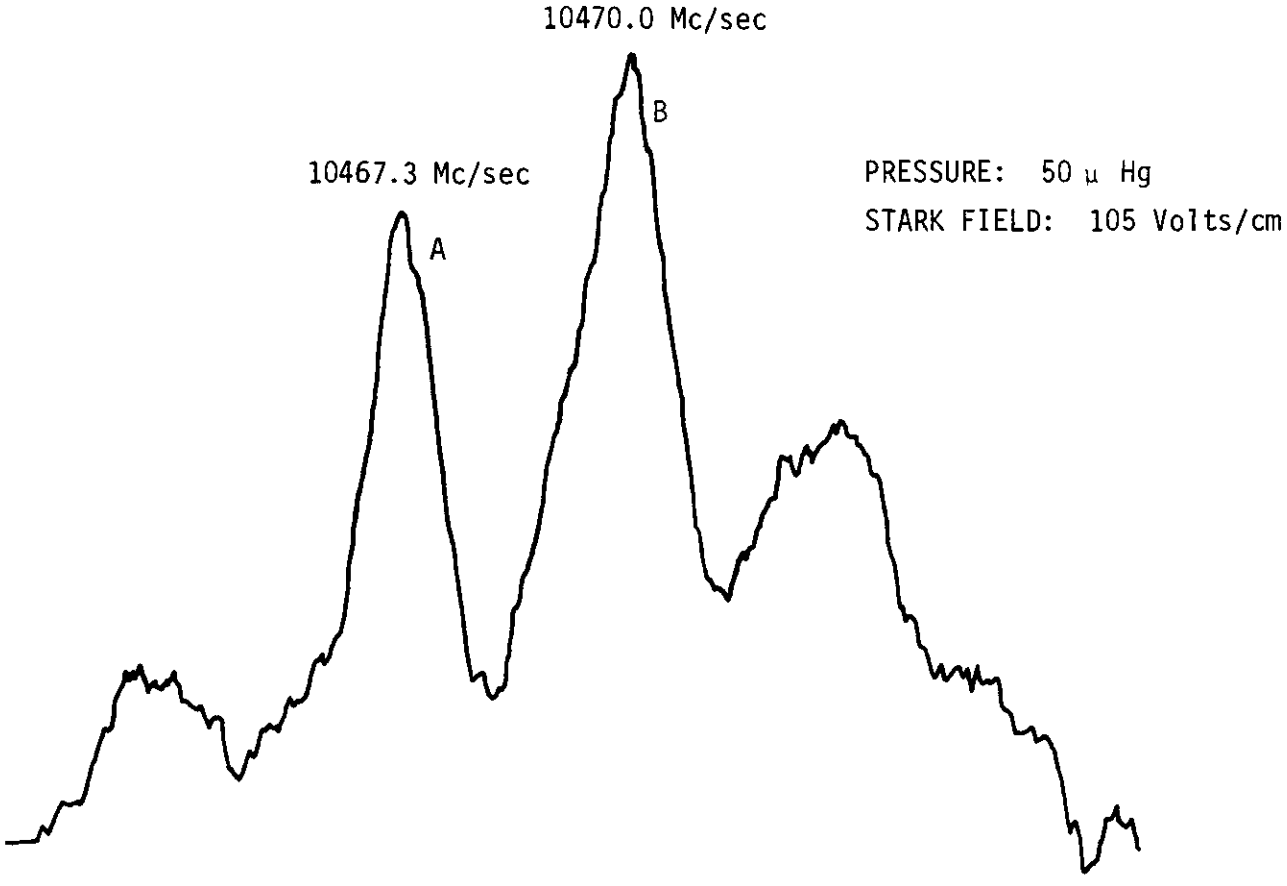

Figure 14. The J = 1 to J = 2 Transition in PCl_3.

tuning rate, and a lower pressure was obtained by pumping continuously on the waveguide.

The relative intensities of the peaks varied somewhat with the microwave power level. Increasing the power tended to lower the peaks. An optimum was obtained by attenuating the microwave power until the relative intensities of the peaks no longer changed with increasing attenuation.

A large number of measurements were made of the separation between lines A and B in Figure 14. The measurements for Stark voltages of 100 volts and less ($\mu E < 60$ Mc/sec) yielded for the separation

$$\Delta\nu_{AB} = 2.69 \pm 0.05 \text{ Mc/sec.}$$

For Stark voltages of 200 volts and higher, the separation decreased slightly as would be expected from the calculation illustrated in Figure 12. At 200 volts the separation was about 2.55 Mc/sec. A. Wolf (14) noted this effect in $CFCl_3$ and $CHCl_3$ and used low Stark voltages in his measurements.

The standard deviation of the average value of a large number of measurements is given by (67)

$$s^2 = \left(\sum_{n=1}^{k} x_n^2 - k\bar{x}^2\right)/(k^2 - k)$$

where $\bar{x}$ is the average of the measurements of x, and k is the number of measurements. This expression applies to cases where the errors in measurement are random. The standard deviation in the case of the separation

above is 0.01 Mc/sec, but the error limits were increased to 0.05 Mc/sec to allow for possible systematic error due to the Stark effect or other sources. The standard deviations were calculated for all the experimental data in this chapter and will be quoted, but more conservative estimates of the probable error will be made in each case.

The above separation measurement leads to a quadrupole coupling constant

$$eqQ = -53.3 \pm 1.0 \text{ Mc/sec.}$$

Measurement of the peak positions yielded the following:

$$\nu_A = 10{,}467.35 \pm .04 \text{ Mc/sec}$$

$$\nu_B = 10{,}470.01 \pm .04 \text{ Mc/sec.}$$

Comparison of these frequencies to the calculated spectrum gives

$$\nu = 10{,}469.26 \pm .08 \text{ Mc/sec}$$

for the line center of the J=1 to J=2 transition. This gives a rotational constant for PCl_3 with the value B = 2,617.31 ± 0.02 Mc/sec compared to the value B = 2,617.1 ± .1 Mc/sec obtained by Kisliuk and Townes (15) from the J=4 to J=5 transition. The standard deviations for the frequencies of the lines A and B were .002 Mc/sec and .01 Mc/sec respectively.

No attempt was made to assign frequencies to the peak labeled D in Figure 14 and the peak to the low frequency side of the peaks A and B. Their positions were not always reproducible, and the calculated spectrum indicated that they were composed of several small lines.

As pointed out in Chapter I, the two most highly populated excited vibrational states should give lines centered 7.6 Mc/sec on each side of the ground state line center. No evidence of such excited state lines was observed. Even if present, such lines would not be expected to alter the peak positions A and B because of their distance from the center line of the ground state transition.

Quadrupole Spectrum of Phosphoryl Chloride

Phosphoryl chloride, $POCl_3$, proved to be more difficult to analyze than PCl_3. The fact that it is a solid at dry ice temperature made necessary the experimental procedure described in Chapter II. The line width was greater than that of PCl_3, making lower pressures a necessity for $POCl_3$. Below 25 microns Hg as indicated on the Pirani gauge, the line separation did not appear to depend on the pressure. To provide further assurance of reliability, the data was taken at pressures below 15 microns Hg.

A reorder trace of the J=1 to J=2 transition is shown in Figure 16. The Pirani gauge pressure is 9 microns Hg in that case. The calculated fit of the spectrum (Figure 15) was made using a line width parameter b = 34 Mc/mm Hg. It should be repeated that the line width parameter has a large margin of error. The spectrum of $POCl_3$ was not as reproducible in appearance as that of PCl_3, although the line separation was reproducible. The relative intensities of the peaks did not seem to be so dependent upon the microwave power level as in the case of PCl_3.

A large number of measurements of the separation of lines A and B were made. Measurements made at several voltages did not yield any dependence of the separation upon the Stark field. The measurements

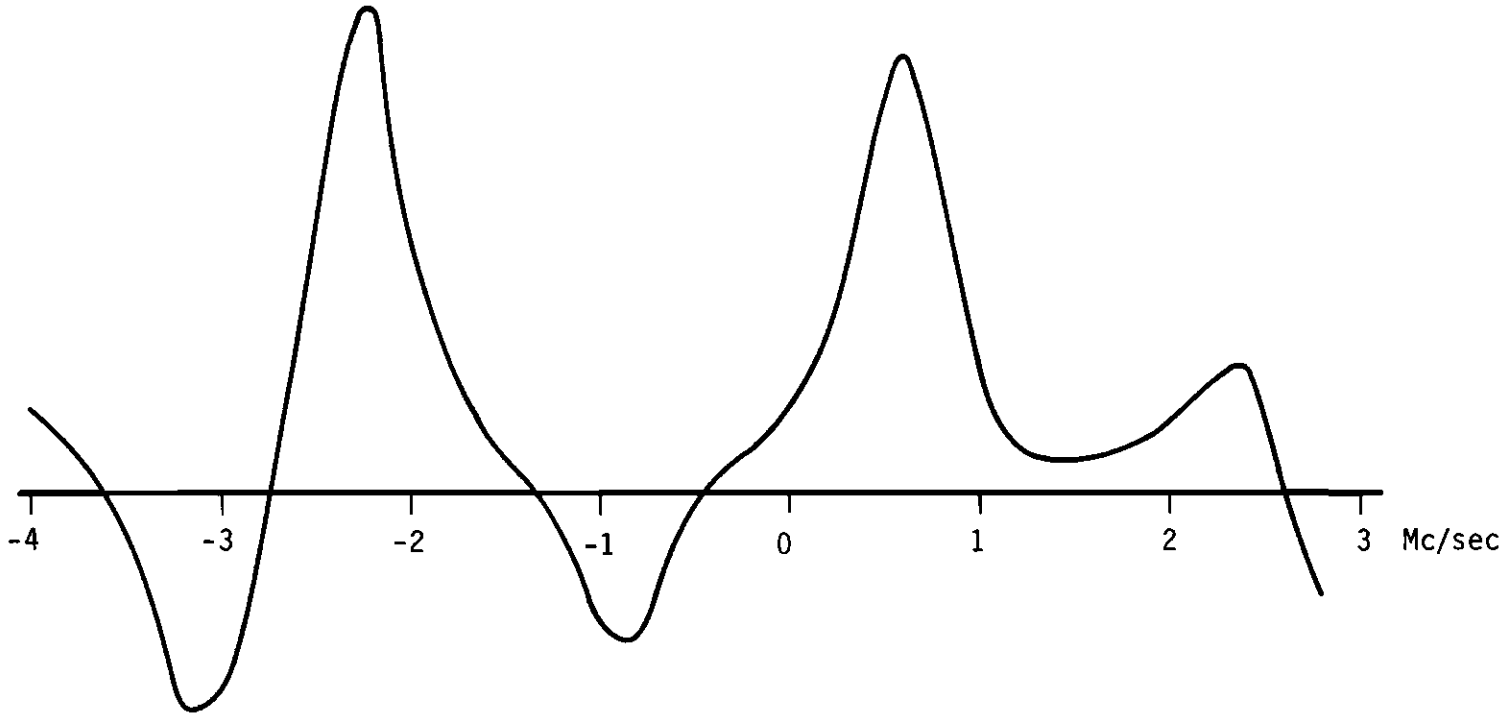

Figure 15. Calculated J = 1 to J = 2 Transition for $POCl_3$.

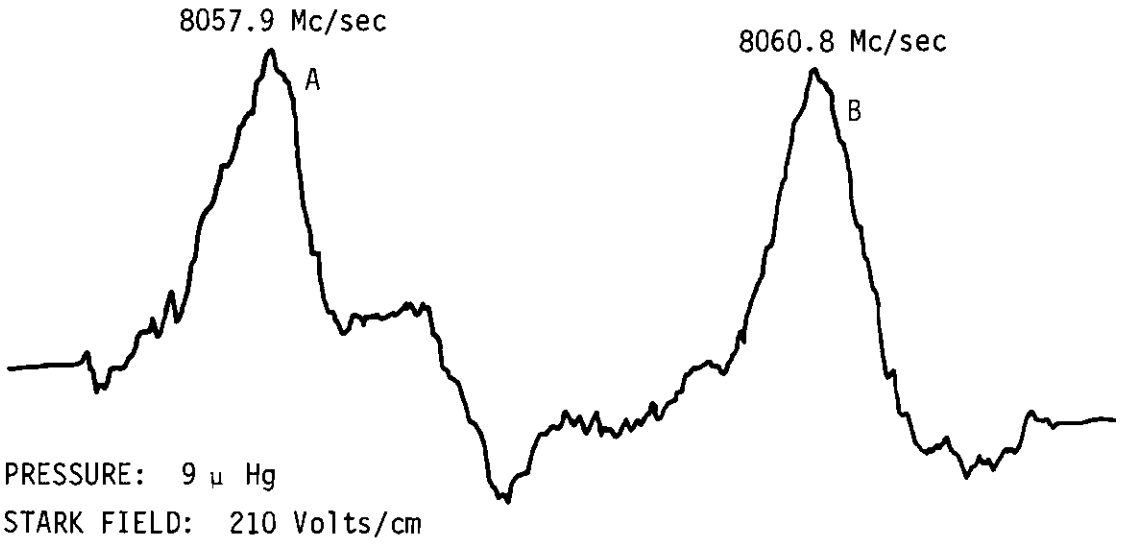

Figure 16. The J = 1 to J = 2 Transition in $POCl_3$.

were made at Stark voltages $\leq$ 100 volts and with pressures low enough that the systematic error due to the Stark effect should be less than one percent. The measured separation of the two strongest lines was

$$\Delta\nu_{AB} = 2.93 \pm .05 \text{ Mc/sec.}$$

This gives a quadrupole coupling constant

$$eqQ = -55.4 \pm 1.2 \text{ Mc/sec.}$$

The probable error in eqQ includes that due to the uncertainty in the bond angle 'a'. The probable error due to the separation measurement alone is 0.9 Mc/sec, including a margin for possible systematic error due to the Stark effect. Measurement of the peak positions A and B yielded:

$$\nu_A = 8{,}057.90 \pm 0.05 \text{ Mc/sec}$$

$$\nu_B = 8{,}060.83 \pm 0.05 \text{ Mc/sec.}$$

Comparison with the calculated spectrum gives a line center frequency

$$\nu = 8{,}060.2 \pm 0.08 \text{ Mc/sec}$$

for the J=1 to J=2 transition in $POCl_3$. The corresponding rotational constant is B = 2,015.04 ± 0.03 Mc/sec compared to the value B = 2,015.20 ± 0.05 Mc/sec obtained by Williams *et al.* (18). The standard deviations in $\Delta\nu_{AB}$, ν_B were 0.01, 0.01 and 0.005 Mc/sec respectively.

Excited vibrational state lines were observed in the J=3→4 and J=4→5 transitions but no satisfactory measurements of their frequencies

were obtained. At temperatures near room temperature, there were some features in the J=1 to J=2 transition which were attributable to excited state transitions, but at the temperatures at which data was taken these features were very small and apparently did not shift the peak positions.

The quadrupole coupling constants for $POCl_3$ and PCl_3 are listed in Table 3. Also listed are those values for $CFCl_3$ and $CHCl_3$ obtained by Wolf (14). The solid state values of Livingston (35) (9) are also listed for comparison. Only the magnitudes of eqQ are listed for the solid state measurements, since the sign is not determined by the pure quadrupole resonance experiment. The quadrupole coupling constant for $POCl_3$, eqQ = -55.4 Mc/sec, is lower than the solid state value while in the other molecules the constant eqQ is above the solid state value. The difference between the measured value and the value which would have been expected on the basis of the other eqQ values is thought to be too large to be attributable to systematic error due to the Stark effect or other factors in the experiment.

To illustrate how different values of eqQ and the bond angle can affect the spectrum, the calculated and experimental results for the J=1 to J=2,K=1 transition in $CFCl_3$ are shown in Figures 17 and 18 respectively. In this case the lines labeled C and D in Figure 8, along with other weak lines, are separated out from line B. The resultant spectrum shows line A higher in intensity than line B, in contrast to PCl_3 and $POCl_3$.

The spectrum for $CFCl_3$ was obtained with the improved klystron stabilization and tuning technique developed for the work on PCl_3 and $POCl_3$. A better signal-to-noise ratio than that obtained by A. A. Wolf

Table 3. Comparison of Microwave and Solid State Measurements of the Quadrupole Coupling Constant eqQ

Molecule	eqQ (Mc/sec)	
	Solid State	Microwave
PCl_3	52.40[a]	-53.3 ± 1.0[c]
$POCl_3$	57.97[a]	-55.4 ± 1.2[c]
$CFCl_3$	79.63[b]	-79.9 ± 0.6[d]
$CHCl_3$	76.98[b]	-77.9 ± 0.5[d]

[a]Reference 35.

[b]Reference 9.

[c]Present investigation.

[d]Reference 14.

(68) was provided by this technique, but no significant improvement in the line separation measurement was obtained. Wolf's value for the quadrupole coupling constant, eqQ = -79.9 Mc/sec, and the bond angle a = 111 degrees were used for the calculated spectrum in Figure 17. The best fit was obtained with a line width parameter b = 10 Mc/mm Hg. Wolf did not consider the possibility of Stark components such as those shown in Figure 10 which cannot be removed by increasing the voltage. However, calculations have shown that no appreciable error should result at the voltages and pressures at which he worked.

Dipole Moment Measurements

From the discussion of Chapter VI and the calculations illustrated in Figures 10 and 11 it appears that a measurement of the dipole moment can be obtained from analysis of the Stark effect in the J=1 to J=2, K=1 transition. The condition for a good measurement of the dipole moment from Chapter VI was $\mu E > 100$ Mc/sec. The Stark displacement of the center of the Stark 'lobe', composed of several lines, is given by equation IV-13. For the J=1 to J=2, K=1 transition the relevant quantum numbers are J=1, $J_J = \pm 1$ and $K = \pm 1$, giving a stark displacement $\pm \mu E/3$.

For the J=2 to J=3 transition there are six Stark components in the absence of the quadrupole interaction. Their positions are given in Table 4. The relative intensities in Table 4 are calculated from the relation (69)

$$I = (J + 1)^2 - M_J^2$$

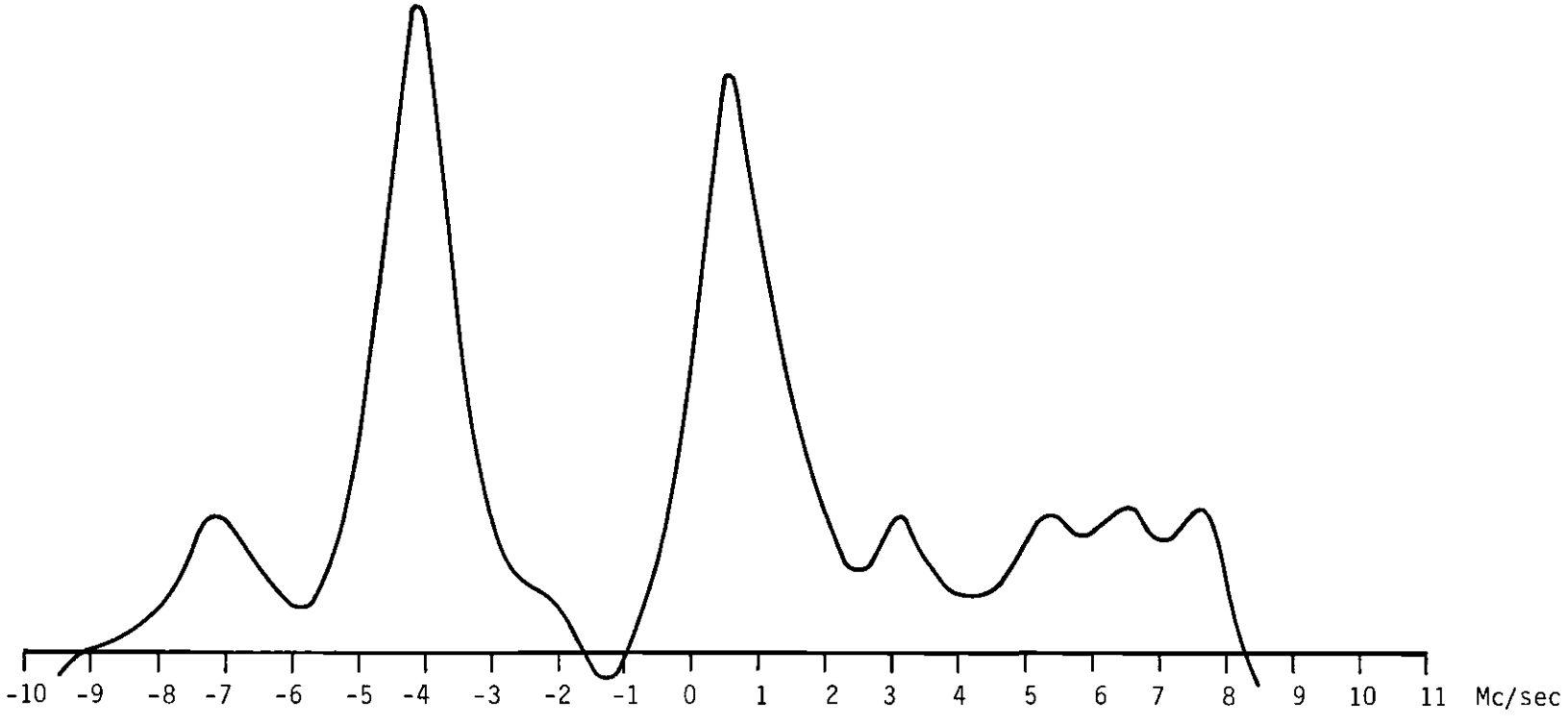

Figure 17. Calculated J = 1 to J = 2 Transition for $CFCl_3$.

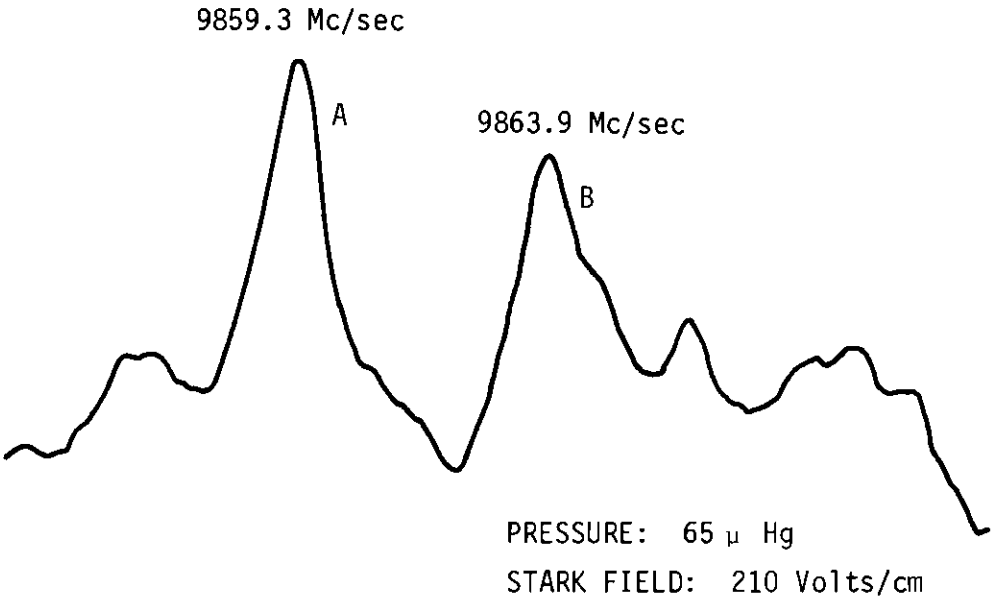

Figure 18. The J = 1 to J = 2 Transition in $CFCl_3$.

Table 4. Displacements and Relative Intensities of Stark Lines in the J=2 to J=3 Spectrum of a Symmetric-top Molecule

$M_J K$	Displacement	Relative Intensity
±1	$\frac{\mu E}{12}$	16
±2	$\frac{\mu E}{6}$	13
±4	$\frac{\mu E}{3}$	5

for transitions J to J+1, $\Delta M_J = 0$. No calculation of the Stark effect with quadrupole interaction was attempted for the J=2 to J=3 transition. However, since the quadrupole splitting is smaller for this transition, it seems reasonable that the same approximations would hold for the Stark displacement is the same as for the J=1 to J=2 transition.

The Stark displacement as a function of field strength for the J=1 to J=2 transition of $POCl_3$ was measured and is shown in Figure 19. The displacements were measured for components both above and below the line center frequency. The Stark displacements for the J=2 to J=3 transition are shown in Figure 20. The dipole moment was measured by varying the slope of the lines for a least-squares fit of the data. The dipole moments obtained are as follows:

J=1 to J=2, $M_J K = \pm 1$ 2.53 ± 0.04 debye

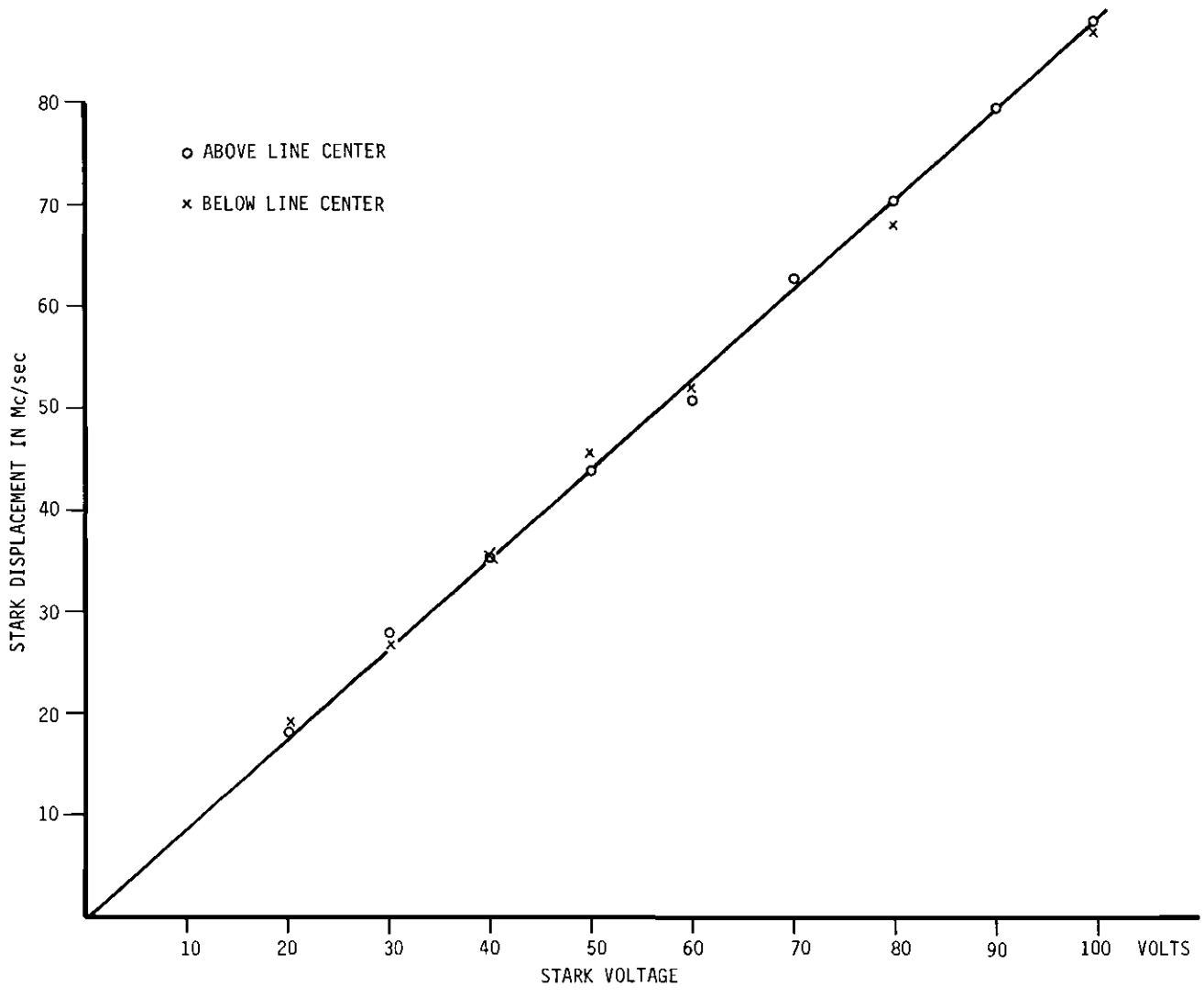

Figure 19. Stark Displacement in the J = 1 to J = 2 Transition of $POCl_3$.

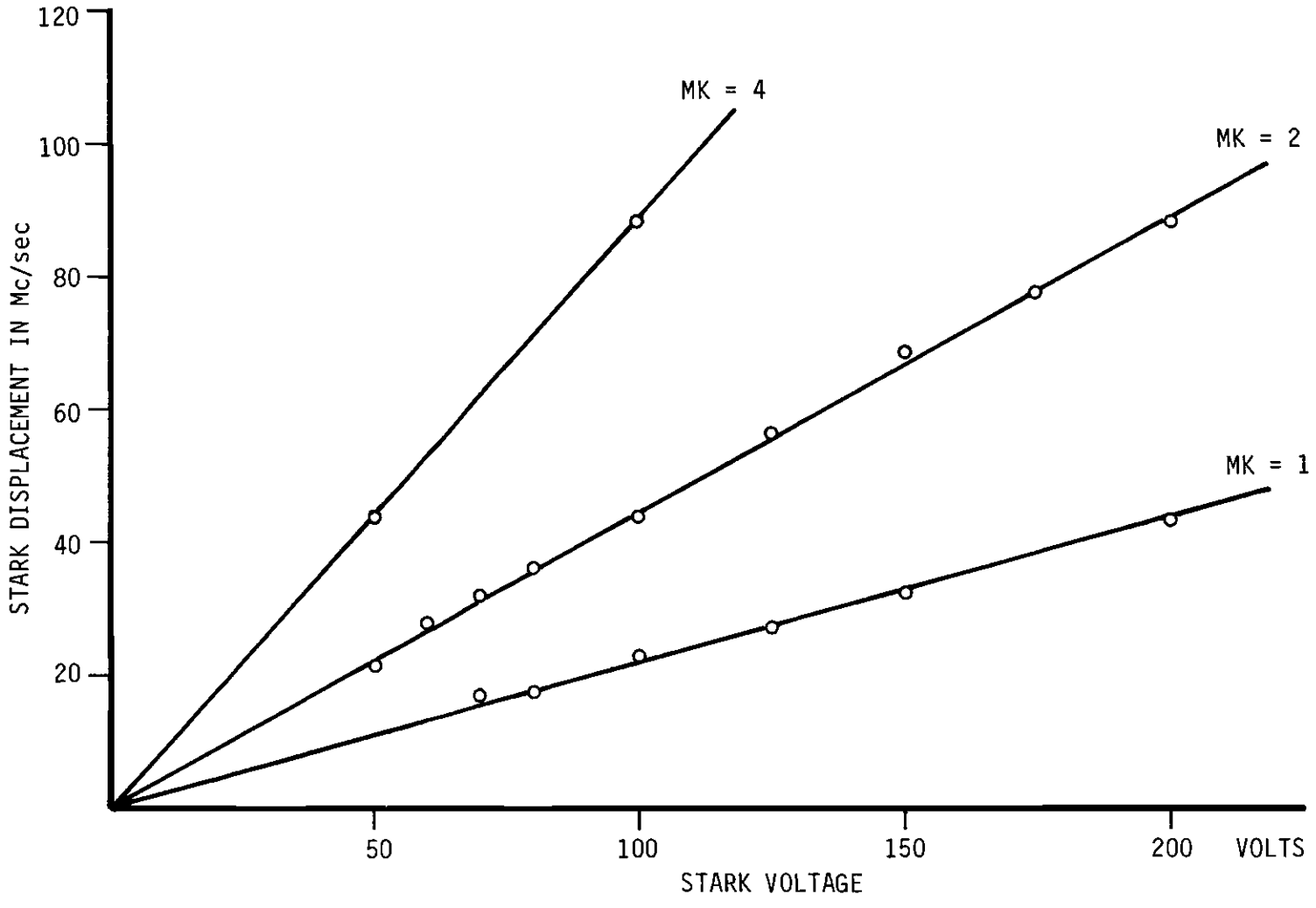

Figure 20. Stark Displacement in the J=2 to J=3 Transition of $POCl_3$.

J=2 to J=3, $M_J K = \pm 1$: 2.53 ± 0.04 debye

J=2 to J=3, $M_J K = \pm 2$: 2.55 ± 0.04 debye.

The estimated probable error limits above are considered to be conservative since the standard deviation of the average dipole moment was in each case less than 0.01 debye. The component for $M_J K = \pm 4$ in the J=2 to J=3 transition was quite weak and could not be measured as well as the others. Two points are plotted on Figure 20 to show its position. The condition suggested to insure that the center of the Stark line gives a good measurement of the dipole moment was $\mu E > 100$ Mc/sec, or a Stark voltage greater than 25 volts for $POCl_3$. The data taken for voltages above this value were in good agreement with the theory.

For higher J transitions, the quadrupole splitting becomes smaller, but the number of Stark components increases so that identification of the components becomes a problem. The Stark components corresponding to the largest values of the product $M_J K$ are the ones which have displacements large enough to be measured, but they have the smallest relative intensity and are therefore difficult to detect. The J=3 to J=4 and J=4 to J=5 transitions in $POCl_3$ were examined, and an attempt was made to measure the Stark displacements for these transitions. The observed Stark lines were very weak, and no satisfactory displacement measurements were obtained. It was concluded that the J=1 to J=2 and J=2 to J=3 transitions provide the most easily analyzed Stark spectra.

Because of poor signal-to-noise ratios, measurements for the Stark displacements of the J=1 to J=2, K=1 transition of PCl_3 were not obtained. The displacements for the J=2 to J=3 transition are shown in Figure 21.

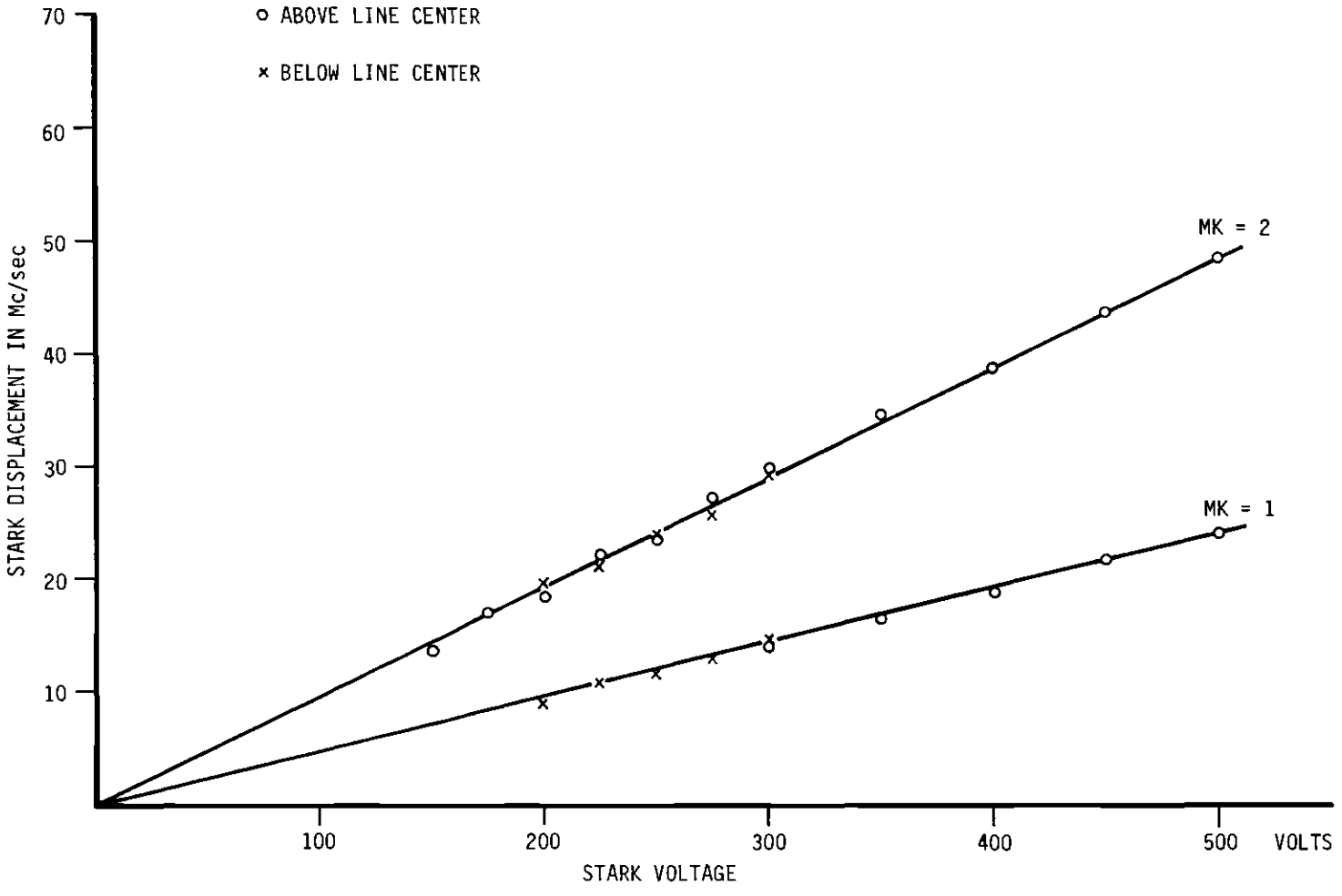

Figure 21. Stark Displacement in the J=2 to J=3 Transition of PCl_3.

The dipole moments obtained from this data were:

$M_J K = \pm 1$: 0.56 ± .01 debye

$M_J K = \pm 2$: 0.56 ± .02 debye.

The Stark components for $M_J K = \pm 4$ were observed but were too weak to be measured satisfactorily.

The Stark lobes are symmetric about the line center for sufficiently high field strengths. By taking the center frequency between the symmetric Stark lobes for several voltages, the J=2 to J=3 transition frequency was measured. The resulting frequency was

$$\nu = 15{,}704.2 \pm 0.4 \text{ Mc/sec}$$

corresponding to a rotational constant B = 2,617.36 ± 0.07 Mc/sec. This is in agreement with the value obtained from analysis of the hyperfine structure in the J=1 to J=2 transition.

Several measurements of the dipole moments of PCl_3 and $POCl_3$ have been made by measurement of the dielectric constant in various solvents. The results of these experiments vary considerably. Some typical results are listed in Table 5 along with the microwave measurements from this investigation.

Table 5. Experimental Dipole Moments for PCl_3 and $POCl_3$

Molecule	Dipole Moment (debye)		State or Solvent
	Microwave[a]	Other[b]	
$POCl_3$	2.54 ± .04		gas
		2.41	benzene
		2.42	benzene
PCl_3	0.56 ± .02		gas
		0.79	gas
		0.70	solid
		0.89	benzene
		0.78	CCl_4

[a]Present investigation.

[b]Obtained from A. L. McClellan, Tables of Experimental Dipole Moments (W. H. Freeman and Company, San Francisco, 1963).

CHAPTER VIII

CONCLUSIONS AND RECOMMENDATIONS

The theory of the quadrupole interaction developed by A. A. Wolf and Svidzinskii and the Stark effect calculations given in this treatment lead to good agreement with the experimental spectra and yield quadrupole coupling constants in general agreement with those obtained from solid state measurements. The work done by Wolf on the molecules $CFCl_3$ and $CHCl_3$ and the present work on PCl_3 and $POCl_3$ provide confirmation of the calculated spectra.

The measured quadrupole coupling constant for PCl_3 is $eqQ = -53.3 \pm 1.0$ Mc/sec compared with the solid state measured value 52.4 Mc/sec. Comparison of the spectrum with the theory yields a rotational constant $B = 2{,}617.31 \pm .02$ Mc/sec compared to the value $B = 2{,}617.1 \pm .1$ Mc/sec obtained by Kisliuk and Townes (15).

In $POCl_3$ the measured value for the quadrupole coupling constant is $eqQ = -55.4 \pm 1.2$ Mc/sec compared to the solid state value 57.9 Mc/sec. Comparison of the spectrum to the theory yields a rotational constant $B = 2{,}015.04 \pm .03$ Mc/sec, compared to the value $2{,}015.20 \pm .05$ Mc/sec obtained at higher-J transitions by Williams et al. (18).

The quadrupole coupling constants, eqQ, measured in the solid and gaseous forms would be expected to differ somewhat because neighboring molecules in the solid can alter q, the second derivative of the potential at the nucleus. The quadrupole coupling constants measured by microwave methods have usually been found to be slightly larger than the solid

state values. PCl_3 is in agreement with this general trend, with a microwave value about two percent higher than the solid state eqQ. $POCl_3$, however, is an exception with a microwave value for eqQ about five percent lower than the solid state value.

The quadrupole coupling constant eqQ is useful in chemical bond theory. Measurement of eqQ for several chlorine compounds gives relative values for the electric field gradient, q, in the compounds. The value of q is one indication of the bond type (i.e., ionic, single covalent, double covalent). The interpretation of the quadrupole coupling constants in terms of chemical bond types has been discussed by Townes and Schawlow (70). Such interpretation is quite complicated and is considered to be outside the scope of this investigation.

Other molecules of this type with three chlorines can now be studied to obtain values for the quadrupole coupling constant. However, the above mentioned molecules were chosen for study because of large eqQ values from the solid state measurements. They were near the limit of resolution with the present instrumentation because of the problem of pressure broadening. Other molecules which may have quadrupole coupling constants large enough to allow microwave measurements are $SiHCl_3$ and $GeHCl_3$. $GeHcl_3$ is particularly interesting since no solid state value for the quadrupole coupling constant has been reported to date.

The measured dipole moments for PCl_3 and $POCl_3$ are 0.56 ± .02 debye and 2.54 ± 0.04 debye respectively. The dipole moments of a number of symmetric-top molecules with three chlorines can be measured by the techniques presented here. The J=1 to J=2 and J=2 to J=3 transitions are appropriate for these measurements. No previous attempts to

measure the dipole moments of such molecules using the low rotational transitions have been published.

Although no reliable measurements of the line width parameter b for the pressure broadening of spectral lines was obtainable from the complex spectra studied here, the techniques employed do offer some promise in the case of less complex spectra. For spectra which are not split by the quadrupole interaction, the stabilization and tuning techniques used in this experiment can give good measurements of the line widths as a function of pressure. If techniques are available to reliably measure the pressure of different molecules in the pressure range 10-100 microns Hg, then presumeably the line width parameter and thus the cross-section for line-broadening interactions can be measured.

APPENDIX A

TABLES REQUIRED IN QUADRUPOLE HYPERFINE STRUCTURE CALCULATION

Table 6. Matrix Representations of the Group of Permutations of Three Objects.

REPRESENTATION	GROUP ELEMENTS					
	(0)	(123)	(132)	(23)	(31)	(12)
$A^{(1)}$	1	1	1	1	1	1
$A^{(2)}$	1	1	1	-1	-1	-1
E	$\begin{pmatrix} 1 & 0 \\ 0 & 1 \end{pmatrix}$	$\begin{pmatrix} -\frac{1}{2} & -\frac{\sqrt{3}}{2} \\ \frac{\sqrt{3}}{2} & -\frac{1}{2} \end{pmatrix}$	$\begin{pmatrix} -\frac{1}{2} & \frac{\sqrt{3}}{2} \\ -\frac{\sqrt{3}}{2} & -\frac{1}{2} \end{pmatrix}$	$\begin{pmatrix} -1 & 0 \\ 0 & 1 \end{pmatrix}$	$\begin{pmatrix} \frac{1}{2} & \frac{\sqrt{3}}{2} \\ \frac{\sqrt{3}}{2} & -\frac{1}{2} \end{pmatrix}$	$\begin{pmatrix} \frac{1}{2} & -\frac{\sqrt{3}}{2} \\ -\frac{\sqrt{3}}{2} & -\frac{1}{2} \end{pmatrix}$

Table 7. Matrix Elements of the Permutation Operators

$$(u(L'I),\ S(123)u)(LI)) = (-1)^{L'}[(2L+1)(2L'+1)]^{1/2} \begin{Bmatrix} 3/2 & 3/2 & L' \\ 3/2 & I & L \end{Bmatrix}$$

$$(u(L'I),\ S(132)u(LI)) = (-1)^{L'-L}(u(L'I),\ S(123)U(LI))$$

$$(u(L'I),\ S(31)u(LI)) = -(-1)^{L'}(u(L'I),\ S(123)u(LI))$$

$$(u(L'I),\ S(12)u(LI)) = -(-1)^{L-2L'}(u(L'I),\ S(123)u(LI))$$

$$(u(L'I),\ S(0)u(LI)) = \delta_{L'L}$$

$$(u(L'I),\ S\ (23)u(LI)) = (-1)^{3-L}\delta_{L'L}$$

The permutation operators defined by Wolf (14) permute the spin coordinates of the three identical nuclei. For example, the operator S(123) assigns the spin of nucleus 1 to nucleus 2, the spin of nucleus 2 to nucleus 3, and the spin of nucleus 3 to nucleus 1. The operator S(0) is the identity operator.

Table 8. The Genealogical Coefficients.

w	$A^{(1)}$			$A^{(2)}$	E_1				E_2			
	I			I	I				I			
L	3/2	5/2	9/2	3/2	1/2	3/2	5/2	7/2	1/2	3/2	5/2	7/2
0				$\mp\sqrt{\frac{1}{6}}$		$\pm\sqrt{\frac{5}{6}}$						
1	$\mp\sqrt{\frac{7}{10}}$	$\sqrt{\frac{8}{15}}$							± 1	$\mp\sqrt{\frac{3}{10}}$	$\mp\sqrt{\frac{7}{15}}$	
2				$\sqrt{\frac{5}{6}}$	± 1	$\pm\sqrt{\frac{1}{6}}$	± 1	± 1				
3	$\sqrt{\frac{3}{10}}$	$\sqrt{\frac{7}{15}}$	1							$\mp\sqrt{\frac{7}{10}}$	$\pm\sqrt{\frac{8}{15}}$	∓ 1

Table 9. The Reduction Coefficients

$C(A^{(1)}, 3/2, 3/2) = 3/5$

$C(A^{(1)}, 3/2, 5/2) = 4\sqrt{6}/5$

$C(A^{(1)}, 5/2, 5/2) = -\sqrt{21}/10$

$C(A^{(1)}, 5/2, 9/2) = -3/2$

$C(A^{(1)}, 9/2, 9/2) = -\sqrt{33}/2$

$C(A^{(2)}, 3/2, 3/2) = -1$

$C(E_1, 1/2, 3/2) = -\sqrt{3}/5$

$C(E_1, 3/2, 3/2) = 11/5$

$C(E_1, 1/2, 5/2) = -3\sqrt{42}/10$

$C(E_1, 3/2, 5/2) = -3/5$

$C(E_1, 3/2, 7/2) = 2\sqrt{3}/5$

$C(E_1, 5/2, 5/2) = 3\sqrt{21}/35$

$C(E_1, 5/2, 7/2) = 36\sqrt{7}/35$

$C(E_1, 7/2, 7/2) = 3\sqrt{42}/7$

$C(E_2, 1/2, 3/2) = -3\sqrt{3}/5$

$C(E_2, 3/2, 3/2) = 3/5$

$C(E_2, 1/2, 5/2) = \sqrt{42}/10$

$C(E_2, 3/2, 5/2) = -9/5$

$C(E_2, 3/2, 7/2) = 6\sqrt{3}/5$

$C(E_2, 5/2, 5/2) = -\sqrt{21}/35$

$C(E_2, 5/2, 7/2) = -12\sqrt{7}/35$

$C(E_2, 7/2, 7/2) = -\sqrt{42}/7$

APPENDIX B

COMPUTER CALCULATIONS

DESCRIPTION OF THE PROGRAM

The purpose of the following computer program is to calculate the J=1 to J=2, K=1 transition spectrum of a symmetric-top molecule with three identical quadrupolar nuclei for direct comparison to the spectrum obtained from a Stark modulation type spectrograph. To this end it calculates the quadrupole component frequencies and intensities both in the presence and absence of an applied Stark field. After broadening all lines according to the Van Vleck-Weisskopf relation, equation V-4, the difference bewteen the two spectra is calculated to obtain a facsimile of the actual recorded spectrum from a phase-sensitive detector.

The input to the program consists of the following parameters: the quadrupole coupling constant eqQ, the Cl-X-Cl bond angle 'a', the dipole moment μ, the field strength E, the line width parameter 'b', and the pressure p. The output is actually dependent only upon the products eqQ cos (a), μE, and bp. This data is contained on cards 223-225 of the program to avoid using a READ statement.

The procedure EAGLE for calculation of eigenvalues and eigenvectors was originally derived from an algorithm written by D. F. Eagle (71) for the Burroughs B-220 computer. It was translated for use on the B-5500 computer (extended ALGOL) and subsequently modified extensively to incorporate an improved Jacobi procedure for eigenvalue and eigenvector calculation. The procedure JACOBI in the program was written by W. Fleming of the staff of the Rich Electronic Computer Center on the

campus of the Georgia Institute of Technology. This procedure is not included in the following list of program cards, but is presently part of the Cast A disk library for the B-5500 computer. Algorithms for calculation of the Wigner 3-J and 6-J symbols were written for the matrix element calculations. Alternative algorithms for the 3-J, 6-J and 9-J symbols have been published by Gunn (72).

Listing of Program Cards

```
    BEGIN
%   QUADRUPOLE HYPERFINE STRUCTURE AND STARK EFFECT FOR SYMMETRIC-TOP      1.0000
%   MOLECULES WITH THREE IDENTICAL QUADRUPOLAR NUCLEI                      2.0000
    INTEGER PAR,N4,MINI,EXC,EXP7,P1,PAR1,F1L,MFL ; %                       3.0000
    INTEGER MF2,I1,I2,R1,C1,MIN4,MIN3,EXP1,D,S,F3,EXP6,F1,F2,V1,V2,        4.0000
      N,I,J,K,M,MIN1,N1,N2,N3,MF3,KQ,JQ,K1,JA,JB,K2,L ;                    5.0000
    REAL SUMINT1,INT1,LWP,SUMINT,IQ1,FQ1,FQ2,MFQ ; %                       6.0000
    REAL MLF,TB1,TB2,MF22,F12,F22,I12,SPLIT3,EQQ3,FREQ,PRESS ; %           7.0000
    REAL SM1,J1,J2,J3,L1,L2,L3,M1,M2,M3,MU,EFIELD,TE3,TE4 ; %              8.0000
   REAL ALPHA1,ALP,SUMI,DIPOLE,INT,SPLIT,T1,T2,CLOCK,CLOCK2,TRA,TRD,       9.0000
        SUMX2,SUMY2,SPROD,ITS,FREQ1,FREQ2,SPLIT2,EQQ ; %                  10.0000
    REAL INT2 ; %
    ARRAY ALP2,BETA2[0:4,0:4],FACT[-10:21] ; %                            11.0000
    ARRAY B1[0:1,1:4,1:5,1:22],B2[0:1,1:4,1:6,1:34],EGY1[0:22],           12.0000
    B[1:2,1:2,0:1,1:4,1:4,1:6],EGY2[0:34] ; %                             13.0000
    ARRAY NU1,PEAK1[0:301],E[1:2,1:2,0:1,1:4,1:6] ; %                     14.0000
    ARRAY A,Y,DG[0:35,0:35],PEAK,NU[1:4,1:8000],SJSY[0:4,0:5,0:6] ; %     15.0000

    ARRAY THJS[1:5,1:5,1:6] ; %                                           15.1000
    FILE OUT LINE 6(1,15) ; %                                             16.0000
    LIST SNAFU (TRA,TRD,TRA-TRD),                                         17.000
         INP (N,FOR I ← 1 STEP 1 UNTIL N DO                               18.000
              FOR J ← 1 STEP 1 UNTIL N DO A[I,J])                         19.000
    FORMAT OUT HEADINT(/"TRANSITIONS J=1,F=",I2,"/2,V=",I2,               20.000
    " TO J=2,F=",I2,"/2,V=",I2), %                                        21.000
         SUMINTF("SUM OF INTENSITIES = ", F10.4) , %                      22.000
    MH("MATRIX FOR J=",I2," MF=",I2,"/2") , %                             23.000
    IL(/"TRANSITIONS J=2 ← J=1 FOR MF=",I2,"/2") , %                      24.000
    PCL3S("STARK PLUS QUADRUPOLE INTERACTION SPECTRUM FOR PHOSPHOROUS"    25.000
   " TRICHLORIDE,PCL3") , %                                               26.000
   POCL3S("STARK PLUS QUADRUPOLE INTERACTION SPECTRUM FOR PHOSPHORYL"     27.000
    " CHLORIDE,POCL3") , %                                                28.000
    CFCL3S("STARK PLUS QUADRUPOLE INTERACTION SPECTRUM FOR"               29.000
           " FLOUROTRICHLOROMETHANE, CFCL3") , %                          30.000
    PLOT(X10,2F20.4) , %
    MUE(/"   DIPOLE MOMENT =",F5.2," DEBYE,ELECTRIC FIELD = ",F8.3,       31.000
    " VOLTS/CM, STARK VOLTAGE =",F7.3/) , %                               32.000
```

```
QUAD1(/"   QUADRUPOLE COUPLING CONSTANT EQQ ="ꜝF8.3ꜝ" BOND ANGLE"      33.000
" CL-X-CL ="ꜝF8.2) ꜝ %                                                 34.000
PBSH("   PRESSURE ="ꜝF6.3ꜝ" MM HGꜝ LINE WIDTH PARAMETER ="ꜝF6.1/)  ꜝ  35.0000
IH(/X5ꜝ"J=1 LEVEL"ꜝX10ꜝ"J=2 LEVEL",X10,"SPLITTING"ꜝX10ꜝ               36.000
  "INTENSITY") ꜝ %                                                     37.000
INTENSITY(X4ꜝF10.4ꜝX9ꜝF10.4ꜝX7ꜝF12.6ꜝX7ꜝF12.8ꜝI6) ꜝ %                38.000
PLOT2(/X10ꜝF6.3ꜝ3F20.4) ꜝ %                                           39.0000
HEADIN2(/"TRANSITIONS J="ꜝI2ꜝ"ꜝF="ꜝI2ꜝ"/2ꜝV="ꜝI2ꜝ                   40.000
     " TO J="ꜝI2ꜝ"ꜝF="ꜝI2ꜝ"/2ꜝV="ꜝI2) ꜝ %                            41.000
JH("TRANSITIONS J="ꜝI3ꜝ" TO J="ꜝI3ꜝ"ꜝK="ꜝI3) ꜝ %                     42.000
PBSH2(/X9ꜝ"FREQUENCY"ꜝX9ꜝ"QUADRUPOLE"ꜝX13ꜝ"STARK"ꜝX11ꜝ                43.000
"QUADRUPOLE "/X11ꜝ"IN MC"ꜝX12ꜝ"SPECTRUM"ꜝX14ꜝ"SPECTRUM",X8ꜝ             44.000
"MINUS STARK") ꜝ %                                                     45.000
     POL3("QUADRUPOLE SPECTRA FOR PHOSPHOROUS TRICHLORIDE"//)ꜝ          46.000
FORMAT OUT CHECK ("TRA="ꜝF13.4ꜝX9ꜝ"TRD="ꜝF13.4ꜝX9ꜝ"DIFF="ꜝF7.4)ꜝ       47.000
POCL3(/"QUADRUPOLE SPECTRA FOR PHOSPHORYL CHLORIDE ꜝ POCL3") ꜝ %       48.000
          EIG ("DEGENERATE EIGENVALUE--ORTHONORMALIZED VECTOR IS-"),    49.000
          DATA ("INPUT MATRIX IS"), %                                  50.000
   PBS12(/"PRESSURE BROADENED SPECTRUM FOR J=1 TO J=2 TRANSITIONS"),   51.000
   PBS23(/"PRESSURE BROADENED SPECTRUM FOR J=2 TO J=3 TRANSITIONS"),   52.000
RUNTIME(/"RUN TIME ="ꜝF9.2ꜝX2ꜝ"SECONDS"/)ꜝ %                         53.000
RT2("TOTAL TIME ="ꜝF9.2ꜝX2ꜝ"SECONDS"/)ꜝ %                            54.000
          DGN ("DIAGONALIZED MATRIX IS") ; %                           55.000
FORMAT DIVZRO("ZERO DENOMINATOR REACHED IN VECTOR CALCULATION"         56.000
"FOR J="ꜝI3ꜝ"K="ꜝI3ꜝ". VECTOR FOLLOWING IS INVALID") ꜝ %              57.000
EXDEG("EXACT DEGENERACY FOR EIGENVALUE"ꜝI3ꜝ". SCHMIDT PROCESS"        58.000
" BREAKS DOWN") ; %                                                    59.000
INTEGER PROCEDURE MIN2(P1ꜝP2ꜝP3ꜝP4) ; %                               60.000
  VALUE P1ꜝP2ꜝP3ꜝP4 ; %                                               61.000
  INTEGER P1ꜝP2ꜝP3ꜝP4 ; %                                             62.000
    BEGIN IF P1≤P2 AND P1≤P3 AND P1≤P4 THEN MIN2←P1 ; %                63.000
          IF P2≤P1 AND P2≤P3 AND P2≤P4 THEN MIN2←P2 ; %                64.000
          IF P3≤P1 AND P3≤P2 AND P3≤P4 THEN MIN2←P3 ; %                65.000
          IF P4≤P1 AND P4≤P2 AND P4≤P3 THEN MIN2←P4 ; END          ; 66.000
   REAL PROCEDURE FACA(S) ; % CALCULATES FACTORIAL OF S                67.000
     VALUE S ; INTEGER S ; %                                           68.000
       FACA←IF S<0 THEN 0 ELSE IF S< 2 THEN 1 ELSE FACA(S-1)×S     ; 69.000
```

```
     REAL PROCEDURE DEL(D1,D2,D3) ; %                                          70.000
          VALUE D1,D2,D3 ; REAL D1,D2,D3 ; %                                   71.000
          DEL ← SQRT(FACT[D1+D2-D3]×FACT[D1-D2+D3]×FACT[-D1+D2+D3]/            73.000
          FACT[D1+D2+D3+1]) ; %                                                74.000
     REAL PROCEDURE SUMK(J1,J2,J3,L1,L2,L3) ;                                  75.000
          VALUE J1,J2,J3,L1,L2,L3 ; %                                          76.000
          REAL  J1,J2,J3,L1,L2,L3 ; %                                          77.000
     BEGIN %                                                                   78.000
     SM1←0 ; MIN3←MIN2(J1+J2-J3,J1+L2-L3,L1+J2-L3,L1+L2-J3) ; %                79.000
     FOR K←0 STEP 1 UNTIL MIN3 DO BEGIN %                                      80.000
     F3← FACT[K]×FACT[J1+J2-J3-K] %                                            81.000
     ×FACT[J1+L2-L3-K]×FACT[L1+J2-L3-K]×FACT[-J1-L1+J3+L3+K] %                 82.000
     ×FACT[-J2-L2+J3+L3+K]×FACT[L1+L2-J3-K] ; %                               83.000
     IF F3>0 THEN SM1←SM1 + (IF BOOLEAN(K) THEN -1 ELSE 1) %                   84.000
                              ×FACT[J1+J2+L1+L2+1-K]/F3 ; END        ; %       85.000
     SUMK ← SM1 ; %                                                           86.000
     END;                                                                     87.000
     REAL PROCEDURE SIXJ(J1,J2,J3,L1,L2,L3) ; %                               88.000
%  CALCULATES WIGNER 6-J COEFFICIENTS                                         88.100
          VALUE J1,J2,J3,L1,L2,L3 ; %                                         89.000
          REAL  J1,J2,J3,L1,L2,L3 ; %                                         90.000
     BEGIN %                                                                  91.000
            EXP1 ← J1+J2+L1+L2 ; %                                            92.000
            IF ABS(J1+J2)≥J3 AND ABS(J1-J2)≤J3 THEN %                         93.000
            SIXJ ←(IF BOOLEAN(EXP1) THEN -1 ELSE 1) %                         94.000
                          ×DEL(J1,J2,J3)×DEL(L1,L2,J3)×DEL(J1,L2,L3)          95.000
            × SUMK(J1,J2,J3,L1,L2,L3)× DEL(L1,J2,L3) %                        96.000
            ELSE SIXJ←0 ; %                                                   97.000
     END; %                                                                   98.000
     REAL PROCEDURE SUMK2(J1,J2,J3,M1,M2,M3) ; %                              99.000
          VALUE J1,J2,J3,M1,M2,M3 ; %                                        100.000
          REAL  J1,J2,J3,M1,M2,M3 ; %                                        101.000
     BEGIN %                                                                 102.000
          SM1←0 ; MIN3←MIN2(J1+J2-J3,J1-M1,J2+M2,100) ; %                    103.000
          FOR K←0 STEP 1 UNTIL MIN3 DO BEGIN %                               104.000
                         F3←(FACT[K]×FACT[J1+J2-J3-K]×FACT[J1-M1-K]×         105.000
            FACT[J2+M2-K]×FACT[J3-J2+M1+K]×FACT[J3-J1-M2+K])                 ;106.000
```

```
      IF F3>0 THEN SM1←SM1 + (IF BOOLEAN(K) THEN -1 ELSE 1)/F3 ; END;  107.000
        SUMK2 ← SM1 ; %                                                108.000
    END; %                                                             109.000
    REAL PROCEDURE THREEJ(J1,J2,J3,M1,M2,M3) ; %                       110.000
%   CALCULATES WIGNER 3-J COEFFICIENTS                                 110.1000
      VALUE J1,J2,J3,M1,M2,M3 ; %                                      111.000
      REAL  J1,J2,J3,M1,M2,M3 ; %                                      112.000
    BEGIN %                                                            113.000
        EXP1 ← J1-J2-M3 ; %                                            114.000
        IF M1+M2+M3≠0 THEN THREEJ←0 ELSE %                             115.000
        THREEJ← (IF BOOLEAN(EXP1) THEN -1 ELSE 1) %                    116.000
                  ×SQRT(FACT[J1+J2-J3]×FACT[J1-J2+J3] %                117.000
         ×FACT[-J1+J2+J3]×FACT[J1+M1]×FACT[J1-M1] ×FACT[J2+M2]         118.000
         ×FACT[J2-M2]×FACT[J3+M3]×FACT[J3-M3]/FACT[J1+J2+J3+1])        119.000
         ×SUMK2(J1,J2,J3,M1,M2,M3) ; %                                 120.000
    END; %                                                             121.000
    REAL PROCEDURE QDP(J,F1,I1,I2,V1,K) ;                              122.0000
%   ALCULATES QUADRUPOLE INTERACTION MATRIX ELEMENT                    122.1000
      VALUE J,F1,I1,I2,V1,K ; %                                        123.0000
      REAL  J,F1,I1,I2,V1,K ; %                                        124.0000
        BEGIN INTEGER EXP4,EXP5 ; %                                    125.0000
        EXP4← 2 + 3/2 +J+F1 ; EXP5← J+V1+3 ; %                         126.0000
    QDP←(IF BOOLEAN(EXP4) THEN -1 ELSE 1)×  SIXJ(2,J,J,F1,I2,I1)×SQRT(5)127.0000
        ×(ALP2[(2×I1+1)/2,(2×I2+1)/2]×SQRT(2×J+1)×(3×K*2-J×(J+1))      128.0000
        ×ALP/SQRT((2×J+3)×(2×J+2)×2×J×(2×J-1)) %                       129.0000
        +(IF BOOLEAN(EXP5) THEN -1 ELSE 1) %                           130.0000
                  ×BETA2[(2×I1+1)/2,(2×I2+1)/2]×SQRT(2×J+1) %          131.0000
        ×J×(J+1)×(ALP-1)/(2×SQRT((2×J+3)×(2×J+2)×2×J×(2×J-1))))×EQQ  ;132.0000
      END ; %                                                          133.0000
    REAL PROCEDURE STARK(J,JP,I1,F1,F2,MF,K) ; %                       134.0000
%   CALCULATES STARK EFFECT MATRIX ELEMENT                             134.1000
      VALUE J,I1,F1,F2,MF,K,JP ; %                                     135.0000
      REAL  J,I1,F1,F2,MF,K,JP ; %                                     136.0000
      BEGIN EXP6←F1+F2+I1-MF-K ; %                                     137.0000
    STARK←(IF BOOLEAN(EXP6) THEN -1 ELSE 1)×THREEJ(F1,1,F2,-MF,0,MF)   138.0000
        ×SQRT((2×F1+1)×(2×F2+1))×SIXJ(J,F1,I1,F2,JP,1) %               139.0000
      ×SQRT((2×J+1)×(2×JP+1))×THREEJ(JP,J,1,K,-K,0)×MU×EFIELD ; %      140.0000
```

```
      END  ; %                                                                  141.0000
    PROCEDURE CLEARA(A)  ; %                                                    142.0000
    ARRAY A[0,0] ; %                                                            143.0000
    BEGIN %                                                                     144.0000
         FOR I←1 STEP 1 UNTIL  4 DO FOR J←1 STEP 1 UNTIL  4 DO A[I,J]←0;        145.0000
    END CLEARA ; %                                                              146.0000
    INTEGER PROCEDURE MIN(P1,P2) ; %                                            147.0000
    VALUE P1,P2 ; %                                                             148.0000
    INTEGER P1,P2 ; %                                                           149.0000
         IF P1 < P2 THEN MIN ← P1 ELSE %                                        150.0000
         MIN ← P2 ; %                                                           151.0000
    PROCEDURE MATRIXPRINT (N,M,A) ; %                                           152.0000
    VALUE N,M ; %                                                               153.0000
    INTEGER N,M ; %                                                             154.0000
    ARRAY A[0,0] ; %                                                            155.0000
         BEGIN %                                                                156.0000
         FORMAT OUT FMT ("ROW",I3,X2,"COL",I3,5F20.8 ) ; %                      157.0000
         INTEGER I,J,K ; %                                                      158.0000
LIST ROW ( I,J,FOR K← J STEP 1 UNTIL MIN1 DO A[I,K] ) ; %                       159.0000
              FOR I ← 1 STEP 1 UNTIL N DO ; %                                   160.0000
              BEGIN  %                                                          161.0000
              MIN1 ← 5 ; %                                                      162.0000
                 J ← 1 ; WHILE J ≤ M DO %                                       163.0000
              BEGIN  %                                                          164.0000
                     WRITE (LINE,FMT,ROW) ; %                                   165.0000
                     J ← K ; %                                                  166.0000
              MIN1 ← MIN(J+4,M) %                                               167.0000
                 END %                                                          168.0000
              END %                                                             169.0000
         END MATRIXPRINT ; %                                                    170.0000
    PROCEDURE EAGLE(N,A) ; %                                                    171.0000
%  CONTROL PROCEDURE FOR EIGENVALUE AND EIGENVECTOR CALCULATION                 171.1000
    VALUE N ; INTEGER N ; ARRAY A[0,0] ; %                                      172.0000
    BEGIN %                                                                     173.0000
    ARRAY REF[0:34,0:34],X,GOUF[0:34] ; %                                       174.0000
    INTEGER ARRAY ID[0:34,0:34] ; %                                             175.0000
  FORMAT OUT  GOOFF("VECTOR CHECK BY SUM OF PRODUCTS FOR ROW",I2,F12.8,         176.0000
```

```
    I4) ; %                                                                 177.0000
    LIST GOOFO (I,GOOF[I],K) ; %                                            178.0000
      LABEL TOM ; %                                                         179.0000
% CALL CASE A TAPE PROCEDURE A016 FOR CALCULATING EIGENVALUES AND          180.0000
% EIGENVECTORS                                                            181.0000
$$ A A016                                                                 00000000
                                                                          99999999
        T1 ← TIME(2) ; %                                                  182.0000
        FOR I ← 2 STEP 1 UNTIL N DO %                                     183.0000
        FOR J ← 1 STEP 1 UNTIL I-1 DO A[I,J] ← A[J,I] ; %                 184.0000
        FOR I ← 1 STEP 1 UNTIL N DO FOR J ← 1 STEP 1 UNTIL N DO           185.0000
        BEGIN %                                                           186.0000
            REF[I,J] ← A[I,J] ; %                                         187.0000
            IF I = J THEN ID[I,J] ← 1 ; %                                 188.0000
            IF I ≠ J THEN ID[I,J] ← 0 %                                   189.0000
        END ; %                                                           190.0000
        TRA ← 0.0 ; %                                                     191.0000
        FOR I ← 1 STEP 1 UNTIL N DO %                                     192.0000
        TRA ← TRA + A[I,I] ; %                                            193.0000
%  CALCULATE EIGENVALUES AND EIGENVECTORS                                 194.0000
    JACOBI(1,N,A,DG) ; %                                                  195.0000
        TRD ← 0.0 ; %                                                     196.0000
        FOR I ← 1 STEP 1 UNTIL N DO %                                     197.0000
        TRD ← TRD + A[I,I] ; %                                            198.0000
%  CHECK INVARIANCE OF TRACE UNDER DIAGONALIZING TRANSFORMATION           198.1000
    IF ABS(TRA - TRD) > 10-6 THEN %                                       199.0000
        WRITE (LINE,CHECK,SNAFU) ; %                                      200.0000
%  CHECK HOMOGENEITY CONDITION ON EIGENVECTORS                            200.1000
        FOR K ← 1 STEP 1 UNTIL N DO BEGIN %                               201.0000
            FOR I ← 1 STEP 1 UNTIL N DO %                                 202.0000
            BEGIN GOOF[I] ← 0.0 ; %                                       203.0000
              FOR J ← 1 STEP 1 UNTIL N DO %                               204.0000
    GOOF[I]←GOOF[I]+(REF[I,J]-A[K,K]×ID[I,J])×DG[J,K] ; %                 205.0000
    IF GOOF[I]>10-6 THEN %                                                206.0000
              WRITE(LINE,GOOFF,GOOFO) %                                   207.0000
            END ; %                                                       208.0000
        END ; %                                                           209.0000
```

```
    END EAGLE ; %                                                          210.0000
    WRITE(LINE[NO]) ; %
    T2 ← TIME(2) ; %                                                       211.0000
    BEGIN REAL DUMMY1  ; %                                                 212.0000
%   BUILD FACTORIAL TABLE                                                  212.1000
    FOR I←-10 STEP 1 UNTIL 20 DO FACT[I]←FACA(I) ; %                       213.0000
%   BUILD TABLE OF REDUCTION COEFFICIENTS C(+) AND C(-)                    213.1000
        ALP2[4,4]← SQRT(42)/7 ; ALP2[3,4]←12×SQRT(7)/35 ; %                214.0000
        ALP2[3,3]←SQRT(21)/35 ; ALP2[2,4]←4×SQRT(3)/5 ; %                  215.0000
        ALP2[2,3]←-6/5 ; ALP2[2,2]←7/5 ; ALP2[1,3]←-SQRT(42)/10 ; %        216.0000
        ALP2[1,2]←-2×SQRT(3)/5 ; BETA2[4,4]←-2×SQRT(42)/7 ; %              217.0000
        BETA2[3,4]←-2×ALP2[3,4] ; BETA2[3,3]←-2×ALP2[3,3] ; %              218.0000
        BETA2[2,4]←2×SQRT(3)/5 ; BETA2[2,3]←-3/5 ;BETA2[2,2]←-4/5          ;219.0000
        BETA2[1,3]←2×SQRT(42)/10 ; BETA2[1,2]←-SQRT(3)/5 ; %               220.0000
    FOR I←1 STEP 1 UNTIL 4 DO FOR L←1 STEP 1 UNTIL I DO %                  221.0000
    BEGIN ALP2[I,L]←ALP2[L,I] ; BETA2[I,L]←BETA2[L,I] END ; %              222.0000
%   DATA CARDS FOR PROGRAM                                                 222.1000
    ALPHA1←1.80641 ; ALP←COS(ALPHA1) ; EQQ←-55.4 ; %                       223.0000
    MU←2.50 ; EFIELD←104.674 ; %                                           224.000
    LWP←45.0 ; PRESS ← 0.005 ; %                                           225.0000
%   BUILD TABLE OF WIGNER 6-J SYMBOLS                                      225.1000
    FOR IQ1←1 STEP 1 UNTIL 4 DO FOR FQ1←1 STEP 1 UNTIL 5 DO %              226.0000
    FOR FQ2←1 STEP 1 UNTIL 6 DO IF ABS(FQ1-FQ2) ≤ 1 THEN %                 227.0000
    SJSY[IQ1,FQ1,FQ2]←SIXJ(1,(2×FQ1-1)/2,(2×IQ1-1)/2,(2×FQ2-1)/2,2,1)     ;228.0000
%   BUILD TABLE OF WIGNER 3-J SYMBOLS                                      228.1000
    FOR MFQ←1 STEP 1 UNTIL 5 DO FOR FQ1←MFQ STEP 1 UNTIL 5 DO %            229.0000
    FOR FQ2←MFQ STEP 1 UNTIL 6 DO IF ABS(FQ1-FQ2) ≤ 1 THEN %               230.0000
    THJS[MFQ,FQ1,FQ2]←THREEJ((2×FQ1-1)/2,1,(2×FQ2-1)/2, %                  231.0000
      -(2×MFQ-1)/2,0,(2×MFQ-1)/2) ; %                                      232.0000
    WRITE(LINE,POCL3S); WRITE(LINE,QUAD1,EQQ,ALPHA1×57.2958) ; %           233.0000
    PAR ←0 ; %                                                             234.0000
        SUMINT←0 ; %                                                       235.0000
%   CALCULATE MATRICES FOR STARK PLUS QUADRUPOLE INTERACTION               235.1000
    FOR MF2←9 STEP -2 UNTIL 1 DO BEGIN KQ←1 ; %                            236.0000
    FOR K1←1 STEP 1 UNTIL 22 DO EGY1[K1]←0 ; %                             237.0000
    FOR K1←1 STEP 1 UNTIL 34 DO EGY2[K1]←0 ; %                             238.0000
    FOR I1←1,2,3,4 DO FOR F1←1,2,3,4,5 DO FOR V1←0,1 DO FOR K1←1 %          239.0000
```

```
     STEP 1 UNTIL 22 DO B1[V1,I1,F1,K1]←0 ; %                                  240.0000
    FOR I1←1,2,3,4 DO FOR F1←1,2,3,4,5 DO FOR V1←0,1 DO FOR K1←1 %              241.0000
     STEP 1 UNTIL 34 DO B2[V1,I1,F1,K1]←0 ; %                                  242.0000
     BEGIN FOR JQ←1,2 DO %                                                     243.0000
       BEGIN R1←C1←N←0 ; %                                                     243.0000
      FOR F1←2×JQ+7 STEP -2 UNTIL ABS(MF2) DO %                                244.0000
       BEGIN MIN4←MIN(7,F1+2×JQ)} FOR I1←MIN4 STEP -2 WHILE I1≥1 %             246.0000
      AND I1≥F1-2×JQ DO FOR V1←0,1 DO BEGIN C1←R1 ; R1←R1+1 ; %                247.0000
       FOR F2←F1 STEP -2 UNTIL ABS(MF2) DO BEGIN MIN3←MIN(7,F2+2×JQ)           }248.0000
       FOR I2← IF F2=F1 THEN I1 ELSE MIN3 STEP -2 WHILE I2≥1 %                 249.0000
      AND I2≥F2-2×JQ DO FOR V2← IF F2=F1 AND I2=I1 THEN V1 ELSE 0 STEP         250.0000
          1 UNTIL 1 DO %                                                       251.0000
       BEGIN C1←C1+1 ; N←C1 ; %                                                252.0000
       IF F1-F2≤2 AND I1=I2 AND V1≠V2 THEN %                                   253.0000
     A[R1,C1]←STARK(JQ,JQ,I1/2,F1/2,F2/2,MF2/2,KQ) ELSE %                      253.0000
       IF F1=F2 AND V1=V2 THEN A[R1,C1]←QDP(JQ,F1/2,I1/2,I2/2,V1,KQ)           254.0000
       ELSE A[R1,C1]←0 ; END END END END  ; %                                  255.0000
     IF MF2=1 AND JQ=2 THEN N←32 ;                                             257.0000
     EAGLE(N,A) ; %                                                            258.0000
%   ASSIGN QUANTUM NUMBERS TO ENERGY EIGENVALUES AND                          258.1000
%   EIGENVECTOR COMPONENTS                                                    258.1100
     FOR K1←1 STEP 1 UNTIL N DO %                                              259.0000
     BEGIN I←0 ; FOR F1←2×JQ+7 STEP -2 UNTIL ABS(MF2) DO %                     260.0000
       BEGIN MIN4←MIN(7,F1+2×JQ)} FOR I1←MIN4 STEP -2 WHILE I1≥1 %             261.0000
     AND I1≥F1-2×JQ DO FOR V1←0,1 DO BEGIN I←I+1 ; %                           262.0000
       IF JW=1 THEN BEGIN B1[V1,(I1+1)/2,(F1+1)/2,K1]←DG[I,K1] ; %             263.0000
         EGY1[K1]←A[K1,K1] ; N1←N END ; %                                      264.0000
       IF JW=2 THEN BEGIN B2[V1,(I1+1)/2,(F1+1)/2,K1]←DG[I,K1] ; %             265.0000
         EGY2[K1]←A[K1,K1] ; N2←N END ; %                                      266.0000
     END END ; %                                                               267.0000
     END END ; %                                                               268.0000
%   BEGINNING OF INTENSITY CALCULATION                                        268.1000
     WRITE(LINE,IL,MF2) ; WRITE(LINE,IH) ; %                                  269.0000
     MFL←ABS((MF2+1)/2) ; %                                                    270.0000
       MF22←MF2/2 ; %                                                          271.0000
     JA←1; JB←2 ; FOR K1←1 STEP 1 UNTIL N1 DO FOR K2←1 STEP 1 UNTIL N2 DO272.0000
     BEGIN SUMI←0 ; FOR F2←6 STEP -1 UNTIL MFL DO %                            273.0000
```

```
  BEGIN ITS←MIN(5,F2←1) ; %                                          274.0000
  F1L←(IF F2=MFL THEN F2 ELSE F2-1) ; %                              275.0000
  FOR F1←ITS STEP -1 UNTIL F1L DO %                                  276.0000
    BEGIN MIN4←MIN2(4,F1←1,F2←2,20) ; %                              277.0000
  F12← (2×F1-1)/2 ; F22←(2×F2-1)/2 ; %                               278.0000
  MEF←-SQRT(6×F1×F2)×THJS[(MF2←1)/2,F1,F2] ; %                       279.0000
                                          FOR I1←MIN4 STEP -1        280.0000
    WHILE I1≥1 AND I1≥F1-1 AND I1≥F2-2 DO %                          281.0000
BEGIN I12←(2×I1-1)/2 ; %                                           282.0000
FOR V1←0,1 DO BEGIN V2←IF V1=0 THEN 1 ELSE 0 ; TB1←B1[V1,I1,F1,K1] ;283.0000
  TB2←B2[V2,I1,F2,K2] ; IF TB1≠0 AND TB2≠0 THEN %                  284.0000
    BEGIN EXP6←F1←F2←I12-MF22 ; %                                    285.0000
      SUMI←SUMI←TB1×TB2×(IF BOOLEAN(EXP6) THEN -1 ELSE 1) %          286.0000
        ×SJSY[I1,F1,F2]×MEF ; %                                      287.0000
END END END END END ; %                                            288.0000
  INT←SUMI*2 ; SPLIT← EGY2[K2]-EGY1[K1] ; PAR←PAR+1 ; %            289.0000
SUMINT←SUMINT+INT ; IF PAR ≤ 800  THEN %                           290.0000
BEGIN PEAK[1,PAR]←INT ; NU[1,PAR]←SPLIT END ELSE IF PAR≤1600 THEN  291.0000
BEGIN PEAK[2,PAR-800 ]←INT ; NU[2,PAR-800 ]←SPLIT END ELSE         292.0000
IF PAR ≤ 2400 THEN %                                               293.0000
BEGIN PEAK[3,PAR-1600]←INT ; NU[3,PAR-1600]←SPLIT END ELSE %       294.0000
BEGIN PEAK[4,PAR-2400]←INT ; NU[4,PAR-2400]←SPLIT END ; %          295.0000
  IF INT > 0.05 THEN %                                             296.0000
  WRITE(LINE,INTENSITY,EGY1[K1],EGY2[K2],SPLIT,INT,PAR) ; %        297.0000
END ; %                                                            298.0000
END END ; %                                                        299.0000
WRITE(LINE[DBL]) ; %                                               300.0000
     WRITE(LINE,SUMINTF,SUMINT) ; %                                301.0000
CLOCK2 ← (TIME(2) - T2)/60 ; %                                     302.0000
WRITE(LINE,RT2,CLOCK2) ; %                                         303.0000
BEGIN   REAL DUMMY2 ; %                                            304.0000
LABEL WORK ; %                                                     305.0000
N3←2 ; FOR JQ←1,2 DO %                                             306.0000
BEGIN N3← IF N3=2 THEN 1 ELSE 2 ; FOR KQ←1 DO FOR F1←1 %           307.0000
  STEP 1 UNTIL 6  DO FOR V1←0,1 DO FOR K1←1,2,3,4 DO FOR I1←1,2,3,4 308.0000
  DO %                                                             309.0000
  BEGIN E[N3,KQ,V1,K1,F1]←0 ; B[N3,KQ,V1,K1,I1,F1]←0  %            310.0000
```

```
      END ; FOR PAR1←1 STEP 1 UNTIL 300 DO PEAK1[PAR1]←NU1[PAR1]←0 ;
    PAR1←0 ; %
      FOR KQ←1 STEP 1 UNTIL JQ DO FOR F1←2×JQ+7 STEP -2 UNTIL 1 DO %
      FOR V1←0,1 DO %
      BEGIN R1←C1←0 ; CLEARA(A) ; MINI←MIN(7,F1+2×JQ) ; %
% BEGINNING OF CALCULATION FOR QUADRUPOLE INTERACTION ALONE
% CALCULATE MATRIX CORRESPONDING TO CURRENT VALUES OF J,K,F AND V
        FOR I1←MINI STEP -2 WHILE I1≥1 AND I1≥F1-2×JQ DO %
        BEGIN C1←R1 ; R1←R1+1 ; %
          FOR I2←I1 STEP -2 WHILE I2≥1 AND I2≥F1-2×JQ DO %
          BEGIN C1←C1+1 ; A[R1,C1]←QDP(JQ,F1/2,I1/2,I2/2,V1,KQ) ; %
          END ; %
        END ; %
    IF JQ=2 AND F1=1 THEN C1←2 ; %
    IF JQ=3 AND F1=3 THEN C1←3 ; %
    IF JQ=3 AND F1=1 THEN C1←2 ; %
% CALL PROCEDURE TO DIAGONALIZE MATRIX AND CALCULATE EIGENVECTORS
        EAGLE(C1,A) ; FOR K1←1 STEP 1 UNTIL C1 DO %
% ASSIGN QUANTUM NUMBERS TO ALL EIGENVALUES AND EIGENVECTOR COMPONENTS
        BEGIN E[N3,KQ,V1,K1,(F1+1)/2]←A[K1,K1] ; I1← MINI +2 ; %
          FOR I←1 STEP 1 UNTIL C1 DO %
          BEGIN I1←I1-2 ; B[N3,KQ,V1,K1,(I1+1)/2,(F1+1)/2]←DG[I,K1] ;
          END ; %
          END ; %
      END ; %
    SUMINT1←0.0 ; %
      IF JQ≠1 THEN FOR KQ←1 STEP 1 UNTIL JQ-1 DO %
     BEGIN WRITE(LINE[PAGE]) ; WRITE(LINE,POCL3) ; %
        WRITE(LINE,QUAD1,EQQ,ALPHA1×57.2958) ;WRITE(LINE,JH,JQ-1,JQ,KQ);
        WRITE(LINE,IH) ; %
% CALCULATE INTENSITIES FOR ALL TRANSITIONS FROM J TO J+1
        FOR F1←2×(JQ-1)+7 STEP -2 UNTIL 1 DO IF EXC≠1 THEN %
        BEGIN F2←F1 ; %
WORK:     FOR V1←0,1 DO %
          BEGIN V2←IF V1=0 THEN 1 ELSE 0 ;%
            WRITE(LINE,HEADIN2,JQ-1,F1,V1,JQ,F2,V2) ; %
            FOR K1←1,2,3,4 DO FOR K2←1,2,3,4 DO %
```

```
            BEGIN SUMI←0 ; FOR I←4 STEP -1 UNTIL 1 DO %                    347.0000
              BEGIN EXP7←1+I+(F2+1)/2 ; N4←IF N3=1 THEN 2 ELSE 1 ; %       348.0000
                SUMI←SUMI+B[N4,KQ,V1,K1,I,(F1+1)/2] %                      349.0000
                ×B[N3,KQ,V2,K2,I,(F2+1)/2]×(IF BOOLEAN(EXP7) THEN -1 %     350.0000
                ELSE 1)×SJSY[I,(F1+1)/2,(F2+1)/2] ; %                      351.0000
              END ; %                                                      352.0000
              INT←(F1+1)×(F2+1)×SUMI*2×(JQ×JQ-KQ×KQ)/(3×JQ) ; %           353.0000
              TE3←E[N3,KQ,V2,K2,(F2+1)/2] ; TE4←E[N4,KQ,V1,K1,(F1+1)/2];  354.0000
              SPLIT←TE3-TE4 ; %                                            355.0000
            IF INT≠0 THEN BEGIN %                                          356.0000
              PAR1←PAR1+1 ; NU1[PAR1]←SPLIT ; PEAK1[PAR1]←INT END ; %      357.0000
            SUMINT1←SUMINT1+INT ; %                                        358.0000
              IF INT>0.001 THEN %                                          358.1000
              WRITE(LINE,INTENSITY,TE4,TE3,SPLIT,INT,PAR1) ; %            358.2000
            END ; %                                                        359.0000
          END ; %                                                          360.0000
          IF F1=F2 THEN BEGIN F2←F1+2 ; GO TO WORK END ; %                 361.0000
          IF F1≠1 AND F2≠F1-2 THEN BEGIN F2←F1-2 ; GO TO WORK END END  ;   362.0000
    END END ; %                                                            363.0000
%  PRESSURE BROADEN ALL LINES ACCORDING TO THE VAN VLECK-WEISSKOPF         365.1000
%  RELATION AND ADD TO GET THE RESULTANT SPECTRUM                          365.1100
       WRITE(LINE,SUMINTF,SUMINT1) ; %                                     366.0000
    BEGIN ; %                                                              368.0000
    WRITE(LINE,POCL3S); WRITE(LINE,QUAD1,EQQ,ALPHA1×57.2958) ; %           369.0000
    WRITE(LINE,MUE,MU,EFIELD,EFIELD×0.9554); WRITE(LINE,PBS12) ; %         371.0000
    WRITE(LINE,PBSH,PRESS,LWP) ; %                                         372.0000
    WRITE(LINE,PBSH2) ; %                                                  373.0000
    FOR FREQ1← -10 STEP 0.2 UNTIL 10.01 DO BEGIN %                         376.0000
    INT←0 ;FOR PAR←1 STEP 1 UNTIL 1560 DO %                                377.0000
    BEGIN IF PAR ≤800  THEN BEGIN P1←1 ; PAR1←PAR END %                    378.0000
      ELSE IF PAR ≤1600 THEN BEGIN P1←2 ; PAR1←PAR-800  END %              379.0000
      ELSE IF PAR ≤2400 THEN BEGIN P1←3 ; PAR1←PAR-1600 END %              380.0000
      ELSE BEGIN P1←4 ; PAR1←PAR-2400 END ; %                              381.0000
    IF PEAK[P1,PAR1]>0.001 AND ABS(FREQ1-NU[P1,PAR1])<10 THEN %            382.0000
    INT←INT+(500×PEAK[P1,PAR1]×PRESS*2)/( %                                383.0000
     (FREQ1-NU[P1,PAR1])*2+(LWP ×PRESS)*2)×2 ; %                           384.0000
    END ; %                                                                385.0000
```

```
 INT1←0 ; FOR PAR1←1 STEP 1 UNTIL 300 DO %                          386.0000
IF ABS(FREQ1-NU1[PAR1])<10 THEN %                                   387.0000
 INT1←INT1 + (500×PEAK1[PAR1]×PRESS×PRESS)/ %                       388.0000
((FREQ1-NU1[PAR1])*2+(LWP ×PRESS)*2) ; %                            389.0000
 WRITE(LINE,PLOT2,FREQ1,INT1,INT,INT1-INT) ; %                      390.0000
 END         END ; %                                                391.0000
 END ; %                                                            392.0000
 CLOCK2 ← (TIME(2) - T2)/60 ; %                                     393.0000
 WRITE(LINE,RT2,CLOCK2) ; %                                         394.0000
 END ; %                                                            395.0000
      END .
```

LITERATURE CITED

1. H. B. G. Casimir, On the Interaction Between Atomic Nuclei and Electrons (Teyler's Tweede Genootschap, E. F. Bohn, Haarlem, 1936).

2. C. H. Townes and A. L. Schawlow, Microwave Spectroscopy (McGraw-Hill Book Co., Inc., New York, 1955).

3. R. Bersohn, Unpublished Ph. D. Thesis, Harvard University (1949).

4. Townes and Schawlow, op. cit., p. 173.

5. P. N. Wolfe, Unpublished Ph. D. Thesis, Ohio State University (1955).

6. P. N. Wolfe, Journal of Chemical Physics 25, 976 (1956).

7. M. W. Long, Unpublished Ph. D. Thesis, Georgia Institute of Technology (1959).

8. M. W. Long, J. Chem. Phys. 33, 508 (1960).

9. R. Livingston, Physical Review 82, 289 (1951).

10. R. C. Johnson, Unpublished Ph. D. Thesis, Georgia Institute of Technology (1961).

11. P. G. Favero and A. M. Mirri, Nouvo Cimento 30, 502 (1963).

12. T. L. Weatherly, private communication.

13. K. K. Svidzinskii, "Theory of the Hyperfine Structure in the Rotational Spectra of Molecules," Soviet Maser Research, ed. D. V. Skobel'tsyn (Consultants Bureau, New York, 1964).

14. A. A. Wolf, Unpublished Ph. D. Thesis, Georgia Institute of Technology (1966).

15. P. Kisliuk and C. H. Townes, J. Chem. Phys. 18, 1109 (1950).

16. P. W. Allen and L. E. Sutton, "Tables of Interatomic Distances and Molecular Configurations Obtained by Electron Diffraction in the Gas Phase," Acta Crystallographica 3, 46 (1950), private communication from S. M. Swingle.

17. K. Hedberg and M. Iwasaki, J. Chem. Phys. 36, 589 (1962).

18. J. Q. Williams, J. Sheridan, and W. Gordy, J. Chem. Phys. 20, 164 (1952).

19. G. R. Badgley and R. Livingston, Journal of the American Chemical Society 76, 261 (1954).

20. J. S. Ziomek and E. A. Piotrowski, J. Chem. Phys. 34, 1087 (1961).

21. A. Langseth, Zeitschrift fur Physik 72, 350 (1931).

22. J. Cabannes and A Rousset, Annales de Physique 19, 229 (1933).

23. L. W. Daasch and D. C. Smith, Analytical Chemistry 23, 853 (1951).

24. M. Baudler, R. Klement, and E. Rother, Chemische Berichte 93, 149 (1960).

25. Y. Nakai and K. Mori, Bulletin of the Chemical Society of Japan 37, 1489 (1964).

26. S. G. Frankiss and F. A. Miller, Spectrochemica Acta 21, 1235 (1965).

27. J. R. Nielsen and N. E. Ward, J. Chem. Phys. 10, 81 (1942).

28. P. W. Davis and R. A. Oetjen, Journal of Molecular Spectroscopy 2, 253 (1958).

29. V. Lorenzelli, Academie des Sciences, Paris, Comptes rendus hebdomadaires des seances 252, 3219 (1961).

30. S. Venkateswarlu, Indian Journal of Pure and Applied Physics 1, 380 (1963).

31. A. M. Mirri, F. S. Scappini, and P. G. Favero, Spectrochimica Acta 21, 965 (1965).

32. Townes and Schawlow, op. cit., p. 78.

33. H. H. Nielsen, Reviews of Modern Physics 23, 90 (1951).

34. A. Narath and W. D. Gwinn, The Review of Scientific Instruments 33, 79 (1962).

35. R. Livingston, Journal of Physical Chemistry 57, 496 (1953).

36. L. Clayton, Unpublished Ph. D. Thesis, Georgia Institute of Technology (1961).

37. M. Hamermesh, Group Theory and its Application to Physical Problems (Addison-Wesley Publishing Co., Inc., Reading, Mass., 1962), p. 161.

38. A. A. Wolf, op. cit., p. 33.

39. Ibid., p. 35.

40. Ibid., p. 45.

41. Ibid., p. 51, equation 40.

42. Ibid., p. 51, equation 41.

43. Svidzinskii, op. cit., p. 112.

44. Ibid., p. 21.

45. Ibid., p. 26.

46. Ibid., p. 57.

47. M. Rotenberg, R. Bivins, N. Metropolis, and J. Wooten, Jr., The 3-j and 6-j Symbols (The Technology Press, Cambridge, Mass., 1959).

48. W. Low and C. H. Townes, Phys. Rev. 76, 1295 (1949).

49. Svidzinskii, op. cit., p. 123.

50. A. R. Edmonds, Angular Momentum in Quantum Mechanics (Princeton University Press, Princeton, 1957), p. 69.

51. Ibid., p. 75.

52. Ibid., p. 111.

53. Svidzinskii, op. cit., p. 119.

54. Rotenberg et al., op. cit., p. 2.

55. Edmonds, op. cit., pp. 125, 130.

56. Townes and Schawlow, op. cit., p. 249.

57. Ibid., p. 250.

58. Ibid., p. 336.

59. Ibid., p. 337.

60. Ibid., p. 374.

61. J. H. Van Vleck and V. F. Weisskepf, Revs. Mod. Phys. 17, 227 (1945).

62. C. H. Townes, Physical Review 70, 665 (1947).

63. Townes and Schawlow, op. cit., p. 338 ff.

64. Ibid., p. 153.

65. A. A. Wolf, op. cit., p. 62 ff.

66. Townes and Schawlow, op. cit., p. 344.

67. Y. Beers, Introduction to the Theory of Error (Addison-Wesley Publishing Co., Inc., Reading, Mass., 1953), pp. 9, 30.

68. A. Wolf, op. cit., p. 71.

69. Townes and Schawlow, op. cit., p. 256.

70. Ibid., p. 225 ff.

71. D. F. Eagle, Unpublished Ph. D. Thesis, Georgia Institute of Technology (1962).

72. J. H. Gunn, Communications of the ACM 8, 492 (1965).

VITA

Carl Rodney Nave was born on July 21, 1939 in Newport, Arkansas. He attended public schools there and was graduated from Newport High School, Newport, Arkansas, in 1957. He received the Bachelor of Electrical Engineering degree from the Georgia Institute of Technology in June, 1961 and entered the graduate school of physics at the same institution in September, 1961.

Mr. Nave was employed as a graduate teaching assistant in the School of Physics at the Georgia Institute of Technology from September, 1962 until June, 1963. He was employed as a research assistant from June, 1963 until June, 1964. He received the degree Master of Science in Physics from the Georgia Institute of Technology in June, 1964. In September, 1964, he received a National Science Foundation Research Assistantship for research toward the Ph.D. degree in physics at the Georgia Institute of Technology.

Mr. Nave was married to the former Brenda Carolyn Duncan of Austell, Georgia, on June 22, 1962.